LOW LEVEL JETSTREAM OF ASIAN SUMMER MONSOON AND ITS VARIABILITY

Thesis submitted in
partial fulfillment of the requirements
for the degree of

Doctor of Philosophy

in

Atmospheric Science

by

S. SIJIKUMAR

Department of Atmospheric Sciences
COCHIN UNIVERSITY OF SCIENCE AND TECHNOLOGY
Cochin 682 016, India

April 2003

CERTIFICATE

This is to certify that the research work presented in this thesis is the original work done by Mr. S. Sijikumar under my guidance and has not been submitted for the award of any Degree or Diploma by any other University or institution.

Cochin
April 12, 2003

K. Mohankumar
Thesis Guide

Dr.K.Mohan Kumar, Ph.D.
Professor & Head
Department of Atmospheric Sciences
Cochin University of Science & Technology
Cochin-682 016, India

CONTENTS

LIST OF FIGURES

LIST OF TABLES

PREFACE

Asian summer monsoon rainfall affecting Indian subcontinent and other Asian regions is the product of the global and local anomaly in the general circulation features. Awareness of the need to understand and predict the monsoon over India have recently generated much interest in the possible relationships between the amount and distribution of Indian monsoon rainfall and antecedent regional and global features. The most important need in monsoon forecasting is to pick out with reasonable degree of success, the years of deficient and excess rainfall.

A strong cross-equatorial Low Level Jet-stream (LLJ) with core around 850 hPa exists over the Indian Ocean and south Asia during the boreal summer monsoon season, June to September. LLJ has strong horizontal shear (vorticity) in the planetary boundary layer and is important for the development of rain producing weather systems. The LLJ is the main conduit for transporting moisture generated over Indian Ocean to the monsoon area. The intraseasonal oscillation of LLJ controls this moisture distribution. Thus LLJ is plays an important role on monsoon rainfall distribution over Indian subcontinent.

The main objectives of the present study are, (i) to study intraseasonal variability of LLJ and its relation with convective heating of the atmosphere, (ii) to establish whether LLJ splits into two branches over the Arabian sea as widely believed, (iii) to study the role of horizontal wind shear of LLJ in the episodes of intense rainfall events observed over the west coast of India, (iv) to perform atmospheric modeling work to test whether small (meso) scale vortices form during intense rainfall events along the west coast; and (v) to study the relation between LLJ and monsoon depression genesis.

Daily wind data, from NCEP/NCAR reanalysis project (1961-1990), Outgoing Longwave Radiation (OLR) data of NOAA (1979-1990), Indian Summer Monsoon Rainfall (ISMR) series are the major data sets used for this study. Fifth

Generation NCAR/Penn State Mesoscale Model (MM5) is used to simulate a few intense rainfall events along the west coast of India during summer monsoon.

During the 30-year period, ISMR had large inter-annual variability with several DRY and WET monsoon years. LLJ winds over the western Arabian Sea and the cross equatorial flow are stronger in the WET composite than in the DRY. In the WET case monsoon westerlies extend eastwards only upto the longitude of Philippines (~120°E). In the DRY composite, monsoon westerlies extend further eastwards. The correlation between ISMR and the monsoon winds over south Asia, Indian Ocean and West Pacific are also discussed.

The intraseasonal variability of LLJ and its association with convective heating has been studied. The 12-year (1979-1990) composite of the onset pentad shows a large area of low OLR or high convection in the low latitudes of Indian Ocean. A well-marked LLJ maximum is present in the southeast parts of India and over Sri Lanka. Composite pentad analysis of OLR for break monsoon conditions during July and August shows that the OLR minimum area of low latitudes at the time of onset has moved northwards and lies over northeast India and neighbourhood. A fresh area of OLR minimum has formed over equatorial Indian Ocean similar to that at monsoon onset. The LLJ of break monsoon is very much similar to the onset time. During active monsoon periods when there is a band of strong convective heating in the latitude belt 10°N-20°N and longitude 70°E and 120°E, the LLJ axis passes eastwards from central Arabian Sea through peninsular India and emerges into the western Pacific Ocean. During this period, LLJ does not show splitting into two branches as widely believed.

The relation between the convective heating of the atmosphere over south Asia and the LLJ through peninsular India is examined. The linear correlation

coefficient between the daily value of OLR-Index and the U-Index for lags of -5 days to +5 days shows that the atmospheric heating by convection can accelerate the LLJ flow through peninsular India in about 3-4 days.

Cases of intense rainfall (24 hr) events of 20 cm per day or more at 5 coastal stations for the period 1975-1990 have been studied. It is found that these rainfall events occur in the region of large cyclonic wind shear at 850 hPa of the LLJ. Literature has speculated on the existence of an offshore trough and a mesoscale vortex embedded in it in the atmospheric boundary layer in association with these intense rainfall events. This aspect is examined with MM5 model. With the inclusion of realistic Western Ghats orography, a mesoscale vortex appears after 24 hours of model run.

The results of a study on the evolution of LLJ prior to the formation of monsoon depressions are presented. A synoptic model of the temporal evolution of monsoon depression has been produced. There is a systematic temporal evolution of the field of deep convection strength and position of the LLJ axis leading to the genesis of monsoon depression.

One of the significant outcomes of the present doctoral thesis is that the LLJ plays an important role in the intraseasonal and the interannual variability of Indian monsoon activity. Convection and rainfall are dependant mainly on the cyclonic vorticity in the boundary layer associated with LLJ. In turn LLJ is maintained by the convective heating of the atmosphere over Bay of Bengal. Monsoon depression genesis and the episodes of very heavy rainfall along the west coast of India are closely related to the cyclonic shear of the LLJ in the boundary layer and the associated deep convection. Case studies by a mesoscale numerical model (MM5) have shown that the heavy rainfall episodes along the west coast of India are associated with generation of mesoscale cyclonic vortices in the boundary layer.

CHAPTER 1

INTRODUCTION

1.1 Relevance of the topic

The Asian monsoon system is an integral component of the earth's climate system, involving complex interactions of the atmosphere, the hydrosphere and the biosphere. The majority of the population of the planet reside in the monsoon regions. India, with a population of nearly a billion people, is located in the central portion of South Asia and is predominantly within the monsoon regime. The annual variation of rainfall and temperature has a major influence on the livelihood and well being of the country. The change in the large scale atmospheric and oceanic circulations due to the redistribution of monsoon heat sources and sinks is also affecting weather and climate in regions far away from the monsoon region. Droughts and floods due to the changes in monsoon affect agricultural and industrial production and cause property damages, human suffering and death and spread of diseases thus posing serious threats not only to the monsoon community but also on the global scale.

The summer monsoon contributes about 80% to the annual rainwater potential of India. Traditionally in India, agricultural practices have been tied to the annual cycle of the monsoon. Variations in the timing and quantity of rainfall significantly affect the productivity of crops. A monsoon year with less total rainfall than normal generally corresponds to low crop yields (*Gadgil*, 1996). An intense monsoon can cause considerable distress as a result of severe flooding and crop destruction . In addition, within the monsoon rainy season there are great variations of precipitation, the so called intraseasonal variations. The long periods of excess rainfall are often referred to as *active* phases of the monsoon and the dry periods of little rain as *break* phases. Since ploughing and planting periods are extremely susceptible to the changes in monsoon rains, the intraseasonal variability has a direct influence on the agricultural sector. Even if the average seasonal monsoon rains are normal, an ill-timed arrival or cessation of rainfall can cause crop destruction (*Webster et al.*, 1998). With accurate forecasts, the impact of variability of the monsoon on agricultural practices, water management, etc., could be optimised. Since the Asian monsoon system is a dominant manifestation of a strongly interactive ocean-atmosphere-land system, understanding the mechanism that produce the variability in the monsoon is very much needed for developing accurate prediction methods.

1.2 Justification for the study

A strong cross-equatorial Low Level Jetstream (LLJ) with core around 850 hPa exists over the Indian Ocean and south Asia during the boreal summer monsoon season, June to September. LLJ has its origin in the south Indian Ocean, north of the Mascarene High as an easterly current, it crosses the equator in a narrow longitudinal belt close to the east African coast as a southerly current with speeds at times even as high as 100 knots, turns into a westerly current

over the Arabian Sea and passes through India and enters the western Pacific Ocean.

LLJ has strong horizontal shear (vorticity) in the planetary boundary layer (maximum vorticity at 850 hPa) and is important for generation of convective rainfall and for the development of rain producing weather systems. The LLJ is the main conduit for transporting moisture generated over Indian Ocean to the monsoon area. The intraseasonal oscillation of LLJ controls this moisture distribution. In active monsoon condition a large convective region over the Bay of Bengal is maintained by the LLJ passes through peninsular India. It is found that this convection maintains the LLJ. When convection over Bay of Bengal decreases and it gets established over the equatorial Indian Ocean at the time of break monsoon, the LLJ bypasses India and is located south of India. It then transports bulk of the moisture evaporated over the Indian Ocean to the west Pacific Ocean and the moisture supply to India is cut off. Thus LLJ plays an important role in monsoon rainfall distribution over the Indian subcontinent.

1.3 Monsoon

The term *monsoon* appears to have originated from the Arabic word *Mausam* which means *season*. With change of season there is also generally a change of wind direction; hence the word monsoon also came to be associated with wind directions. In a true monsoon climate, seasonal wind shifts typically cause a drastic change in the general precipitation and temperature patterns. Monsoons have been subject of considerable research work for more than a century. According to *Ramage* (1971) the main characteristics of monsoon regions are as follows

- *The prevailing wind direction shifts by at least 120° between January and July.*
- *The average frequency of the respective prevailing wind directions in January and July exceeds 40%.*
- *The mean resultant wind speed in at least one of the months exceeds 3* ms^{-1}.
- *Fewer than one cyclone-anticyclone alternation occurs every two years in either month in a 5° latitude-longitude region.* This ***monsoon region*** which includes parts of the African continent, South Asia and North Australia is shown as shaded area in Figure 1.1.

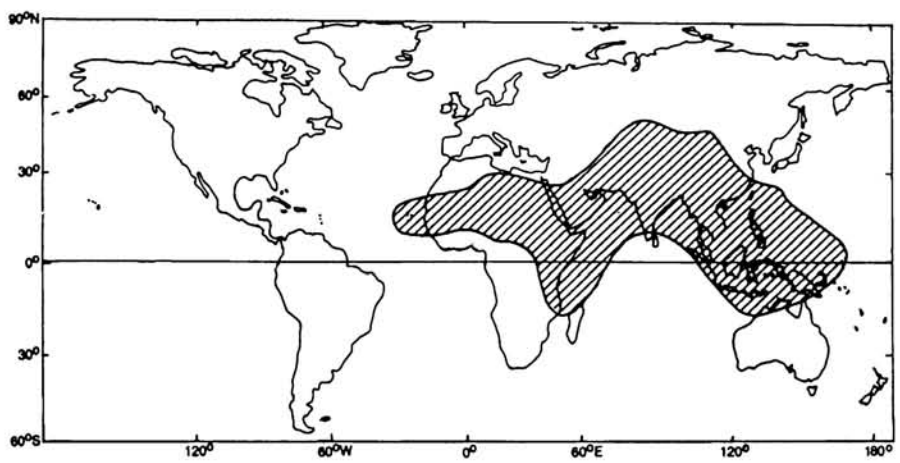

Figure 1.1: Areas with monsoon circulations according to Ramage criteria (*Ramage*, 1971)

There are three fundamental driving mechanisms of the planetary-scale monsoon. These are *(i) the differential heating of the land and the ocean and the resulting pressure gradient (ii) the impact of the rotation of the planet and (iii) moist processes in the atmosphere.* Thus monsoon is a complex, nonlinear phenomenon involving atmosphere, oceanic, and land-based processes (*Webster*, 1987). Ocean can store energy more efficiently than land and therefore retain heat longer than land mass. So over large ocean basins, seasonal changes

in tropical circulation are limited to minor latitudinal shifts and small variations in the intensity. However, over land important seasonal temperature and pressure changes take place that produce seasonal reversal of pressure gradient force. As a result there are major seasonal wind reversals (Figures 1.2 and 1.3).

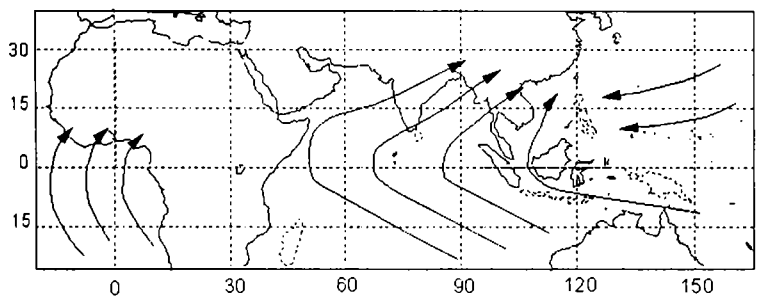

Figure 1.2: Surface wind flow during northern hemispheric summer (*Webster*, 1987)

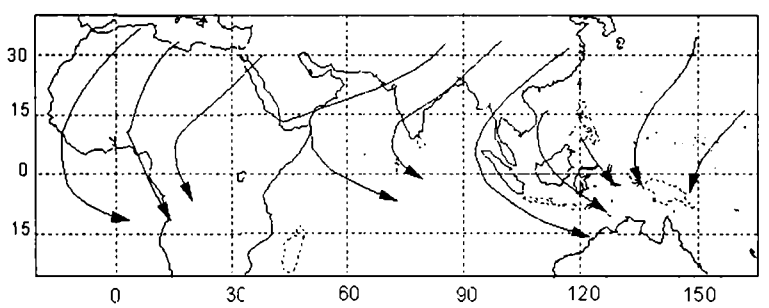

Figure 1.3: Surface wind flow during northern hemispheric winter (*Webster*, 1987)

Because of the Coriolis force due to earth's rotation, air in the monsoon currents moves in curved paths. Inter–hemispheric difference in the direction of the Coriolis force also cause winds to change direction as they cross the equator. As moist warm air rises over summer–time heated land surfaces, the moisture eventually condenses, releasing energy in the form of latent heat of condensation. This extra heating increases the summer land–ocean pressure differences to a point higher than they would be in the absence of moisture in the atmo-

sphere. Moisture processes therefore add to the vigour of the monsoons (*McGregor and Nieuwolt*, 1998).

Monsoon is essentially an annual oscillation in the state of the atmosphere. The relationship among the general mechanisms that generate the monsoons, the seasonal climate cycle and the annual monsoon cycle are shown in Figure 1.4. In the transitional months between the southern and northern hemispheric summers, the Inter Tropical Convergence Zone (ITCZ) is located in the equatorial regions (Figure 1.4 (a)), where maximum surface heating can be found. At this stage, the northern hemispheric tropical–subtropical latitudes are begin to warm up and weak vertical motion is present. The northern hemispheric Hadley cell still predominates at this stage. With the northward movement of the Sun in May to June, the heating of northern tropical land masses intensifies, as does the vertical motion over these land masses (Figure 1.4 (b)). At this time, precipitation belts associated with ITCZ have moved north of the equator, signaling the onset of the summer monsoon.

From June to July, sensible heat input at the surface is close to a maximum, as also the vertical motion and atmospheric moisture over the northern hemispheric tropical land masses (Figure 1.4 (c)). Maximum values of pressure gradient force have also been attained at this stage and the monsoon reaches its maximum intensity with maximum amount of precipitation. By September, surface temperature has decreased markedly with maximum insolation positioned close to that of the April position. The structure of the monsoon at this time of the year is therefore similar to that of April (Figure 1.4 (d)). September heralds the cessation of the northern hemispheric monsoon season. By December, the southern hemispheric wet season is well under way as precipitation belts associated with ITCZ have moved south of the equator (Figure 1.4 (e)) (*McGregor and Nieuwolt*, 1998).

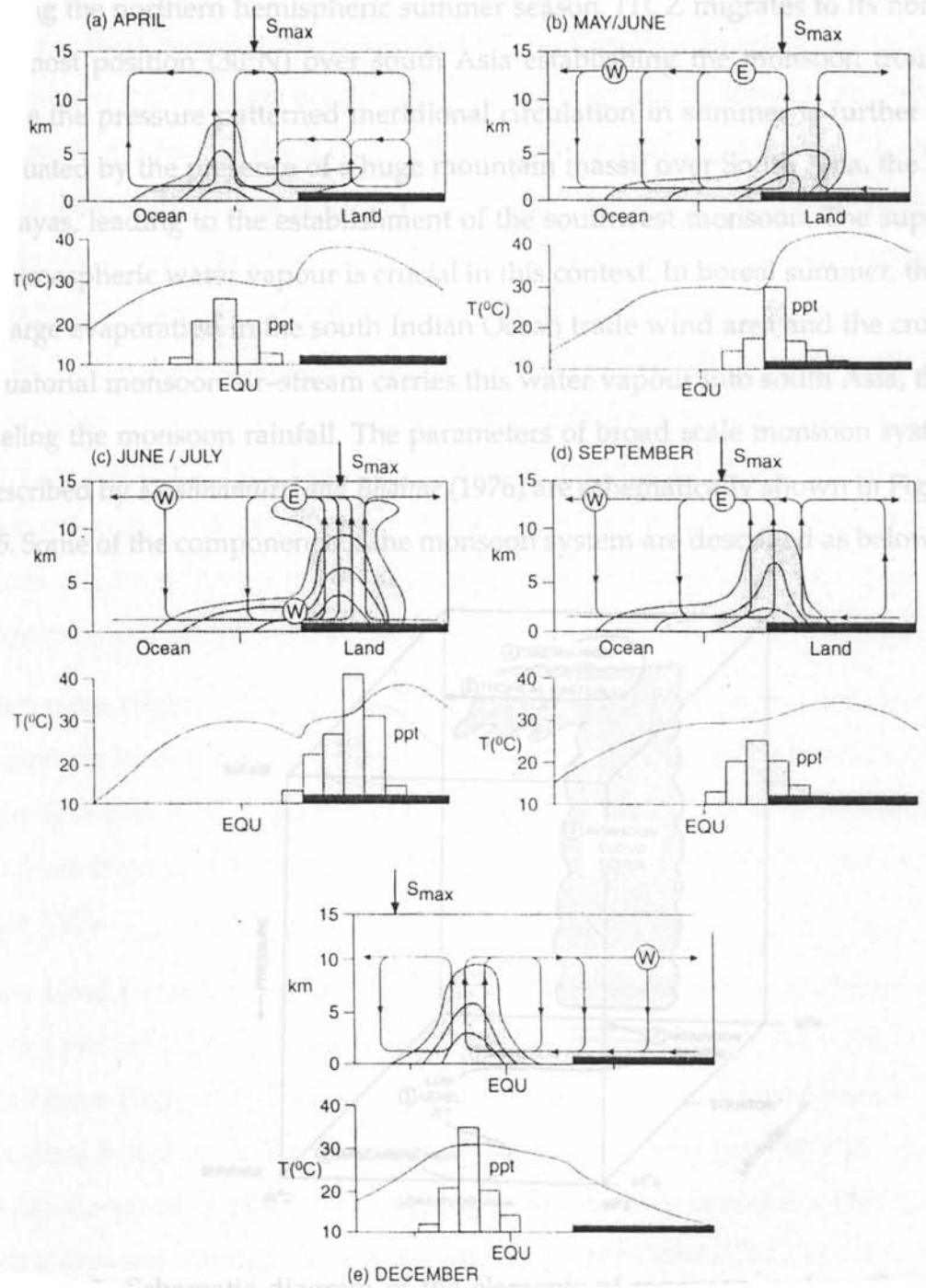

Figure 1.4: The annual monsoon cycle (*Webster et al.*, 1998)

1.4 Asian Summer Monsoon

During the northern hemispheric summer season, ITCZ migrates to its northern most position (30°N) over south Asia establishing the monsoon trough. There the pressure patterned meridional circulation in summer is further accentuated by the presence of a huge mountain massif over South Asia, the Himalayas, leading to the establishment of the southwest monsoon. The supply of atmospheric water vapour is crucial in this context. In boreal summer, there is large evaporation in the south Indian Ocean trade wind area and the cross–equatorial monsoon air–stream carries this water vapour into south Asia, thus fueling the monsoon rainfall. The parameters of broad scale monsoon system described by *Krishnamurti and Bhalme* (1976) are schematically shown in Figure 1.5. Some of the components of the monsoon system are described as below.

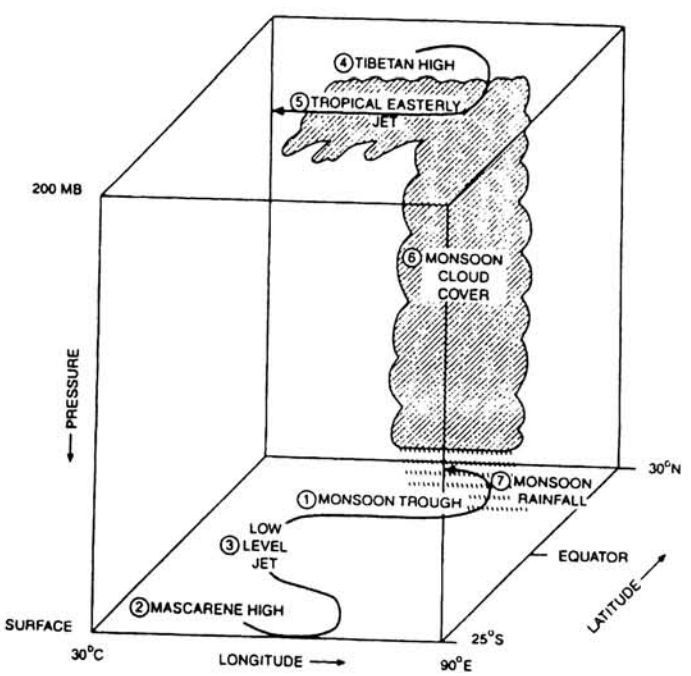

Figure 1.5: Schematic diagram of the elements of monsoon system (*Krishnamurti and Bhalme*, 1976)

Monsoon Trough : During the summer monsoon season, at the surface there is a trough extending southeastwards from the heat low over Pakistan upto Gangetic West Bengal. It is called the Monsoon Trough. The heat low over central parts of Pakistan and neighboring regions is generally linked to the region of maximum heating which are out of reach of the maritime air mass. The heat low is shallow extending upto about 1.5 km and above it is a well marked ridge extending to the upper troposphere, which is part of the subtropical high pressure belt. The monsoon trough is regarded as a part of the equatorial trough of the northern summer in Indian longitudes. The position of this trough line varies from day–to–day and has a vital bearing on the monsoon rains. No other semi–permanent feature has such a control on monsoon activity. When monsoon trough is south of its normal position, we get the active monsoon phase. When monsoon trough moves to the foot hills of the Himalayas we get the break monsoon phase (*Rao*, 1976).

Mascarene High : This is a high pressure area south of the equator near the Mascarene Islands east of Madagascar. The centre of this anticyclone is located near 30°S and 50°E. Variation in the location and strength of the Mascarene High are important in relation to the summer monsoon circulation and rainfall over India.

Low Level Cross Equatorial Jet : This is the well known northern summer Low Level Jet (LLJ). LLJ has its origin in the south Indian Ocean north of the Mascarene High as an easterly current, it crosses the equator in a narrow longitudinal belt close to the east African coast as southerly current with speeds at times even as high as 100 knots, turns into Arabian Sea as a westerly current and passes through India to the western Pacific Ocean. The LLJ is the main conduit for transporting moisture generated over the Indian Ocean into the monsoon area.

Tibetan High : This is a large anticyclone known to have its largest amplitude near 200 hPa during the northern summer months. Between 500 hPa and 200 hPa, the high pressure belt is well to the south of Tibet during June and September and over Tibet during July and August. The combination of the Tibetan High in the upper troposphere and the Monsoon Trough at sea level is accompanied by warm hydrostatic tropospheric columns over the northern India and over the foot hills of the mountains. The warm troposphere is another important feature of broad-scale monsoon system.

Tropical Easterly Jet : A strong easterly flow of air south of the Tibetan High, a tropical easterly jetstream (TEJ), develops in the upper troposphere at around 150 hPa during the monsoon season. This jet has winds of 80–100 knots and has its axis approximately around 10°N and 100°E. Normally, TEJ is in an accelerating stage from south China Sea to south India and decelerates to the west. Upper divergence associated with TEJ is regarded as favourable for convection upstream of 70°E. Subsidence occurs downstream. The fact that the tropical easterly jet only occurs in the summer suggests that its development is related to the seasonal cycle of surface heating and convective heating in the area over which jet lies.

Monsoon Cloudiness and Rainfall : The Indian longitudes are characterized by a large seasonal excursion of the maximum cloud zone (MCZ). It is found that during June–September there are two favourable locations for MCZ over these longitudes. On a majority of days the MCZ is present north of 15°N in the monsoon zone. Often a secondary MCZ occurs in the equatorial region between the equator and 10°N. The monsoon MCZ gets established by northward movement of the MCZ occurring over the equatorial Indian Ocean in April and May. The secondary MCZ appears intermittently, and is characterized by long spells of persistence only when the monsoon MCZ is absent. The

monsoon MCZ cannot remain for more than a month without re–establishment by the the secondary MCZ (*Sikka and Gadgil*, 1980). The rainfall shows similar temporal variation like the cloudiness in MCZ

All these components are connected through the monsoon Hadley circulation. *Krishnamurti and Bhalme* (1976) found that interaction among solar radiation, conditional instability of the monsoon atmosphere and the cloudiness in the monsoon trough region lead to a quasi biweekly oscillation of the components of the monsoon system.

1.4.1 Onset and Withdrawal of Monsoon

Onset of Asian Summer Monsoon is one of the most dramatic seasonal transition exhibited by the atmosphere. The *onset of monsoon* refers to the burst of rains over Kerala on the southern tip of the peninsula and is associated with the commencement of organised monsoon rainfall over Indian region and the establishment of the monsoon trough. The onset phase of monsoon commences in late May/early June. The mean date of onset over Kerala is 1 June, with standard deviation of 8 days. It takes about six weeks from the time of onset over Kerala for the monsoon rains to cover the entire country (India). Figure 1.6 shows the normal onset dates of southwest monsoon over India.

The nature of the onset of the monsoon and the significant factors in the energetics have been extensively studied (*Krishnamurti et al.*, 1981; *Pearce and Mohanty*, 1984; *Ananthakrishnan and Soman*, 1988; *Joseph et al.*, 1994). The main circulation features of the onset can be summarised as follows *(i) formation and northward movement of a cyclonic system (onset vortex) in the southwest Arabian Sea in many years; (ii) strengthening and deepening of westerlies in the lower troposphere and organisation and strengthening of easterlies in the upper troposphere over peninsular India; (iii) the subtropical westerly jet over north India tending to weaken and shift*

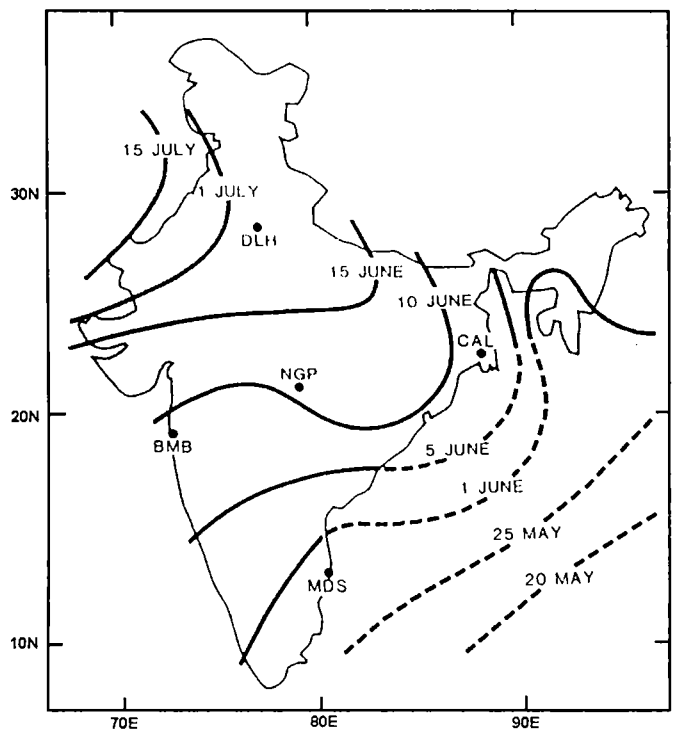

Figure 1.6: Mean dates of onset of the summer monsoon over India. Broken lines denote isolines based on inadequate data. (From India Meteorological Department)

northward; (iv) persistent heavy cloudiness over the southeast Arabian Sea (*Soman and Krishnakumar*, 1993).

On the synoptic scale, the onset of monsoon over Kerala is associated with the genesis and movement of either a depression/cyclone in the Indian seas, or a low pressure area off the coast of Kerala or mid–tropospheric disturbances in the east–west trough zone at the tip of the peninsula. The onset involves the genesis of a well–defined onset vortex (*George and Mishra*, 1993) in about 50% of the years. It usually forms on the cyclonic shear side of the low–level jet in the lower troposphere over eastern Arabian Sea and subsequently its motions are more westward, usually toward the Arabian coast, where it is known to dissipate. It has been noted to first form in the middle troposphere over the eastern

Arabian Sea and subsequently cyclogenesis occurs in the lower troposphere (*Krishnamurti*, 1985).

Krishnamurti and Ramanathan (1982) showed that convective heating has by far the largest effect in determining the structure and strength of the divergent wind. They also demonstrate that unless the moisture is present in the initial profile, no onset occurs in the model. *Sikka* (1980) suggested that passage of deep mid-latitude westerlies across the Mozambique channel in late May triggers the surge in cross–equatorial flow leading to the onset of the monsoon. Analysis of Outgoing Longwave Radiation (OLR) data by *Joseph et al.* (1994) has shown that around the time of monsoon onset over Kerala (MOK), an active belt of convection extends from the south China through the Bay of Bengal, with suppressed convection in the equatorial trough region of the western North Pacific. They also point out that the delayed MOK is associated with El Niño particularly in its year +1. Of the 22 years between 1870–1989 when MOK was delayed by 8 days or more, 16 cases were associated with moderate or strong El NiñoOf the 13 strong El Niños during the same period, 9 were associated with moderate to large delays in MOK.

While the onset of the monsoon over India is invariably gradual, its withdrawal is relatively rapid. Withdrawal from the northwestern parts of India normally commences by September 1 (Figure 1.7). Cooling of the the land masses of northern India and further north and a shift in the activity of the troughs in the westerly wind belt to a relatively lower-latitude belt result in the southward shift of the monsoon trough and withdrawal of the monsoon from northwest India. As these factors vary from year to year, the withdrawal of the monsoon undergoes interannual variation. In general, the withdrawal of the monsoon from western Rajastan, Haryana, and Punjab takes place during the first fortnight of September, and withdrawal from most of the remaining

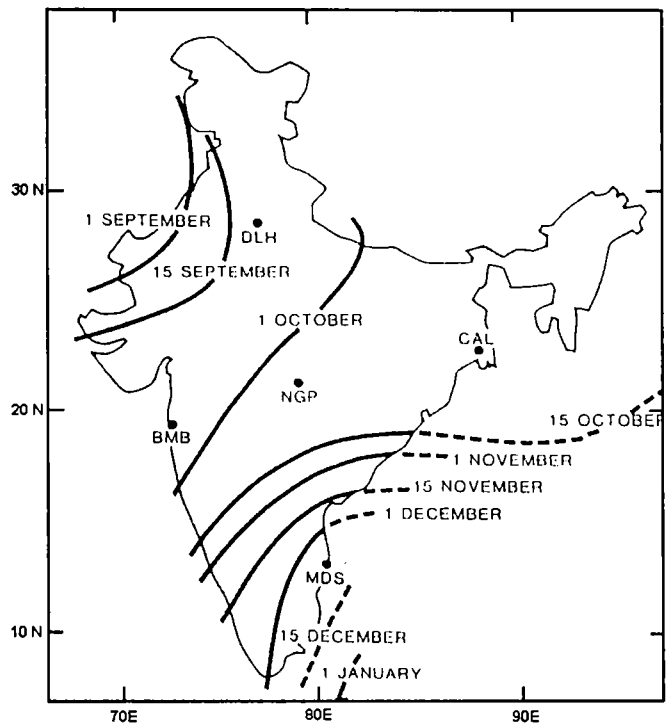

Figure 1.7: Mean dates of withdrawal of the summer monsoon from India. Broken lines denote isolines based on inadequate data. (From India Meteorological Department)

parts of the country occurs during the period mid–September to mid-October (*Mooley and Shukla*, 1987).

1.4.2 Annual Cycle

During Asian summer monsoon season, there are two principal rainfall maxima. The first lies around 15°N and contains two principal sub–maxima: over the Bay of Bengal and in the eastern Arabian Sea next to Ghat mountain range. The second and weaker maximum lies close to and south of the equator and extends from 60°E to 110°E. The northern precipitation zone matches the location of the monsoon trough. The southerly maximum coincides with the weaker surface pressure trough lying just to the south of the equator. During winter the

precipitation patterns extend as a broad zone from the western Indian Ocean to the date line to the south of the equator and is located closer to the equator than during the summer. The heating gradients in both seasons associated with precipitation and radiative processes are largest on the planet, dominating the planet's annual cycle and defining circulation structures on a planetary scale (*Webster et al.*, 1998).

The major precipitation zone in northern summer is in a tilted position with its center in the Indian region (between 15°N and 20°N) while its position in the western Pacific remains around 5°N. This mean displacement of the precipitation zone over the Indian region represents a strong asymmetric heat source. The heating gradients associated with such a heat source drives a regional Hadley circulation with ascending motion around 20°N, and descending motion from the equator to the southern hemisphere subtropics. The precipitation maximum and hence the ascending part of the Hadley circulation during the northern summer over the rest of the globe is closer to the equator and centered around 5°N. It was first noted by *Schulman* (1973) that the regional monsoon Hadley cell with reverse meridional circulation in the Indian monsoon region is strong enough to make the zonally averaged Hadley cell appear to be very week during the northern summer. The importance of the regional Hadley circulation in the monsoon rainfall was recognised by *Joseph* (1978) who showed that the mean meridional wind at 150 hPa in June, July and August over India was related to the seasonal monsoon precipitation. However, there is also an east–west Walker circulation with major ascending motion in the equatorial western Pacific and Indonesia and subsidence over the equatorial Indian Ocean. Thus, the Indian monsoon may be viewed as a superposition and interaction between a regional Hadley circulation and a planetary-scale Walker circulation (*Goswami*, 1994; *Goswami et al.*, 1999).

Through out the annual cycle, the Sea Surface Temperature (SST) in the Indian Ocean undergoes major changes. The SST is the most important characteristics of the coupled ocean–atmosphere system and determines, to a large degree, the manner in which the ocean and the atmosphere interact. The atmosphere feels the SST but the future SST depends on the surface thermal structure and particularly on the heat content of the upper ocean. A warm SST anomaly without warm heat content will quickly be eliminated by the atmosphere. On the other hand, warm SST region with warm heat content can be very persistent to the climate system. The north Indian Ocean SST reaches maximum in spring and early summer (more substantially in the Arabian Sea). With the arrival of the monsoon due to mixing and enhanced Ekman transports SST seems to fall rapidly. Negative feedbacks occur between the atmospheric component of the monsoon and the ocean.

1.4.3 Interannual Variability

The year to year variation of the Asian monsoon is one of the strongest signals of the earth's climate variability. The mean rainfall over Indian peninsula (June–September) is about 852 mm and the standard deviation of the seasonal mean is about 84 mm (*Parthasarathy et al.*, 1994). A large fraction of interannual variability is determined by the slowly varying surface boundary conditions such as SST, surface albedo and soil moisture (*Charney and Shukla*, 1981). Several workers have shown that there is a significant relationship between drought in the Indian summer monsoon and El Niño-Southern Oscillation (ENSO) (*Sikka*, 1980; *Rasmusson and Carpenter*, 1983; *Shukla and Paolina*, 1983). *Webster et al.* (1998) point out that nearly all El Niño years are drought years in India but not all drought years correspond to El Niño years. Although the relationship is not fully understood, it is clear that the monsoon and ENSO are related in some fundamental manner.

Soman and Slingo (1997) showed that the modulation of the Walker circulation (additional subsidence) is the dominant mechanism by which El Niño weakens the Asian summer monsoon for the years 1983 and 1984. However, the delayed onset during El Niño may be associated with the complementary cold SST anomalies in the western Pacific that delay the northward transition of the Tropical Convective Maximum (TCM). They further suggest that during cold events it is primarily the warm SST anomalies in the western Pacific that enhances the TCM and lead to an early onset and stronger monsoon. Although numerous studies have focused on ENSO links to the Indian monsoon, *Lau and Wu* (1999) mentioned that India is not a major center of action in the dominant coupled precipitation–SST relationships. *Arpe et al.* (1998) studied the differences between 1987 and 1988 summer monsoons and suggest that, while large scale dynamics over India are mainly governed by Pacific SST, the variability of precipitation over India is impacted by a number of other factors including SST anomalies over the northern Indian Ocean, soil wetness, initial conditions, and the quasi–biennial oscillation. They show that the two direct effects of El Niño are to reduce precipitation over India and reduce the surface winds over the Arabian Sea. They suggest that the latter leads to an increase in SST and more precipitation over India acting to counteract the direct effect of El Niño .

Another school of thought believe that the monsoon in turn influence ENSO (*Yasunari*, 1990). Several recent studies have examined the possibility of modification of the ENSO characteristics by the summer monsoon by simple coupled models. *Wainer and Webster* (1996) argued that the interannual variation of the summer monsoon may contribute to irregularities of El Niño. *Chung and Nigam* (1999) showed that, based on results from an intermediate ocean–atmosphere coupled model, that monsoon forcing may increase the frequency of occurrence of El Niño. *Lau et al.* (2000) suggested that boreal spring warming in the north Arabian Sea and subtropical western Pacific may play a role in

the development of strong South Asian monsoon. *Kumar et al.* (1999) showed that the inverse relationship between ENSO and Indian Summer Monsoon, that was clearly evident before 1980, weakened considerably in recent decades. They suggest that this is associated with a southward shift in Walker Circulation, and increased Eurasian surface temperature during winter and spring seasons. Using NCEP/NCAR reanalysis data and Atmospheric General Circulation model *Goswami and Jayavelu* (2001) have shown that the Indian Monsoon, by itself, does not produce significant surface wind anomalies in the the equatorial Pacific either during or following the monsoon season and thus the Indian monsoon by itself is unlikely to influence the ENSO in a significant way.

The interannual variability of monsoon rainfall shows a biennial variability during certain periods of the data record. This biennial oscillation, referred to as tropospheric biennial oscillation (TBO) is reported in the rainfall of Indonesia (*Yasunari and Suppiah*, 1988) and east Asia (*Tian and Yasunari*, 1992; *Shen and Lau*, 1995) as well as in Indian rainfall (*Mooley and Parthasarathy*, 1984). The rainfall TBO appears as a part of the coupled ocean–atmosphere system of the monsoon regions, increasing rainfall in one summer and decreasing in the next.

A strong biennial tendency has also been noted in ENSO cycles for some time (*Lau and Sheu*, 1988; *Rasmusson et al.*, 1990). Except for the different time scales, the evolutionary features of the biennial oscillation in SST, sea level pressure, wind and precipitation are very similar to that of ENSO. In the last several years, there have been increasing evidences showing the presence of the TBO in the monsoon regions (*Yasunari*, 1990; *Shen and Lau*, 1995; *Meehl*, 1997). Recently a number of theories have emerged suggesting that the TBO may be related to the air–sea interaction in the Asian Summer Monsoon region, modified by coupled ocean–atmosphere processes (*Meehl*, 1997; *Chang and Li*, 1999). Recent studies have also suggested that strong monsoon-ENSO interactions may result

in a strong biennial tendency in ENSO cycles in the form of rapid development of La Niña approximately one year after an El Niño (*Lau et al.*, 2000; *Lau and Wu*, 2001). *Kim and Lau* (2000) investigated the mechanism of the quasi-biennial tendency in ENSO–monsoon coupled system using an intermediate coupled model. They found that the strong coupling of ENSO to monsoon wind forcing over the western Pacific is the key mechanism.

1.4.4 Intraseasonal Variability

Among the many time scales of Asian Monsoon variations, the intraseasonal variation is most distinctive. Observational evidence shows the existence of three different quasi–periodic oscillations with periods of 4–6 days, 10–20 days and 30–60 days (*Krishnamurti and Bhalme*, 1976). The 4–6 day oscillations are largely observed in monsoon trough region. The dynamical system associated with the 4–6 day scale is the monsoon disturbance. A dominant characteristic of intraseasonal fluctuations during summer in the monsoon region is the active–break cycles of precipitation with periods of 10–20 days or 30–60 days . Active spells of the summer monsoon region are associated with an intense trough over India with heavy rainfall over monsoon trough zone. During the break monsoon condition, the monsoon trough moves northward to the foot of the Himalayas, resulting in decrease in rainfall over much of India but enhanced rainfall in the far north and south (*Ramanadham et al.*, 1973). These anomalies are large scale and extend across the entirety of South Asia.

The active–break cycles are linked to observed northward propagation of convection from Indian Ocean on to the Asian subcontinent in summer (*Kesavamurty et al.*, 1980; *Sikka and Gadgil*, 1980). This northward propagation has a time scale of 30–60 days and has been noted in many studies (*Yasunari*, 1981; *Krishnamurti and Subrahmanyam*, 1982; *Lau and Chan*, 1986; *Wang and Rui*, 1990; *Gadgil and Asha*, 1992). Similar northward propagation is also found over the west Pa-

cific during northern summer (*Murakami*, 1984; *Wang and Rui*, 1990). *Hartman and Michelsen* (1989) analysed daily precipitation from Indian stations during 1901–70 and confirmed the existence of 30-50 day variability over peninsular parts of the country. *Yasunari* (1981) suggested that the northward migrating monsoon cloud bands are maintained by a transient local Hadley cell and also may be related to the low–frequency Madden Julian Oscillation (MJO) (*Madden and Julian*, 1972, 1994). The MJO can be defined as a 30–50 day oscillation in the large scale circulation cells that move eastward from at least the Indian Ocean to the central Pacific Ocean. Even though the association of active and break periods of the monsoon with MJO is not fully understood, there is abundant evidence of frequency peaks in south Asian rainfall and wind in the same period bands as the MJO (*Julian and Madden*, 1981; *Wang and Rui*, 1990; *Madden and Julian*, 1994).

Wang and Rui (1990) classified the intraseasonal movement of convection anomaly in three categories. They are (i) eastward (ii) independent northward and (iii) westward. The eastward propagating convection anomaly exhibit three major tracks: (a) equatorial eastward from Africa all the way to the mid-Pacific, (b) first eastward along the Indian Ocean, then either turning northeast toward the northwest Pacific or southeast toward southwest Pacific at the maritime continent, and (c) eastward propagation along the equator with split center(s) moving northward in the Indian and/or west Pacific Oceans. Independent northward propagation which is not associated with eastward propagation is found over two longitude sectors: the Indian monsoon region and western Pacific monsoon region. The mechanism responsible for meridional propagation may differ from that for the eastward propagation. However, climatologically, the most active period of the MJO (at least in its equatorial manifestation) is in the boreal fall and winter (*Webster et al.*, 1998).

A number of theories have been proposed to explain the northward movement of convection during summer. *Lau and Peng* (1990) showed that the interaction of tropical diabatic heating associated with the 30–60 day oscillation and the summer monsoon mean flow induces the development of westward propagating synoptic scale cyclonic vortices over the monsoon region leading to the active and break phases of the monsoon. They suggest that the rapid development of these disturbances, and associated weakening of equatorial convection *via* changes in the low–level moisture convergences accounts for the observed northward migration of the monsoon trough. *Webster* (1983); *Srinivasan et al.* (1993) emphasized the important role of land surface heat fluxes in the boundary layer that destabilize the atmosphere ahead of the ascending zone, causing a northward shift of convective activity. *Goswami and Shukla* (1984) suggested that the northward propagation is due to a convection–thermal relaxation feedback where in the convective activity increases static stability while dynamic and radiative relaxation decreases the moist static stability, bringing the atmosphere to a convectively unstable state. Based on results of a modelling study of summer ISO's, *Wang and Xie* (1997), described the northward *propagation* as a convection *front* formed by the equatorial Rossby waves emanating from the equatorial convection. *Krishnan et al.* (2000) suggest that monsoon breaks are initiated by rapid northwest propagating Rossby waves emanating from convectively–stable anomalies over the Bay of Bengal.

Using principal oscillation pattern (POP) technique *Annamalai and Slingo* (2001) describes the origin and propagation of 15 day and 40 day mode of intraseasonal oscillations. The 40 day mode originates and intensifies over the equatorial Indian Ocean and it has poleward propagation on either side of the equator, as well as eastward propagation into the equatorial west Pacific. The Rossby waves emanating from the west Pacific appear to be responsible for the northwestward propagation of convection. The 15 day mode originates

over the equatorial west Pacific, associated with westward propagating Rossby waves, amplifies over the northwest tropical Pacific and modulates both the continental and oceanic TCZs over the Indian longitudes. By separating summertime ISOs based on their zonal propagation characteristics in the Indian Ocean and the western Pacific Ocean, *Lawrence and Webster* (2002) have shown that the eastward propagation of convection along the equator is a fundamental feature of the majority of summertime ISOs. The eastward propagation appears to be directly related to the northward movement of convection that is associated with active and break cycles of precipitation across India.

There is some evidence that interannual variations of intraseasonal oscillation activity may influence monsoon strength. Several modelling studies show that a significant fraction of the interannual variation of the seasonal mean Indian summer monsoon is governed by internal chaotic dynamics (*Goswami et al.*, 1998; *Harzallah and Sadourny*, 1995; *Rodwell and Hoskins*, 1995). *Goswami and Ajayamohan* (2001) have shown that the intraseasonal and interannual variations are governed by a common mode of spatial variability. The spatial pattern of standard deviation of intraseasonal variability of low–level vorticity and spatial pattern of the dominant mode of intraseasonal variability of the low level winds are similar to that of interannual variability. In another recent study *Lawrence and Webster* (2001) have shown that intraseasonal activity–Indian monsoon relationship is essentially independent of the ENSO–Indian monsoon relationship.

1.5 Low Level Jetstream

Low Level Jetstream (LLJ) according to a definition suggested by *Reiter* (1961) *should have marked gradients of wind speed in the horizontal and vertical.* There are several places where strong low–level currents are observed. The LLJs are gen-

erally located in the lowest 1 to 2 km of the troposphere. These are strongly influenced by orography, friction, diurnal cycle of heating and corresponding variations of pressure gradient and static stability (*Asnani*, 1993). The following geographical locations are favourable for the occurrence of these LLJs.

1. *Slopes of the mountains parallel to the anti–cyclonic flow around the sub–tropical anti–cyclones; for example, low–level jet over west central USA, along the Peru coast in South America and along Namibian coast in South African continent.*
2. *Narrow mountain gaps, like Marsabit (North Kenya) Jet stream.*
3. *North–south oriented continental coasts near cross–equatorial flow, e.g., East–African LLJ during Asian summer monsoon.*

Bunker (1965) using Aircraft observations of wind in the Arabian Sea during the International Indian Ocean Expedition (IIOE) traced a LLJ with large vertical wind shears off Somalia and across the Central parts of Arabian Sea. He showed that monsoon winds attained a speed of 50 knots in the southwestern parts of the Arabian Sea at the top of a 1000 meter layer of air cooled by contact with the upwelled water off the Somali–Arabian coasts.

Analysing the wind data of five years collected by the radiosonde/rawinsonde network of India, *Joseph and Raman* (1966) established the existence of a westerly low level jet stream over peninsular India with strong vertical and horizontal wind shears (Figure 1.8). This jet is seen over peninsular India on many days in the month of July with core at about 1.5 km above mean sea level and core speeds of the order of 40-60 knots. It showed persistence of a few days at one latitude. South to north movement of the jet core was also reported. *Findlater* (1969a) found that the Asian summer monsoon LLJ has its origin in the south Indian Ocean north of the Mascarene High as an easterly current, it crosses the equator in a narrow longitudinal belt close to the east African coast as southerly current with speeds at times even as high

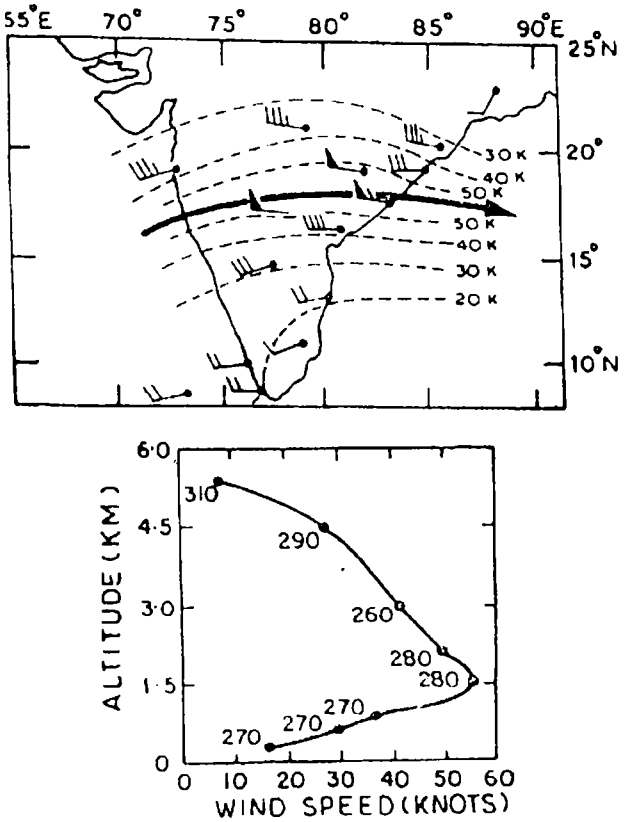

Figure 1.8: Low Level Jet stream over peninsular India at 00 UTC on 9 July 1961. (a) winds and isolines of wind (magnitude) in knots at 850 hPa level. LLJ axis is marked by a thick line. (b) vertical profile of wind speed at Visakhapatnam (17.1°N, 83.3°E) on the jet axis . The three digit numbers marked are the directions of wind. (adapted from *Joseph and Raman* (1966))

as 100 knots, turns into a westerly current over the Arabian Sea and passes through India. This jet according to their computations accounts nearly for half the inter–hemispheric transport of air in the lower troposphere. Using monthly mean winds *Findlater* (1971) showed that the LLJ splits into two branches over the Arabian Sea, the northern branch intersecting the west coast of Indian near 17°N, while the southerly branch passes eastward just south of India. Figure 1.9 shows the monthly mean airflow at the 1.0 km level for August.

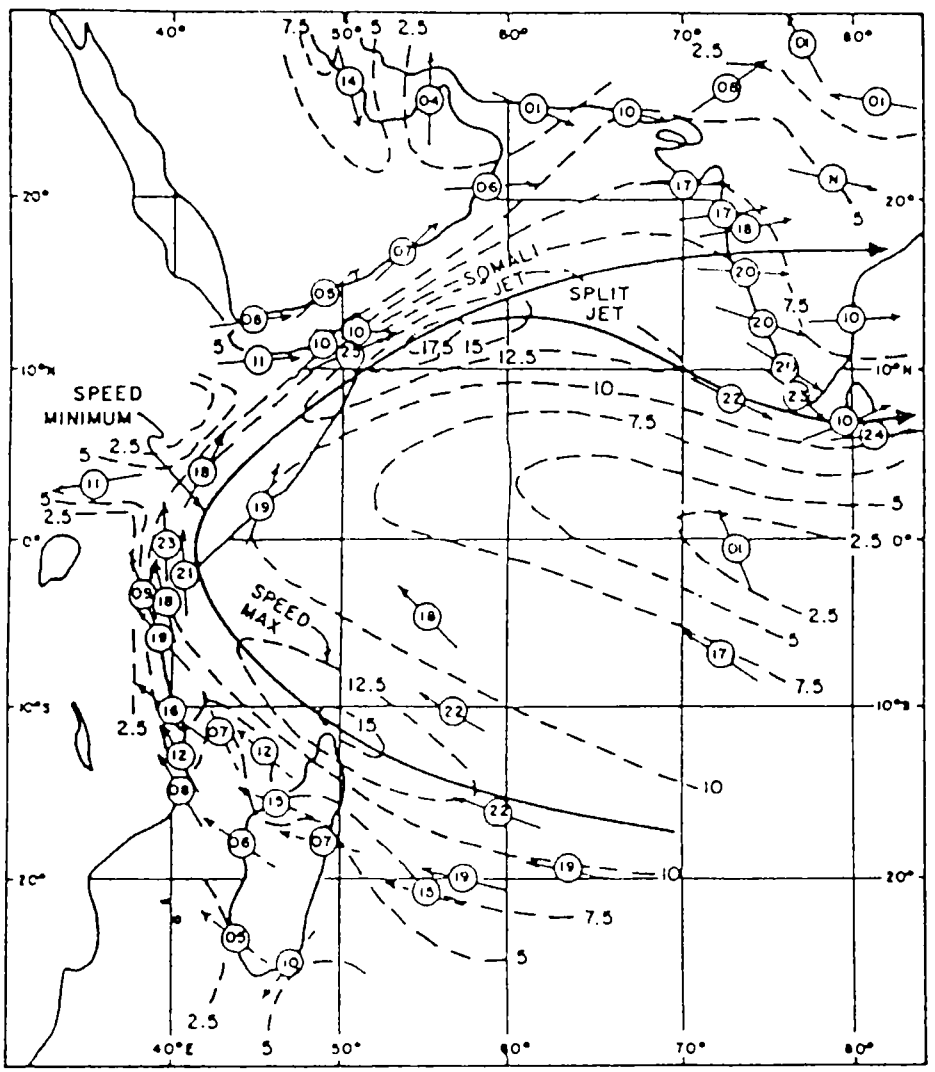

Figure 1.9: Wind field at 1 km for August over the Indian Ocean from *Findlater* (1971). Thick lines marked are the LLJ axes. Isotachs in ms^{-1} are shown as broken lines.

Krishnamurti et al. (1976) studied the LLJ using a single–level, time–dependent, primitive equation model with bottom topography and a prescribed flow on the eastern boundary. They concluded that the broad–scale low–level jet is forced by the differential heating over India and barotropic instability is a possible mechanism for the splitting of the jet. Other one layer models such as those of *Anderson* (1976); *Hart* (1977); *Bannon* (1979, 1982) have indicated how a cross equatorial jet can be formed and have described some of the dynamics involved. *Anderson* (1976) invoked the effects of lateral friction along the mountains located at the East African coast and showed that a balance between the β effect and lateral friction leads to a reasonable strength of the East African Low Level Jet and a location at a reasonable distances away from the mountains. *Hart* (1977) presented a number of analytical models in which the stratification of the observed atmosphere was represented by a free surface under the influence of a reduced gravity. An impermeable western wall barrier simulated the effects of the East African Highlands, and a realistic zonal inflow was prescribed at the eastern boundary. This simplified picture of the observed situation represented the idea that it is the inversion that forces the incident flow to go around rather than the mountain barrier. One of the models of *Hart* (1977) represented the idea of potential vorticity conservation and the advection of the potential vorticity across the equator resulting in the formation of a low level jet in the presence of western boundary mountains.

With a fine–mesh (200m) vertical resolution numerical model *Krishnamurti and Wong* (1979) studied the planetary boundary layer dynamics of the low level monsoonal flow over the Arabian Sea. They concluded that the meridional motion of air across the equator from the Southern to the Northern Hemisphere toward lower pressure results in an acceleration and an enhancement of the horizontal advective terms in the balance forces. As an extension of this study *Krishnamurti et al.* (1983)–using a three dimensional model that removes

the restriction of symmetry–modeled the jet's vertical structure and simulated more realistically its curvature and the position of its maximum strength over the Arabian Sea. The quadratic bulk formulation drag coefficient used was dependent on orographic height. Away from the equator in both hemispheres, the modeled momentum balance was found to be mainly geostrophic at the level of 1 km, with surface friction producing an Ekman balance at 200 m. Near the equator, the balance was cyclostrophic above with friction again important near the ground. An important feature of their results was that the confluence associated with the intertropical convergence zone (ITCZ) over the Arabian Sea did not appear to be accounted for by geostrophic flow. The imbalance between Coriolis and pressure gradient forces to the south of the ITCZ tended to accelerate air parcels northward and so produce the confluence.

Krishnamurti and Ramanathan (1982) showed that the overall development and strengthening of the low–level zonal flow during onset is highly sensitive to the large scale field of differential heating. *Joseph et al.* (1994) suggested that the intensification of the Low Level Jetstream occurs only after the ITCZ over the Indian Ocean has moved north of the equator. A time depended primitive equation model with specified zonal flow, mountains and diabatic heating was used to study the LLJ by *Hoskins and Rodwell* (1995); *Rodwell and Hoskins* (1995). The east African highlands and a land–sea contrast in surface friction are shown to be essential for the concentration of the cross equatorial low level flow into LLJ. They found that surface friction and diabatic heating provide mechanisms for material modification of potential vorticity (PV) of the flow and both were found important for the maintenance of the LLJ. The study identified the strong sensitivity of the LLJ to changes in convective heating over Indian Ocean. When there is a little modification of the PV, the LLJ turns anticyclonically over the Arabian Sea and the flow tends to avoid India.

Arpe et al. (1998) explained the teleconnection between the Somali Jet over the Arabian Sea and El Niño/ La Niña. During El Niño the convection area over the Indian subcontinent, which is the attractor for the Somali Jet, would move eastward and consequently subsidising air would replace rising air and the intensity of the rising air would be reduced. *Halpern and Woiceshyn* (1999) defined the onset of the Somali Jet to be the date when National Aeronautics and Space Administration (NASA) Scatterometer (NSCAT) surface wind speeds off Somalia reached 12 ms^{-2} over a 3°× 3°region in the western Arabian Sea for at least six days. The minimum duration was about three inertial periods, which is the approximate time for development of Ekman currents. The zonal component of wind direction must be eastward. Using Special Sensor Microwave Imager (SSM/I) wind data *Halpern and Woiceshyn* (2001) studied the interannual variations of the Somali Jet in the Arabian Sea during 1988-99 linked with El Niño and La Niña episodes. According to them the average date of Somali jet onset was two days later in El Niño events in comparison with La Niña conditions. Monthly mean strength of the Somali Jet 0.4 ms^{-1} weaker during El Niño episodes than during La Niña intervals. They also reported that the monthly mean intensity of the Somali Jet is above (below) normal, there is an excess (deficit) of rainfall along the Indian west coast.

1.6 Monsoon Depressions

The monsoon season in summer over Asia is punctuated by intermittent emergence and subsequent decay of well–defined, synoptic scale propagating disturbances. One of such synoptic scale tropical disturbance is the Monsoon Depression (MD). These are the important rain producing disturbances of Indian southwest monsoon. Climatology shows that monsoon depressions generally form in the northern portion of the Bay of Bengal and move west-northwestwards (*Rao*, 1976; *Sikka*, 1977). The general features of monsoon

depressions were studied by several workers (*Koteswaram and George*, 1958; *Pisharoty and Asnani*, 1957; *Sikka*, 1977; *Mak*, 1987). The horizontal wavelength of a depression is typically about 2000 km and generally extend vertically up to about 10 to 12 km. The radial gradient of surface pressure ranges from 2 to 5 hPa per 100 km and a surface wind of 8 to 16 ms^{-1}. The disturbance has cold core in the lower troposphere and warm core above (*Sikka*, 1977). Maximum rainfall and cloudiness is found southwest of the depression center (*Pisharoty and Asnani*, 1957). *Lindzen et al.* (1983) ascribed the growth of a Bay of Bengal monsoon depression to the horizontal shear flow instability mechanism. *Douglas* (1992a,b) investigated the structure and dynamics of the monsoon onset vortex and Bay of Bengal depression by special observing systems of MONEX 1979. They found many similarities between the structure of the mature onset vortex and the Bay of Bengal monsoon depression.The observed lower tropospheric positive vorticity tendency west of both depressions (indicating the direction of motion) was primarily a result of an excess of cyclonic vorticity generation by convergence over anticyclonic vorticity advection. Heat-budget calculations for the rain areas showed an approximate balance between warm advection and adiabatic cooling at 850 hPa, though diabatic heating was large above this level. For both depressions the region of maximum rainfall was coincident with the location of the maximum warm advection in the lower troposphere.

1.7 Heavy Rainfall Events Along West Coast of India

Weather during the monsoon period varies from one area to another and from one day to another over the same area. These variations are connected with synoptic patterns in surface and upper air. Formation of off–shore vortices in the trough in westerlies along the west coast of India and associated heavy rainfall is an important synoptic system during monsoon (*Rao*, 1976). Offshore vortices are mesoscale in character with linear dimensions of the order of 100

km or even less and their presence is detected by weak easterly winds at coastal stations. Notwithstanding their small dimension, they are effective in giving spells of very heavy rain in their vicinity. The peculiarity of the rainfall associated with these vortices is that the rainfall over the coast is heavier than that over hill stations a few kilometers east. Their normal duration is of the order of 1 to 3 days. The dynamics of these vortices has not been examined in much detail so far. Existence of these vortices has not been firmly established because of the lack of mesoscale data. They are suspected to be forming when the monsoon is normal or strong over the Arabian Sea. Available data show that they are very small both horizontally and vertically and can be located by coastal surface winds. For the forecasting of heavy rainfall the approach was mainly a statistical correlation, lacking the proper understanding of their dynamics (*George*, 1956; *Mukherjee*, 1980).

CHAPTER 2

DATA AND METHODOLOGY

2.1 NCEP/NCAR Reanalysis

The National Center for Environmental Prediction and National Center for Atmospheric Research (NCEP/NCAR) reanalysis data (*Kalnay et al.*, 1996) are utilised to study the structure and variability of Low Level JetstreamṪhe NCEP/NCAR is a joint project between NCEP and NCAR to produce a multi-decadal record of global atmospheric analysis with data–assimilation system that is unchanged. The NCEP/NCAR Reanalysis System has three major modules (1) data decoder and quality control (QC) preprocessor, (2) data assimilation module with an automatic monitoring system, and (3) archive module (Figure 2.1).

The purpose of the preprocessing Reanalysis module is to reformat the data coming from many different sources into a uniform BUFR format, and to preprocess one or more years at a time, before the actual Reanalysis module is

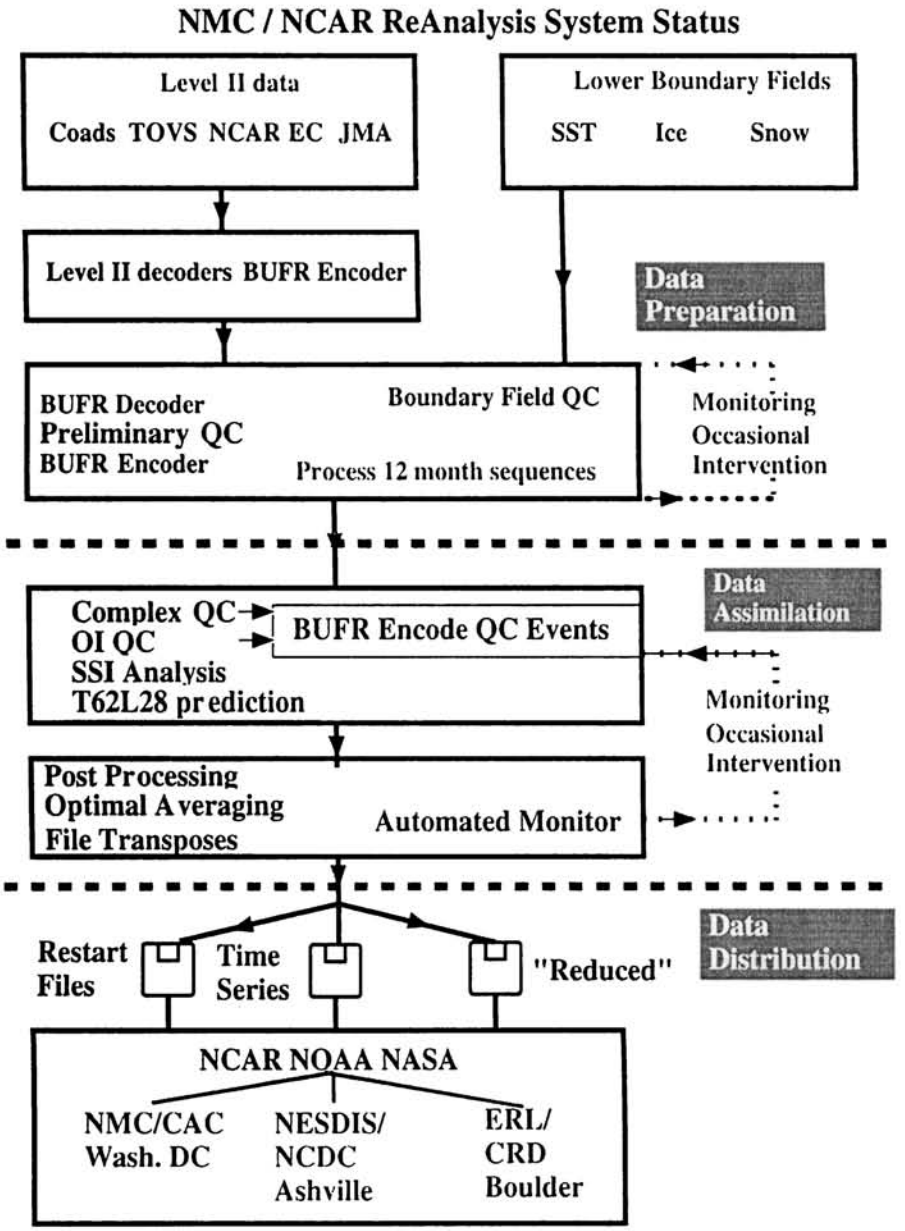

Figure 2.1: Schematic of the main components of the NCEP/NCAR reanalysis system and their state of readiness on January 1995 (NMC has changed to NCEP) (*Kalnay et al.*, 1996).

executed at the rate of one month per day. This allows detection of major data problems with sufficient lead time (a few days before the execution of the Reanalysis), so that human monitors can try to take corrective action. The preprocessor thus minimises the need for reanalysis re–runs due to the many data problems that frequently appear, such as data with wrong dates, satellite data with wrong longitudes, etc. The preprocessor also includes preparation of the surface boundary conditions (SST, sea ice, etc.).

The Spectral Statistical Interpolation (SSI), a 3-dimensional variational analysis scheme (*Derber et al.*, 1991; *Parrish and Derber*, 1992) is used as the analysis module. An important advantage of the SSI is that the balance imposed on the analysis is valid throughout the globe, thus making unnecessary use of nonlinear normal mode initialization. Recent enhancements, such as improved error statistics, and the use of full tendency of the divergence equation in the cost function (replacing the original linear balance of the increments constraint), have also been included (*Derber et al.*, 1991; *Parrish and Derber*, 1992). The T62/28 level NCEP global spectral model is used in the assimilation system. The model has 5 levels in the boundary layer and about 7 levels above 100 hPa. The lowest model level is about 5 hPa from the surface, and the top level is at about 3 hPa. This vertical structure was chosen so that the boundary layer is reasonably well resolved and the stratospheric analysis at 10 hPa is not much affected by the top boundary conditions. The model includes parameterisations of all major physical processes, i.e., convection, large scale precipitation, shallow convection, gravity wave drag, radiation with diurnal cycle and interaction with clouds, boundary layer physics, an interactive surface hydrology, and vertical and horizontal diffusion processes. The reanalysis gridded fields have been classified into four classes, depending on the relative influence of the observational data and the model on the gridded variable.

- **A** indicates that the analysis variable is strongly influenced by observed data, and hence it is in the most reliable class (e.g., upper air temperature and wind).
- The designation **B** denotes that, although there are observational data that directly affect the value of the variable, the model also has a very strong influence on the analysis value (e.g., humidity and surface temperature).
- The letter **C** indicates that there are no observations directly affecting the variable, so that it is derived solely from the model fields forced by the data assimilation to remain close to the atmosphere (e.g., clouds, precipitation and surface fluxes).
- Finally, the letter **D** represents a field that is obtained from climatological values, and does not depend on the model (e.g., plant resistance, land–sea mask).

We have used reduced *Time Series* archive data for the present study. This archive contains basic upper air parameters on standard pressure levels, selected surface flux fields and diabatic heating and radiation terms for each analysis cycle for the entire Reanalysis period. The pressure level data is on a 2.5° lat/lon grid, while the surface flux fields and radiation/diabatic heating data is on a T62 Gaussian grid (192×94).

2.2 NOAA OLR data

To study the relationship between Low Level Jetstream and convective heating, National Oceanic and Atmospheric Administration (NOAA) interpolated Outgoing Longwave Radiation (OLR) data for the period 1974-1990 are used. The data have been taken from the *Interpolated OLR Data* provided by the *NOAA-CIRES Climate Diagnostics Center, Boulder, Colorado, USA,* from their Web site at *http://www.cdc.noaa.gov*. The OLR data contain a major data gap of several

months during 1978 due to the failure of satellite. The resolution of data are at 2.5°×2.5°latitude–longitude (*Gruber and Krueger*, 1984).

2.3 All India Summer Monsoon Rainfall Data

Parthasarathy et al. (1994) have derived a long homogeneous Indian Summer Monsoon Rainfall (ISMR) series for the whole of India using data from 306 rainguage stations having long period records at the same location and well distributed over the country. The mean seasonal rainfall is 852 mm and its standard deviation is 84.5 mm. The variation of the ISMR during 1961–1990 derived by *Parthasarathy et al.* (1994) is shown in Figure 2.2 .

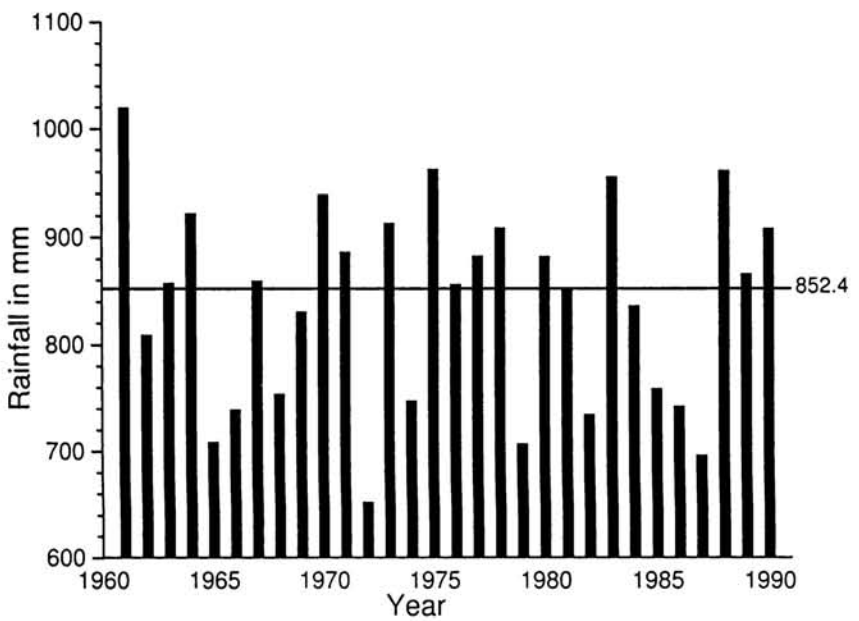

Figure 2.2: Indian Summer Monsoon Rainfall of each year of 1961–1990 in millimeters. The long term mean of 852.4 mm is marked (data from *Parthasarathy et al.* (1994)).

It is seen that on the seasonal scale, the most prominent variation is on the interannual scale between the so called good monsoons (WET) seasons, with above average rainfall and poor monsoon (DRY) seasons with deficit rainfall.

Generally a deficient monsoon year is followed by an excess monsoon year and vice–versa (a biennial oscillation) (*Meehl*, 1987). ISMR has also a prominent decadal scale variability. A 30–year epoch of frequent DRY years (about 3 in ten years) is followed by a 30 year period of much frequent DRY years (less than 1 in ten years) (*Joseph*, 1976; *Parthasarathy et al.*, 1994). Studies of the variation of the monsoon using drought/flood area index (*Bhalme et al.*, 1983; *Mooley and Parthasarathy*, 1983), arid area variations (*Singh et al.*, 1992) and the dry area index (*Singh*, 1995) also bring out these major features of interannual and decadal variation. We have taken a WET year as a year when ISMR is one standard deviation or more above the long term mean and a DRY one standard deviation or below the long term mean. For making composites of WET and DRY cases we have chosen 5 DRY years with the lowest ISMR during 1961–1990 and 5 WET years with the highest ISMR. The DRY years are 1965, 1972, 1979, 1982 and 1987 and the WET years are 1961, 1970, 1975, 1983 and 1988. The ISMR of these years and their departures from the long term mean are given in Table. 2.1.

Table 2.1: Indian Summer Monsoon Rainfall and their departures in units of standard deviation for the 5 (a) DRY and (b) WET years

DRY Years			WET Years		
Year	ISMR (mm)	Normalised departure	Year	ISMR (mm)	Normalised departure
1965	709.4	-1.69	1961	1020.3	1.99
1972	652.9	-2.36	1970	939.8	1.03
1979	707.8	-1.71	1975	962.9	1.31
1982	735.4	-1.38	1983	955.7	1.22
1987	697.3	-1.84	1988	961.5	1.29

2.4 Date of Monsoon Onset

The onset of monsoon over Kerala has a remarkable punctuality and monsoon arrive over Kerala coast around the end of May or beginning of June. The date of Monsoon Onset over Kerala (MOK) is published for each year by the India Meteorological Department (IMD). The mean date of onset over Kerala is 1 June, with standard deviation of eight days. During individual years the date of onset varies widely; the earliest was 11 May (in 1918) and the most delayed was 18 June (in 1972). These are subjective estimates, prepared by several forecasters over the years.

Ananthakrishnan and Soman (1988) prepared homogeneous time series of the onset dates during 1891–1980 as rainfall as sole criterion. They have used the daily rainfall data at 44 rainguage stations in south Kerala and 31 rainguage stations in north Kerala. The daily area–averaged rainfall series of south and north Kerala show spells of light and heavy rain of varying durations. Light rain spells from a feature of the pre–monsoon months, which dramatically give way to rain spells heralding the onset of the southwest monsoon. The transition is sharp and abrupt. The date of monsoon onset is taken as the first day of the transition from light to heavy rainfall category, with the provision that the average daily rainfall during the first 5 days after the transition should not be less than 10 mm. The time series of onset dates has been extended up to 1990 by *Soman and Krishnakumar* (1993), using the same criterion. The mean date of onset of the southwest monsoon over south Kerala is found to be 31 May, with a standard deviation of 8.5 days during 1891–1990. The extreme date of onset during this period were 7 May 1918 and 22 June 1972. The Table 2.2 shows dates MOK for the period 1960–1990 by IMD and *Ananthakrishnan and Soman* (1988); *Soman and Krishnakumar* (1993).

Joseph et al. (1994) have given a critique of the methods for determination of date of MOK. They pointed out that each series has its own merits. *Ananthakrishnan and Soman* (1988) have defined MOK in terms of rainfall from large number of stations in Kerala and an objective method. The IMD series has the merit of using features other than rainfall that are also known to be associated with MOK (e.g., the lower tropospheric wind and humidity fields), but the determination of the date is subjective and has been done by several meteorologists over the course of years.

2.5 Break Periods

Break monsoon conditions are one of the major causes for the intraseasonal variability of the Indian Summer Monsoon. *Ramamurthy* (1969) has studied the details of break period upto 1967. The main criteria used for the study is monsoon trough running close to the foothills of the Himalayas and absence of easterly winds to the north of monsoon trough in the lower tropospheric levels. *De et al.* (1998) identified the break periods from 1968 to 1997 with the help of daily weather charts of India Meteorological Department. He has used the same criteria as by *Ramamurthy* (1969) with some additional features. During the period studied (1968–1997) there were 193 break days with 33 break situations. Most of these occurred in July and August. We have taken for this study the break spells in July and August lasting 3 days or more of the twelve years 1979–1990. We have thus 17 break spells of total duration 84 days. These break spells are listed in Table 2.2.

2.6 Active Periods

Data on the dates of MOK and break monsoon spells are available in the literature for more than 100 years (*Ramamurthy*, 1969; *De et al.*, 1998). But similar long period data on active monsoon spells are not available. *Magna and Webster*

Table 2.2: Date of monsoon onset over Kerala, and duration of Active and Break Monsoon spells during 1979 to 1990. Dates of monsoon onset as given by India Meteorological Department(IMD), also by *Ananthakrishnan and Soman* (1988); *Soman and Krishnakumar* (1993) (AS/SK). Active spells are during June to August (as defined in text) and Break spells during July and August (*De et al.*, 1998), both of duration three or more days

Year	Monsoon Onset over Kerala		Active Monsoon	Break Monsoon
	(IMD)	(AS/SK)		
1979	13 Jun	11 Jun	23 Jun – 02 Jul 31 Jul – 12 Aug	17 Jul – 23 Jul 15 Aug – 31 Aug
1980	01 Jun	31 May	21 Jun – 07 Jul	17 Jul – 20 Jul
1981	30 May	29 May	05 Aug – 08 Aug	26 July – 30 Jul 23 Aug – 27 Aug
1982	01 Jun	01 Jun	11 Aug – 16 Aug	
1983	13 Jun	12 Jun	11 Aug – 15 Aug	22 Aug – 25 Aug
1984	31 May	01 Jun	14 Jun – 18 Jun	20 Jul – 24 Jul
1985	28 May	24 May		22 Aug – 25 Aug
1986	04 Jun	13 Jun	19 Jun – 27 Jun 16 Jul – 21 Jul 06 Aug – 11 Aug	23 Aug – 26 Aug 29 Aug – 31 Aug
1987	02 Jun	01 Jun		28 Jul – 01 Aug
1988	26 May	02 Jun	15 Jul – 20 Jul 31 Jul – 02 Aug	05 Jul – 08 Jul 13 Aug – 15 Aug
1989	03 Jun	01 Jun	21 Jul – 26 Jul	10 Jul – 12 Jul 29 Jul – 31 Jul
1990	19 May	17 May	22 Jun – 08 Jul	08 Jul – 10 Jul 27 Jul – 31 Jul
Total Days			113	84

(1996); *Webster et al.* (1998) have used indices based particularly on the strengths of 850 hPa wind flow and convection in the latitude belt 10°N–20°N over south Asia to define active and break monsoon spells. *Goswami and Ajayamohan* (2001) have also used circulations–based definition of active and break monsoon conditions. They have used 30–60 day filtered zonal wind at 850 hPa at a reference point 90°E, 15°N and the days for which the filtered zonal winds at 850 hPa are greater than +1 standard deviation are considered as active days, while those less than −1 standard deviation are considered break days. Active monsoon is generally understood as the period when strong LLJ passes through the 10°N–20°N latitude belt accompanied by active convection (rainfall) in the same belt over south Asia, formation of monsoon lows and depressions in the head Bay of Bengal, etc (*Rao*, 1976).

We define an active monsoon spell arbitrarily as one in which for each day of the spell the area averaged zonal wind at 850 hPa in the latitude-longitude box 10°N–20°N and 70°E–80°E in a five day period centered on that day is 15 ms^{-1} or more. Figure 2.3 gives the variation of the daily zonal wind at 850 hPa derived in this manner for the period 1 June to 30 September 1979 showing two active spells of monsoon (as given in Table 2.2). During June to August months of the 12–year period 1979–1990 we could thus get 14 active monsoon spells of total duration 113 days as shown in Table 2.2.

2.7 Heavy Rainfall Events

West coast of India experiences rainfall events 20–30 cm or more during the monsoon season. We have taken daily rainfall of 5 stations Kozhikode (Calicut), Honavar, Goa, Ratnagiri and Mumbai (Bombay) from 1975 to 1990 for the monsoon months, June to September, to study the heavy rainfall events. Only data of 15 cm per day and more are taken. Data source is India Meteorological Department. Details of the data are described in Chapter 5 of this thesis.

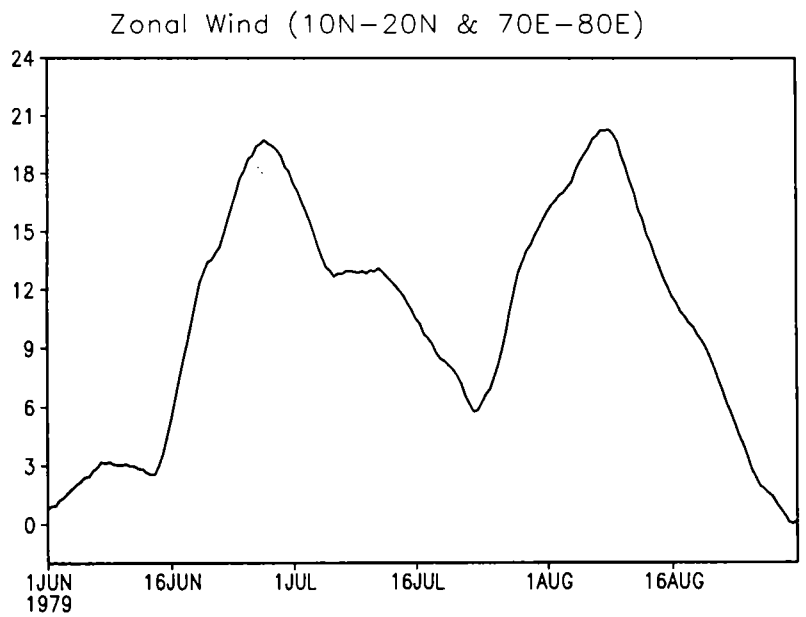

Figure 2.3: Five day moving average of daily mean zonal wind at 850 hPa in the latitude longitude box (10°N–20°N, 70°E–80°E) for the period 1 June 31 August 1979 in ms^{-1}.

2.8 Tropical Cyclones over Western North Pacific

Number of tropical cyclone activity over Western North Pacific (WNP) is very high during the monsoon season, June to September. In order to study the latitude genesis of tropical cyclones and the low level jetstream of summer monsoon we have taken tropical cyclones over WNP during the period 1970 to 1990. Information concerning tropical cyclone activity in WNP was obtained from the Annual Tropical Cyclone Reports (ATCR) issued by the Joint Typhoon Warning Center (JTWC) on Guam. Each year's ATCR contains a summary of the best–track position and intensity (at 6–hr intervals) for all storms warned upon by the JTWC during that calendar year.

2.9 Monsoon Depressions

Monsoon depression is one of the important synoptic scale tropical disturbances which forms periodically on the quasi-stationary monsoon circulation prevailing over the Indian region during the southwest monsoon season of June to September. They generally originate over the northern Bay of Bengal in the seasonal monsoon trough and move west–northwest (*Sikka*, 1977). Systematic records about monsoon depressions are available from year 1891 onwards. The data published by India Meteorological Department shows that depressions form over Bay of Bengal, east Arabian Sea and even over land but the contribution of the Bay of Bengal systems is by far largest (*Sikka*, 1977). In this study data on monsoon depression genesis dates, duration and tracks have been taken from India Meteorological Department (*IMD*, 1996) and is given in Table 2.3.

Table 2.3: Monsoon depressions whose data have been used in the composites

Depression	Year	Date and month of formation	Date and month of dissipation	Duration (days)
A	1979	6 August	10 August	5
B	1981	7 August	10 August	4
C	1981	12 August	16 August	5
D	1983	4 August	10 August	7
E	1984	30 July	6 August	8
F	1984	15 August	19 August	5
G	1985	6 August	9 August	4
H	1986	11 August	14 August	4
I	1987	26 August	29 August	4
J	1988	2 August	6 August	6
K	1989	22 July	25 July	4
L	1990	20 August	24 August	5

2.10 Mesoscale Modelling

The Fifth–Generation NCAR/Penn State Mesoscale Model MM5 (Version 3) is used to study the generation of mesoscale vortices during the monsoon season. The MM5 is the latest in a series that developed from a mesoscale model used by Anthes at Penn State in the early '1970's that was later documented by *Anthes and Warner* (1978). It is a three dimensional nonhydrostatic model with multiple–nest capability and a four dimensional data assimilation capability (*Dudhia*, 1993).

The model is supported by several auxiliary programs, which are referred to collectively as the MM5 modelling system. A schematic diagram representing complete modelling system is shown in Figure. 2.4. Terrestrial and isobaric meteorological data are horizontally interpolated (programs TERRAIN and REGRID) from a latitude–longitude mesh to a variable high–resolution domain on either a Mercator, Lambert conformal, or polar stereographic projection. Since the interpolation does not provide mesoscale detail, the interpolated data may be enhanced (program RAWINS or little_r) with observations from the standard network of surface and rawinsonde stations using either a successive–scan Cressman technique or multiquadric scheme. Program INTERPF performs the vertical interpolation from pressure levels to the sigma coordinate system of MM5. Sigma surfaces near the ground closely follow the terrain, and the higher–level sigma surfaces tend to approximate isobaric surfaces. Since the vertical and horizontal resolution and domain size are variable, the modelling package programs employ parameterised dimensions requiring a variable amount of core memory. Some peripheral storage devices are also used (*PSU/NCAR MM5 User's guide*, 2002).

The modelling system usually gets and analyses its data on pressure surfaces, but these have to be interpolated to the model's vertical coordinate be-

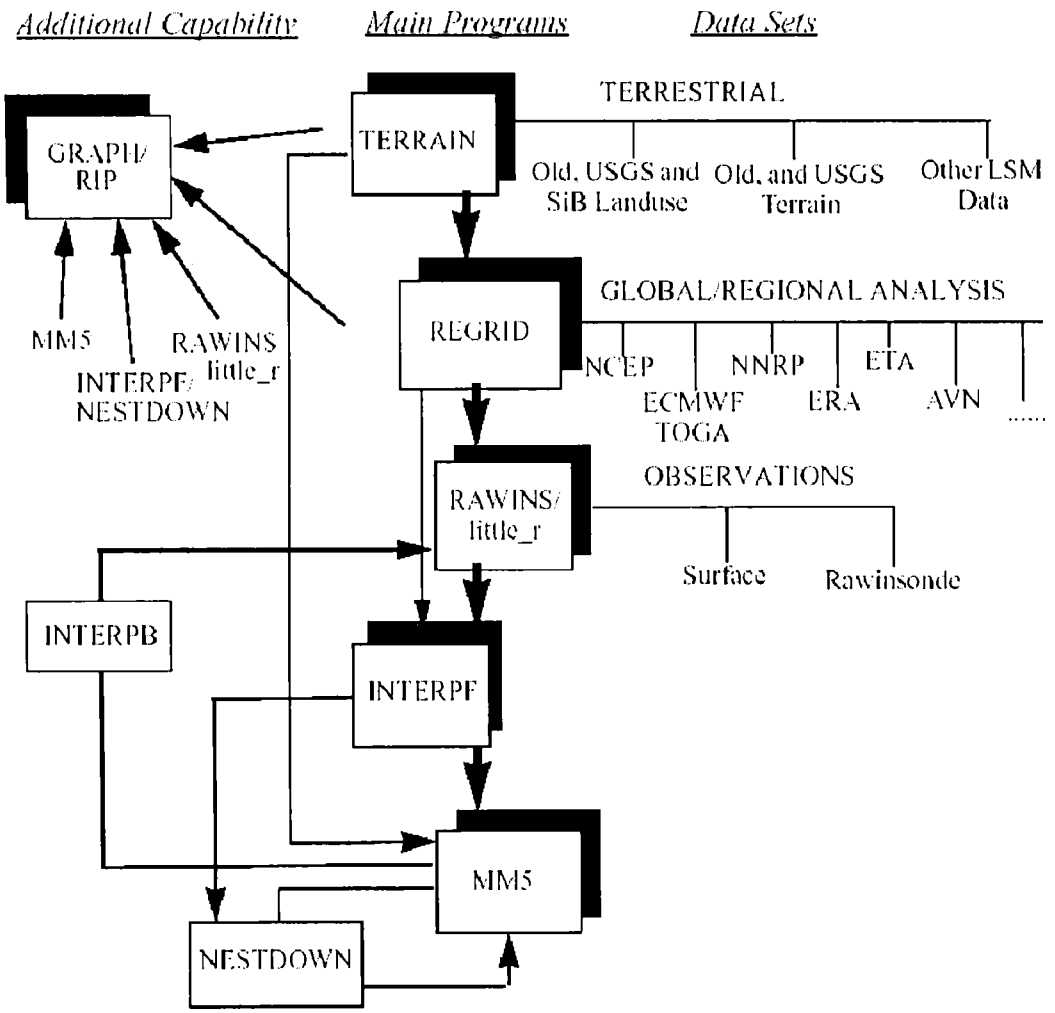

Figure 2.4: The MM5 modelling system flow chart

fore being input to the model.The vertical coordinate of the MM5 model is terrain following (Figure 2.5) meaning that the lower grid levels follow the terrain while the upper surface is flat. Intermediate levels progressively flatten as the pressure decreases toward the chosen top pressure. A dimensionless quantity σ is used to define the model levels where

$$\sigma = \frac{p - p_t}{p_s - p_t} \tag{2.1}$$

where p is the pressure, p_t is a specified constant top pressure, p_s is the surface pressure.

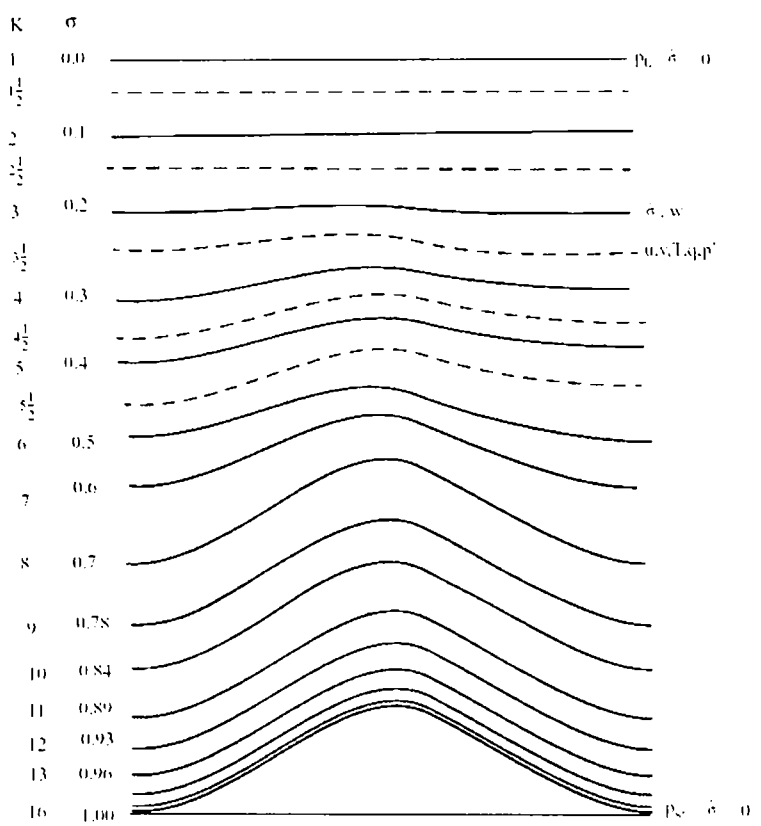

Figure 2.5: Schematic representation of the vertical structure of the model. Dashed lines denotes half–sigma levels, solid lines denote full–sigma levels

It can be seen from the equation and Figure 2.5 that σ is zero at the top and one at the surface, and each model level is defined by a value of σ. The model vertical resolution is defined by a list of values between zero and one that do not necessarily have to be evenly spaced. Commonly the resolution in the boundary layer is much finer than above, and the number of levels may vary from ten to forty, although there is no limit in principle.

The horizontal grid has an Arakawa–Lamb B–staggering of the velocity variables with respect to the scalars. This is shown in Figure 2.6 where it can be seen that the scalars (T, q, etc.) are defined at the center of the grid square, while the eastward (u) and northward (v) velocity components are co–llocated at the corners. The center points of the grid squares will be referred to as cross points, and the corner points are dot points. Hence horizontal velocity is defined at dot points, for example, and when data is input to the model the preprocessors do the necessary interpolations to assure consistency with the grid.

MM5 contains a capability of multiple nesting with up to nine domains running at the same time and completely interacting.The nesting ratio is always 3:1 for two-way interaction. ***Two–way interaction*** means that the nest's input from the coarse mesh comes *via* its boundaries, while the feedback to the coarser mesh occurs over the nest interior.

To run any regional numerical weather prediction model requires lateral boundary conditions. In MM5 all four boundaries have specified horizontal winds, temperature, pressure and moisture fields, and can have specified microphysical fields (such as cloud) if these are available. Therefore, prior to running a simulation, boundary values have to be set in addition to initial values for these fields. The boundary values come from analysis at the future times, or a previous coarser–mesh simulation (1–way nest), or from another model's forecast (in real–time forecasts). For real-time forecasts the lateral boundaries

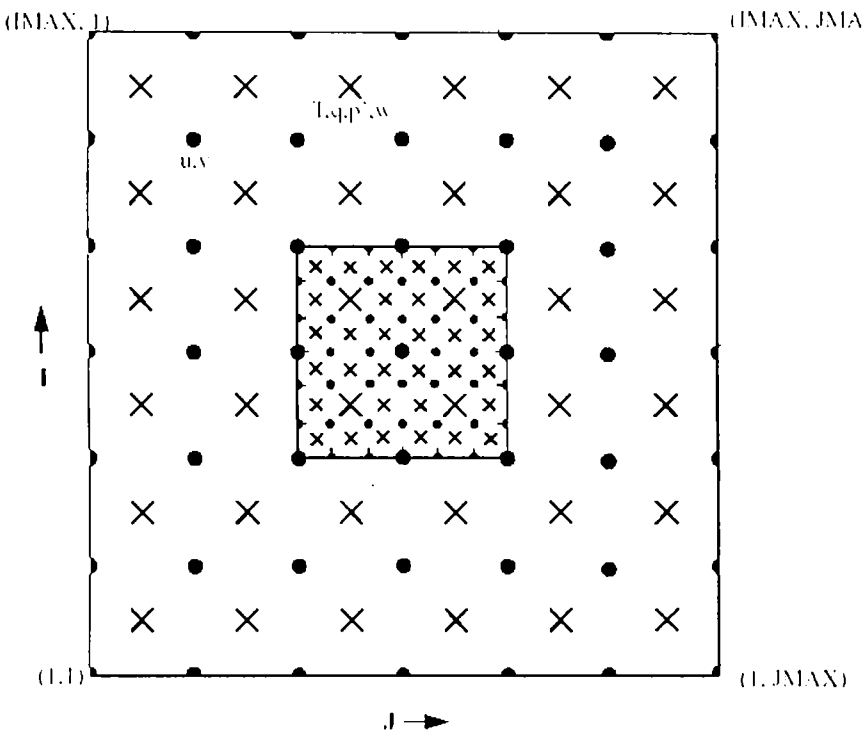

Figure 2.6: Schematic representation showing the horizontal Arakawa B–grid staggering of the dot and cross grid points. The smaller inner box is a representative mesh staggering for a 3:1 coarse–grid distance to fine–grid distance ratio.

will ultimately depend on a global–model forecast. In studies of past cases the analysis providing the boundary conditions may be enhanced by observation analysis (RAWINS or little_r) in the same way as initial conditions are. Where upperair analysis are used the boundary values may only be available 12–hourly, while for model-generated boundary conditions it may be a higher frequency like 6–hourly or even 1–hourly.

The model uses these discrete–time analysis by linearly interpolating them in time to the model time. The analysis completely specify the behavior of the outer row and column of the model grid. In the next four rows and columns

in from the boundary, the model is nudged towards the analysis, and there is also a smoothing term. The strength of this nudging decreases linearly away from the boundaries. To apply this condition, the model uses a boundary file with information for the five points nearest each of the four boundaries at each boundary time. This is a rim of points from the future analysis described above. The interior values from these analysis are not required unless data assimilation by grid–nudging is being performed, so disk-space is saved by having the boundary file just contain the rim values for each field. Two-way nest boundaries are similar but are updated every coarse–mesh time step and have no relaxation zone. The specified zone is two grid–points wide instead of one.

MM5 modelling system requires the following data sets to run

- *Topography and land use.*
- *Gridded atmospheric data that have at least these variable; sea–level pressure, wind, temperature, relative humidity and geopotential height; and at these pressure levels: surface, 1000, 850, 700, 500, 400, 300, 250, 200, 150, 100 mb.*
- *Observation data that contains soundings and surface reports.*

Three resolutions of elevation data; 30 minute, 10 minute, and 5 minute are used for this present study. All these data are created from the 30 seconds United States Geological Surveys (USGS) data. Vegetation/land–use data are also in the same resolution of elevation data and from USGS version 2 land-cover data. Data from NCEP/NCAR Reanalysis Projects (NNRP) are used for the atmospheric variables. The NNRP data are at resolution 2.5°×2.5°latitude–longitude.

CHAPTER 3

STRUCTURE AND CLIMATOLOGY OF LOW LEVEL JETSTREAM AND ITS ASSOCIATION WITH INDIAN SUMMER MONSOON RAINFALL

Asian summer monsoon is an extremely complex phenomenon that has variabilities over a wide range of spatial and temporal scales. It has been recognised for many years that studies of the monsoon must be intimately related to the seasonal climatology of the general atmospheric and oceanic circulations. As far as the atmospheric component is concerned the Low Level Jetstream (LLJ) is one of the main features of the summer monsoon. Importantly, the 850 hPa flow captures important elements of large scale and regional scale monsoon circulation on interannual and subseasonal timescales (*Webster et al.*, 1998; *Annamalai et al.*, 1999; *Sperber et al.*, 2000). Several studies have already been conducted using different data sets and are reported in the literature.

In order to get a comprehensive knowledge about the structure and characteristics of the LLJ during the monsoon season, a detailed study has been carried out using NCEP/NCAR reanalysis data for 30 years (1961–1990) and

the results are reported in this chapter. Horizontal and vertical structure of LLJ, its correlation with Indian Summer Monsoon Rainfall , interannual variability of LLJ and its association with latitude genesis of cyclones in the Western North Pacific (WNP) ocean are studied and the results are discussed.

3.1 Structure and Climatology of LLJ

Thirty year mean (1961-1990) monsoon flow at 850 hPa separately for June, July, August and September are shown in Figure 3.1 a–d, respectively. Westerly monsoon flow extends upto the Philippines (about 120°E) in June. The maximum wind speed is around 14 ms^{-1} and is over western Arabian Sea. Over the Indian peninsular region the flow is weak and core of the flow passes through the southern tip of India and Sri Lanka. By July monsoon flow strengthens and the maximum wind speed is around 18 ms^{-1}. By this time the monsoonal flow has become strong over peninsular India and extends to the east of the Philippines as weak westerlies. The monsoon westerlies of western Pacific strengthen during August. The strongest westerly flow through peninsular India is during July and August. By September the flow weakens over peninsular India.

The latitude–height cross section of mean zonal wind (u) profile of the monsoon flow over central Arabian Sea and peninsular India during July and August is shown in Figures 3.2 (a) and 3.2 (b). Central Arabian Sea cross section is represented by averaging zonal wind between the longitude 62.5°E and 67.5°E and the peninsular India section between 77.5°E to 82.5°E. The zonal wind is plotted from latitudes 50°S to 50°N and vertically from 1000 to 300 hPa. Monsoon westerlies extend from the surface to about 400 hPa level between latitudes 5°S and 25°N. The westerly mean monsoon current is strongest close to 850 hPa. Over the central Arabian Sea (see Figure 3.2 a) the LLJ of the monsoon westerlies has only one core at latitude around 15°N and in the peninsular India (Figure 3.2 (b)) it has two cores (wind maxima) one at about 8°N and the

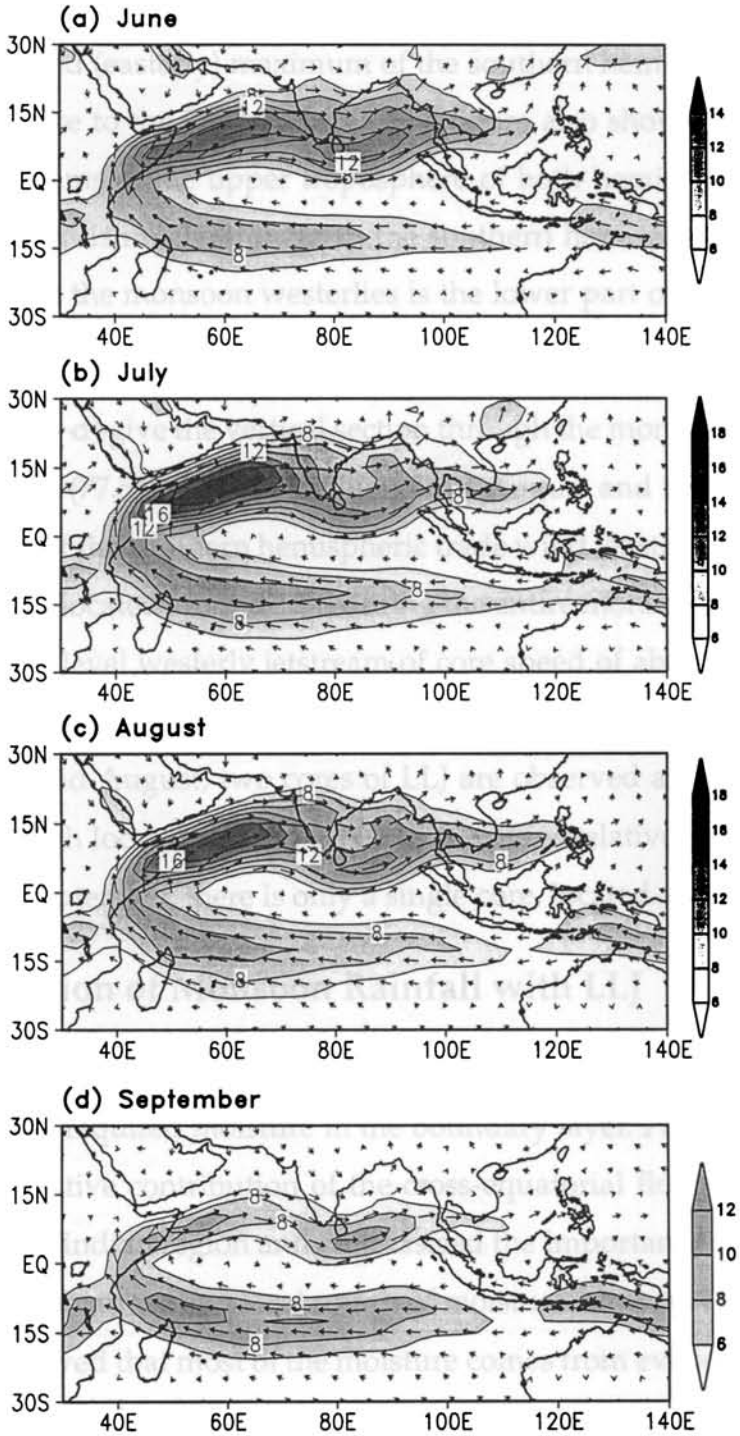

Figure 3.1: Monthly mean 850 hPa wind vectors of the 30 year period 1961–1990 for the months of (a) June, (b) July, (c) August and (d) September using NCEP/NCAR reanalysis data.

other at about 17°N in agreement the splitting of LLJ suggested by *Findlater* (1971). Trade wind (easterly) maximum of the southern hemisphere is at about 12°S latitude close to the 925 hPa level. The figure also shows the subtropical westerly jet streams at the upper troposphere of both hemispheres. The subtropical jet stream is much stronger in the southern hemisphere. The easterly wind seen above the monsoon westerlies is the lower part of the tropical easterly jetstream.

Figures 3.3 (a–d) give the vertical section through the monsoon westerlies of peninsular India (77.5°E–82.5°E) for June, July, August and September respectively. The core of the southern hemispheric trade wind (easterly) of magnitude about 11 ms^{-1} is located around 12°S during the entire monsoon season. On the other hand, low level westerly jetstream of core speed of about 12 ms^{-1} is observed as a single core during June at 850 hPa level around 8°N. During the month of July and August, two cores of LLJ are observed at the same height, one strong branch located around 8°N and the other relatively weaker branch over 17°N. In September, there is only a single core, located around 5°N.

3.2 Association of Monsoon Rainfall with LLJ

The cross–equatorial low level flow is the main artery of the monsoon flow transporting the required moisture in the boundary layer. *Pisharoty* (1965) first assessed the relative contribution of the cross-equatorial flow in transporting water vapour to Indian region and emphasised the importance of the evaporation over the Arabian sea as a local source of moisture. However, *Hastenrath and Lamb* (1980) showed that most of the moisture comes from evaporation over the southern tropical Indian Ocean. The common conclusion emerging from these and subsequent studies is that significant amounts of water vapour and momentum are transported across the equator by the strong wind associated with the Low Level Jetstream .

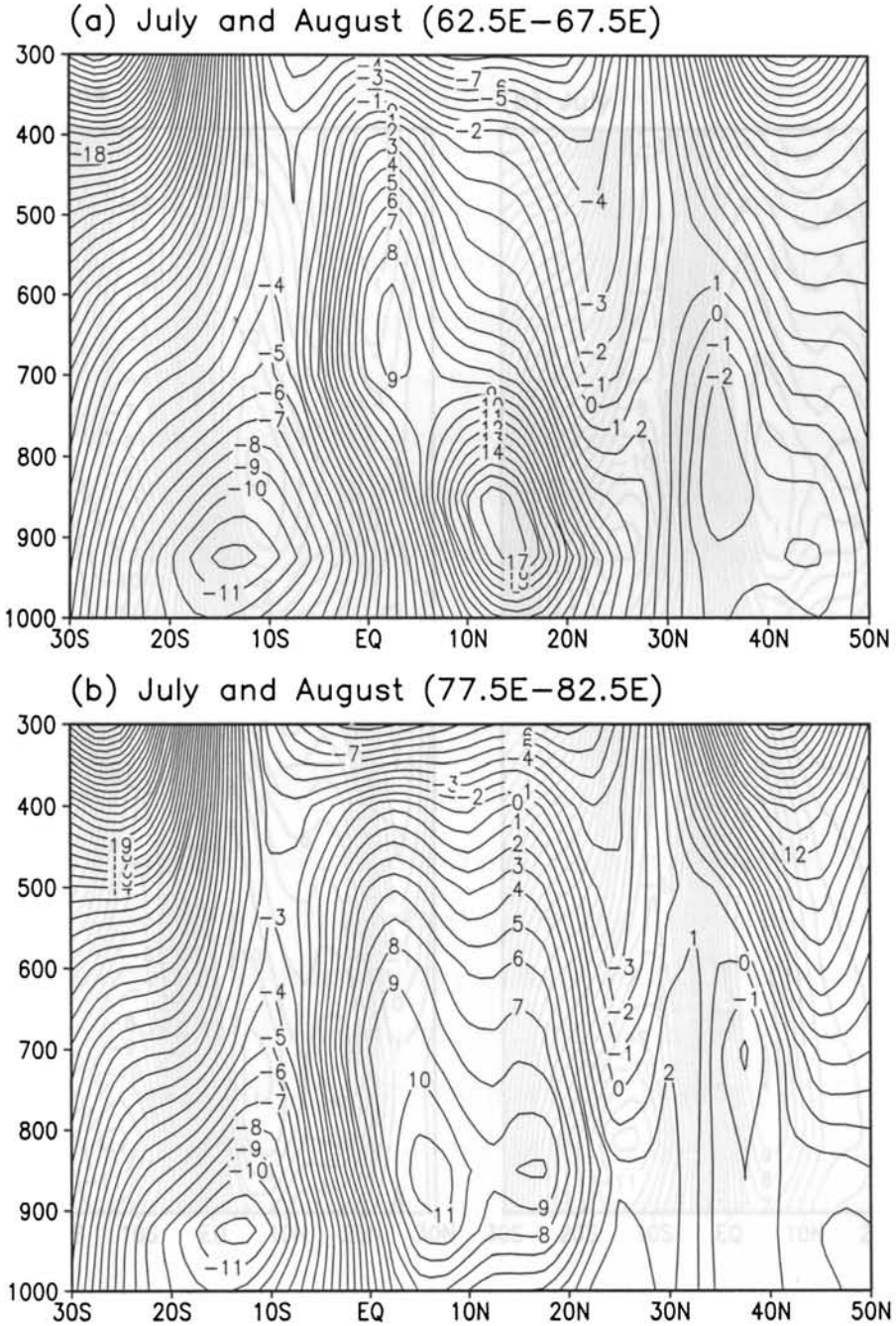

Figure 3.2: Vertical profile of the mean zonal component of wind of July and August, averaged over the longitudes (a) 62.5°E to 67.5°E representative of longitude 65°E and (b) 77.5°E to 82.5°E representative of longitude 80°E as averages for the 30 year period 1961 to 1990.

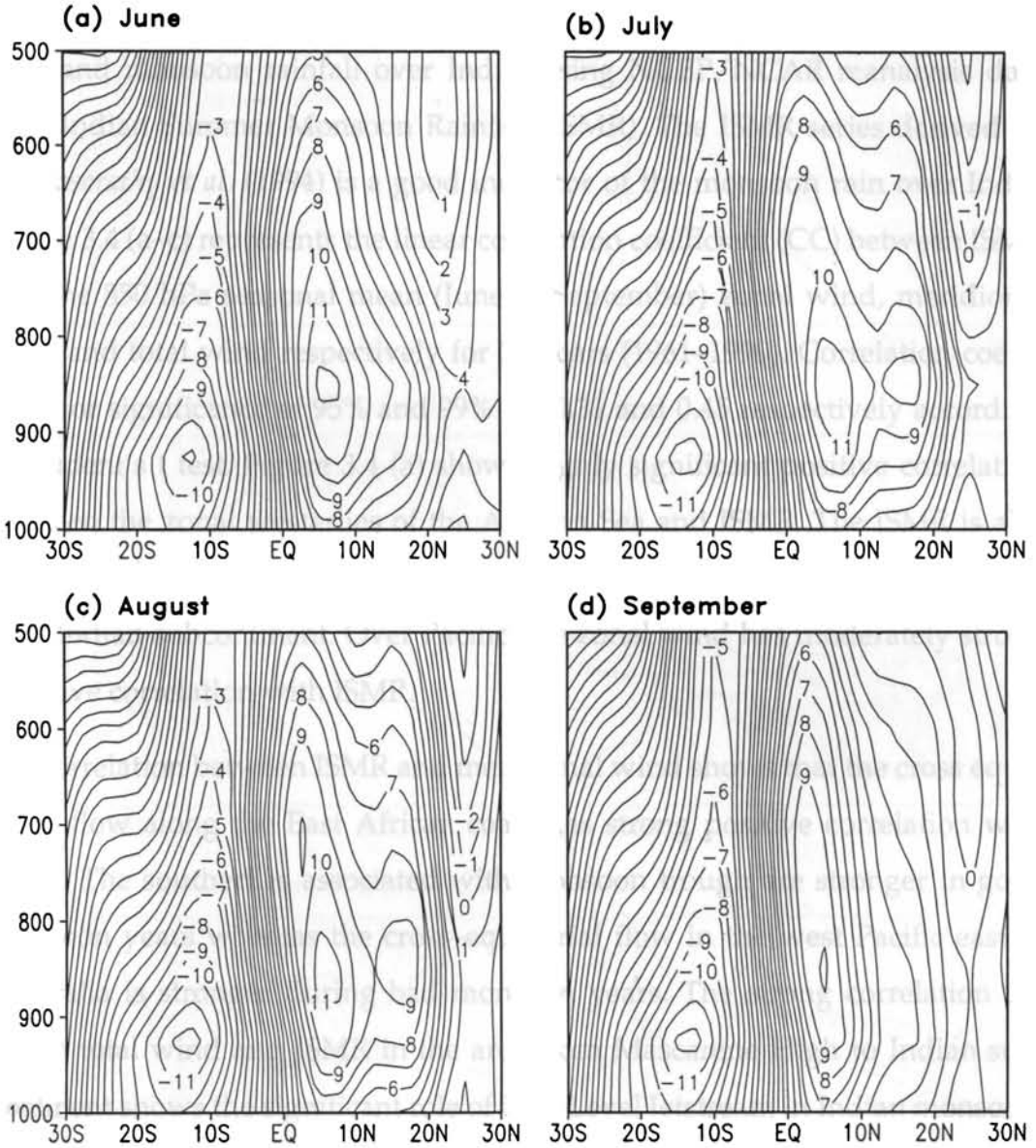

Figure 3.3: Vertical profile of the mean zonal component of wind averaged over the longitudes 77.5°E to 82.5°E representative of longitude 80°E as averages for the 30 year period 1961 to 1990 for (a) June, (b) July, (c) August and (d) September.

Findlater (1981) found significant correlation between cross-equatorial wind index in the years 1953–76 and mean July rainfall of groups of stations in the western India. *Rajan et al.* (1999) studied the relation between the 850 hPa flow and monsoon rainfall over India, using NCEP/NCAR reanalysis data and Indian Summer Monsoon Rainfall (ISMR). The ISMR series derived by *Parthasarathy et al.* (1994) is a good indicator of the monsoon rain over India. Figure 3.4 (a–c) represents the linear correlation coefficient (CC) between ISMR and the 850 hPa seasonal mean (June to September) zonal wind, meridional wind and total wind respectively for 30 years (1961–1990). Correlation coefficient for significance of 95% and 99% are 0.31 and 0.45 respectively according to student's t test. Figure 3.4 (a) shows highly significant positive correlation between the zonal westerlies of the Arabian Sea and ISMR. The ISMR is also correlated with south Indian Ocean easterlies and with easterlies north of 20°N over Indian subcontinent. Over Pacific, the zonal wind has moderately strong negative correlation with ISMR.

Correlation between ISMR and meridional wind shows that the cross equatorial flow along the East African coast has strong positive correlation with ISMR. The southerlies associated with monsoon trough are stronger in good monsoon years whereas the cross–equatorial flow in the west Pacific east of Australia is stronger during bad monsoon years. The strong correlation between total wind and ISMR in the area from Mascarene High to Indian subcontinent shows the significant role of Low Level Jetstream in Indian monsoon.

3.3 Interannual Variability of LLJ

During the 30 year period (1961–1990) Indian Summer Monsoon Rainfall showed large interannual variability. It is interesting to see how the LLJ behaved in the composites of 5 DRY and 5 WET monsoons over this period. Fig-

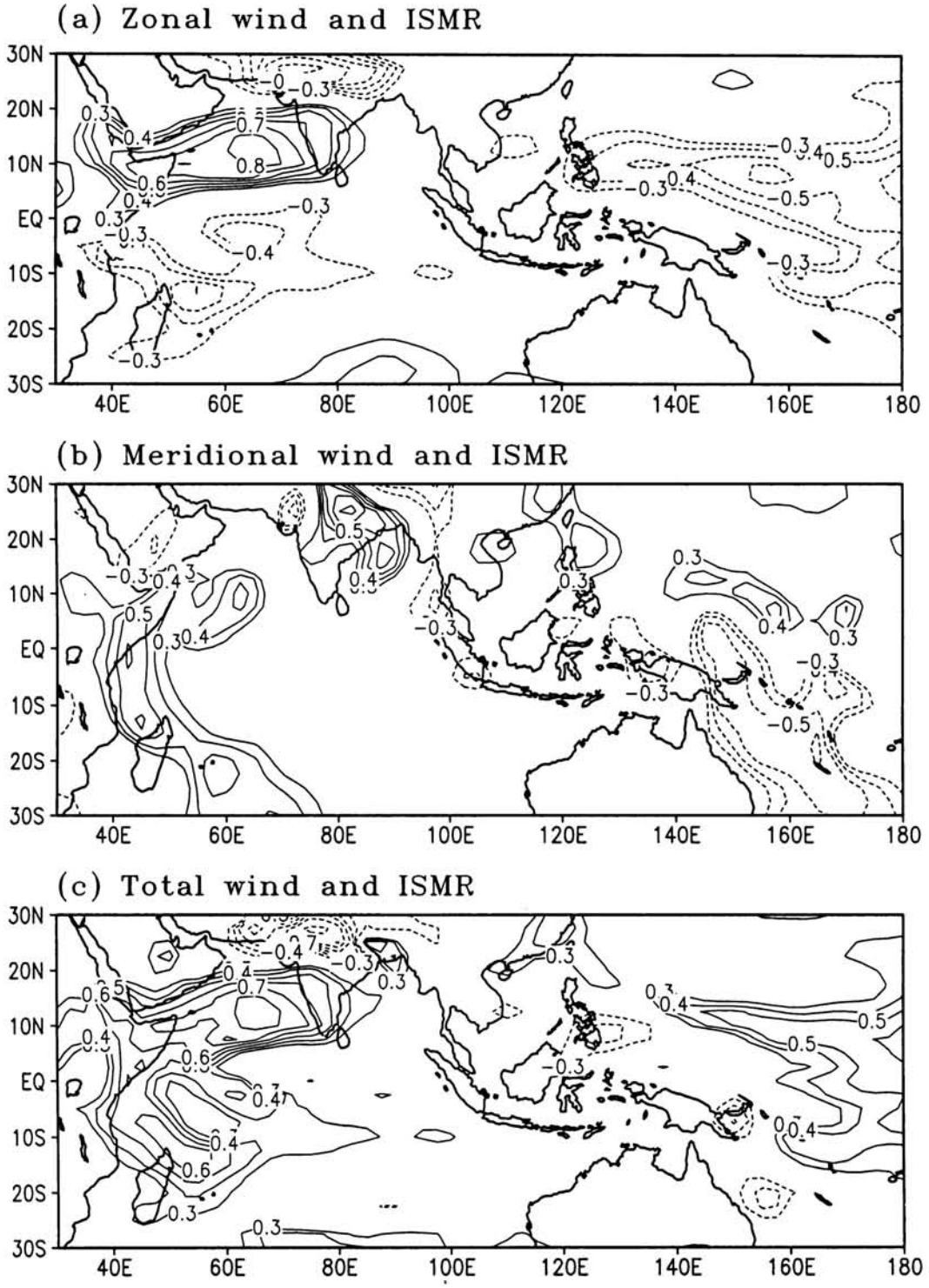

Figure 3.4: Linear correlation coefficients between June to September of 1961-1990 Indian Summer Monsoon Rainfall (*Parthasarathy et al.*, 1994) and mean (a) zonal wind, (b) meridional wind, (c) total wind at 850 hPa. Negative values are shown by dashed line.

ure 3.5 (a) gives the June to September mean values of 850 hPa vector wind and the isotachs of wind speed for the DRY composite years and Figure 3.5 (b) the same for the WET composite years. The LLJ wind over the western Arabian Sea and the cross–equatorial flow are stronger in WET composites than in the DRY. In DRY composite the maximum wind speed is around 14 msms^{-1}, but in WET composite it is upto 16 ms^{-1}. DRY composite flow through Indian subcontinent is generally weak.

Halpern and Woiceshyn (2001) studied the interannual variations of the Somali Jet in the Arabian Sea during 1988–99 linked with El Niño and La Niña episodes using Special Sensor Microwave Imager (SSM/I) wind data. According to them, the monthly mean strength of the Somali Jet is 0.4 ms^{-1} weaker during El Niño episodes than during La Niña intervals. They also reported that the monthly mean intensity of the Somali Jet is above (below) normal, there was an excess (deficit) of rainfall along the Indian west coast. They used surface wind for the study and considered only the rainfall of west coast of India.

Figure 3.6 shows the zonal velocity for (a) DRY composite, (b)WET composites and (c) for DRY minus WET. In the case of WET composite, westerlies are seen west of 130°E and easterlies observed to its east. On the other hand during DRY composite years the westerly regime extends up to 170°E. The axis of the westerlies slopes to lower latitudes from longitude 120°E to 170°E. This is important in relation to genesis of tropical cyclone described in section 3.4.

Over the Arabian Sea, westerlies are stronger by 2 ms^{-1} during WET composites than the DRY composite years (see Figure 3.6 (c)). But over the Bay of Bengal, there is hardly any difference between DRY and WET composite. The protrusion of westerlies into the Pacific Ocean in DRY years is well brought out in Figure 3.6 (c). *Webster et al.* (1998); *Rajan et al.* (1999) observed that in weak (DRY) monsoon years westerlies prevail over Tropical Pacific ocean and east-

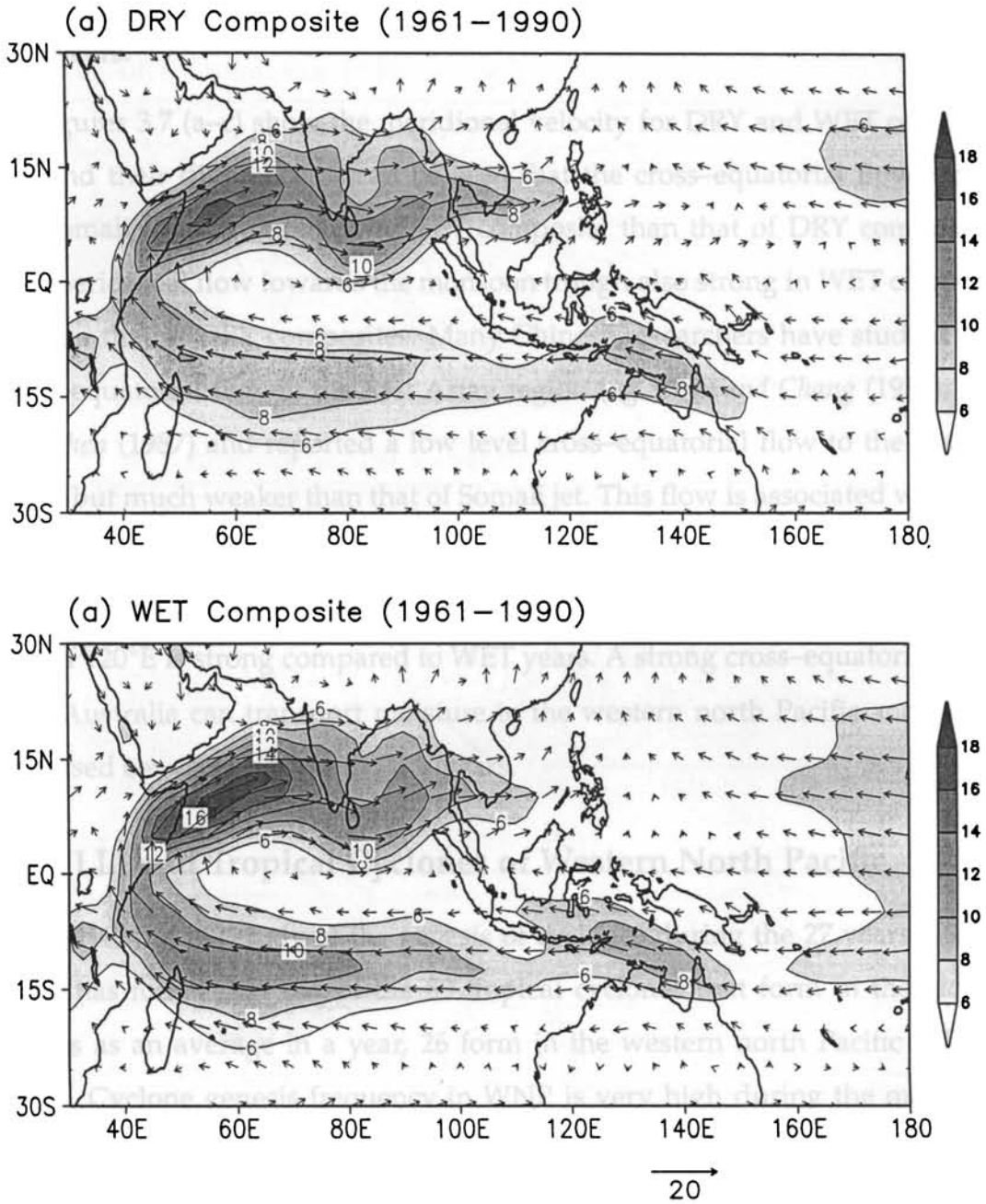

Figure 3.5: Wind vectors and isotachs in ms^{-1} of wind speed at 850 hPa for the composites of (a) five DRY monsoons and (b) five WET monsoons. Averaging is done for the period June to September.

erlies prevail during strong (WET) monsoon years. They also pointed out that over the Pacific ocean trades are strong during WET years and weak during DRY years.

Figures 3.7 (a–c) show the meridional velocity for DRY and WET composites and their difference. It can be seen that the cross–equatorial flow along the Somali coast is stronger in WET composite than that of DRY composite. The meridional flow towards the monsoon trough also strong in WET composite than that of DRY composites. Many Chinese researchers have studied the cross–equatorial flow in the East Asian region (eg. *Chen and Chang* (1980); *Tao and Chen* (1987) and reported a low level cross–equatorial flow to the east of 100°E but much weaker than that of Somali jet. This flow is associated with the circulations around a large anticyclone located near Australia. From the Figure 3.7 (c) it can be seen that in DRY composite years the cross equatorial flow east of 120°E is strong compared to WET years. A strong cross–equatorial flow near Australia can transport moisture to the western north Pacific and cause increased convection there in DRY years.

3.4 LLJ and Tropical Cyclones of Western North Pacific

Gray (1985) in his study of the genesis of cyclones during the 27 years (1958–1984) has found that out of the 80 tropical cyclones that form in the global oceans as an average in a year, 26 form in the western north Pacific (WNP) ocean. Cyclone genesis frequency in WNP is very high during the monsoon season, June to September with about 60% out of 26 having their genesis in that season. In a study on the genesis of cyclones of WNP using data of the period 1960 to 1990, *Lander* (1994) found that in years of low (high) Southern Oscillation Index the mean location of cyclone genesis in WNP is east (west) of the mean location.

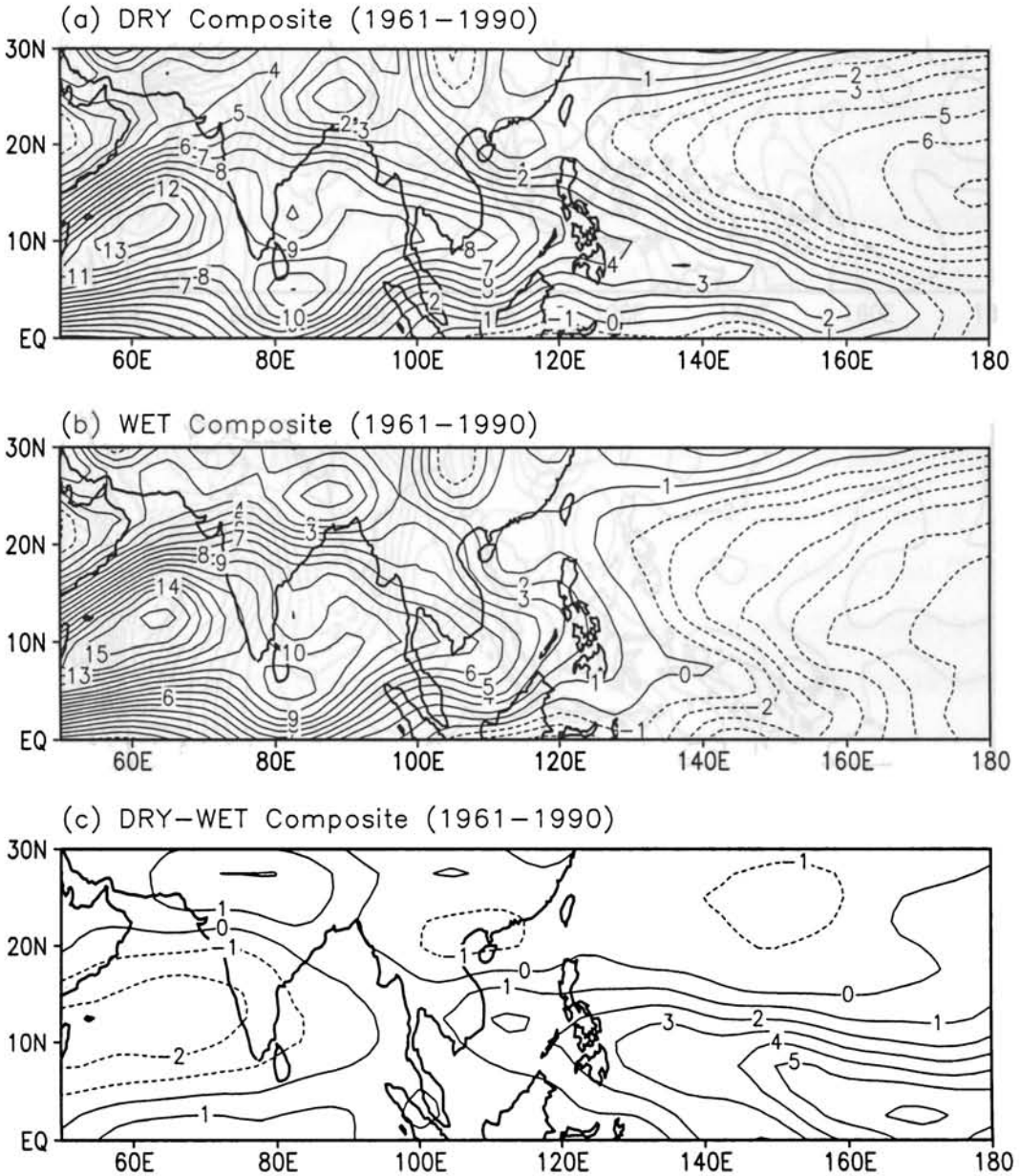

Figure 3.6: (a) Composite of zonal component of wind at 850 hPa for DRY monsoons, (b) for WET monsoons and (c) the difference between DRY and WET.

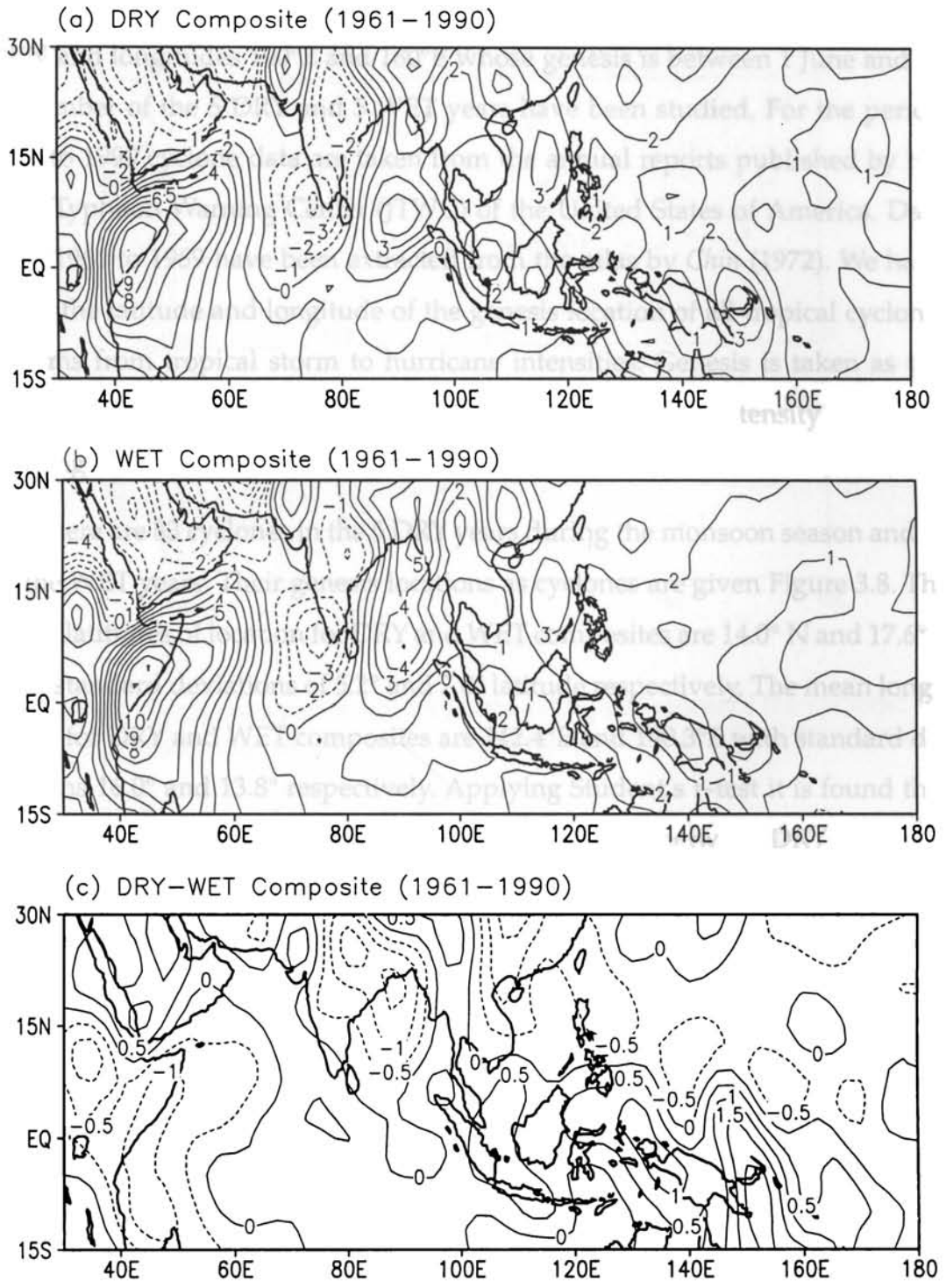

Figure 3.7: (a) Composite of meridional component of wind at 850 hPa for DRY monsoons, (b) for WET monsoons and (c) the difference between DRY and WET.

Tropical cyclones that formed over WNP bounded by latitudes of 0° and 50°N and longitudes 100°E and 180°E whose genesis is between 1 June and 30 September of the 5 DRY and 5 WET years have been studied. For the period 1970 to 1990 cyclone data are taken from the annual reports published by the Joint Typhoon Warning Center (JTWC) of the United States of America. Data from 1961 to 1969 have been extracted from the atlas by *Chin* (1972). We have taken the latitude and longitude of the genesis location of all tropical cyclonic systems from tropical storm to hurricane intensities. Genesis is taken as the spatial location where the system attained tropical cyclone intensity in the beginning.

There are 83 cyclones in the 5 DRY years during the monsoon season and 65 in the WET years. Their genesis locations as cyclones are given Figure 3.8. The mean latitudes of location for DRY and WET composites are 14.0° N and 17.6°N with standard deviations of 5.2° and 7.0° latitude respectively. The mean longitudes for DRY and WET composites are 142.4°E and 140.3°E with standard deviations 16.0° and 13.8° respectively. Applying Student's t–test it is found that the difference in the mean latitudes of cyclone genesis between DRY and WET composites is statistically significant at 95% level. The difference in the mean longitude of cyclogenesis between DRY and WET composites is not statistically significant.

In Dry composite of 850 hPa zonal wind (Figure 3.6 (a)) westerlies extend as a low latitude LLJ axis even up to 170°E longitude. Most of tropical cyclones that form in the WNP originate somewhere along the axis of the low–level monsoon trough (*Lander,* 1994). One of the factors favourable for the cyclogenesis is the cyclonic vorticity in a deep layer of the atmosphere from the sea surface. Figures 3.9 (a–d) give the vorticity at 850 hPa and 600 hPa for the DRY and WET composites. Large positive vorticity at 850 hPa level can be seen south of

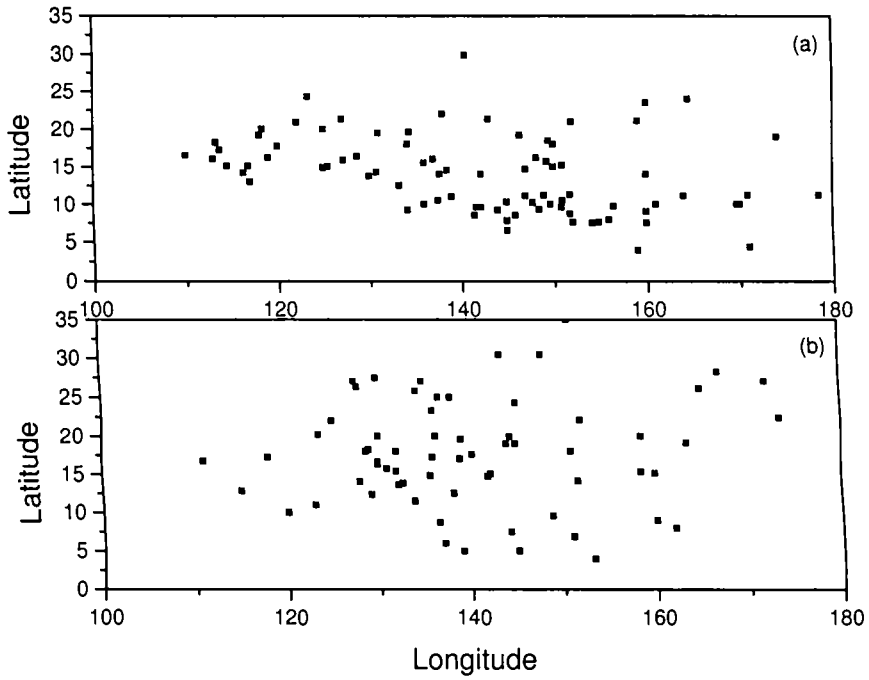

Figure 3.8: Composite genesis of locations as tropical storm of the cyclonic systems of intensity tropical storms and higher in (a) DRY and (b) WET monsoons

20°N for the DRY composite (see Figure 3.9 (a)). At 600 hPa level also cyclonic vorticity covers the area south of 20°N. Thus a deep layer of cyclonic vorticity extending from the surface upwards to the 600 hPa level present in DRY years, south of latitude 20°N is one of the reasons for cyclone genesis in low latitudes in DRY composites. In WET years the 850 hPa vorticity is comparable with DRY composite, whereas at the 600 hPa level the vorticity is very weak.

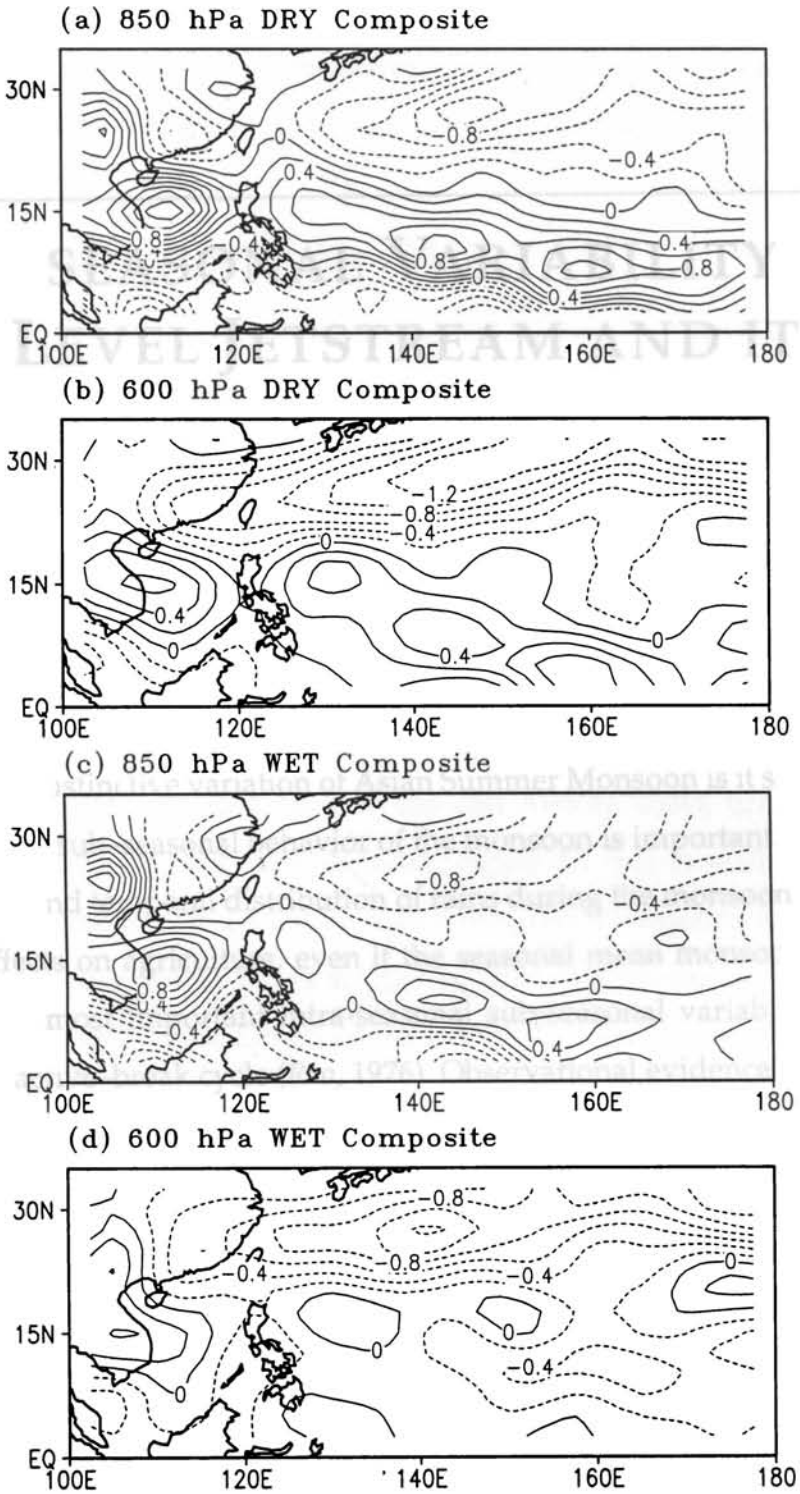

Figure 3.9: Mean relative vorticity (cyclonic in continuous lines anticyclonic broken lines multiplied by 10^5) (a) at 850 hPa for DRY composite (b) at 600 hPa for DRY composite (c) at 850 hPa for WET composite (d) at 600 hPa for WET composite

CHAPTER 4

INTRASEASONAL VARIABILITY OF LOW LEVEL JETSTREAM AND ITS RELATION WITH CONVECTIVE HEATING

The most distinctive variation of Asian Summer Monsoon is it sub–seasonal variation. The sub–seasonal behavior of the monsoon is important because uneven spatial and temporal distribution of rains during the monsoon season has adverse effects on agriculture, even if the seasonal mean monsoon rainfall is normal. The most important intra-seasonal sub-seasonal variability of monsoon is the active–break cycle (*Rao,* 1976). Observational evidence that years of below normal rainfall over central India is characterised by prolonged breaks in Indian monsoon rainfall and years of near normal or above normal rainfall tend to be characterised by fewer breaks of shorter duration *Krishnamurti and Bhalme* (1976); *Sikka and Gadgil* (1980); *Gadgil and Asha* (1992). Detailed examination of the daily NCEP/NCAR reanalysis 850 hPa wind and NOAA OLR data over the Indian sub-continent and the adjacent regions of twelve monsoons (1979–1990) provided clear insight into the characteristic features of the

LLJ on the intra-seasonal time scale. Following sections give details about LLJ and areas of active monsoon convection during composite onset phases and composites of spells of active and break monsoons of the period 1979-1990.

4.1 Intraseasonal Oscillation of LLJ

The date of Monsoon Onset over Kerala (MOK) is taken as 0 and the days before and after onset are taken as negative $(-)$ and positive $(+)$ respectively. The composite pentad 850 hPa wind and OLR data are examined separately for onset, active and break monsoon conditions. The 12-year composite of the onset pentad corresponding to -2 to $+2$ days of MOK of OLR (see Figure 4.1 (a)) shows a large area of low OLR or high convection in the low latitudes of north Indian Ocean. 850 hPa wind composite of the corresponding pentad shows a strong LLJ beginning from the Mascarene High area of south Indian Ocean, crossing the equator passing close to the east African coast, turning east off Somalia coast and moving towards India (Figure 4.1 (b)). A well–marked LLJ maximum is present over the Indian region between the equator and 10°N. The onset phase is characterised by a single LLJ core with maximum wind speeds over south Asia and Indian Ocean. Monsoon westerlies are generally weak over central India.

Figures 4.2 (a–b) give the composite mean of the OLR and the 850 hPa wind in the study area for active monsoon spells of June to August as defined in Chapter–2 of this thesis. The dates on which active monsoon conditions prevailed are given in Table 2.2. The areas of maximum wind (LLJ) and the maximum convection (lowest OLR) are in the latitude belt 10°N–20°N. The composite LLJ has only one axis and LLJ shows no splitting. A convection maximum is seen over Bay of Bengal.

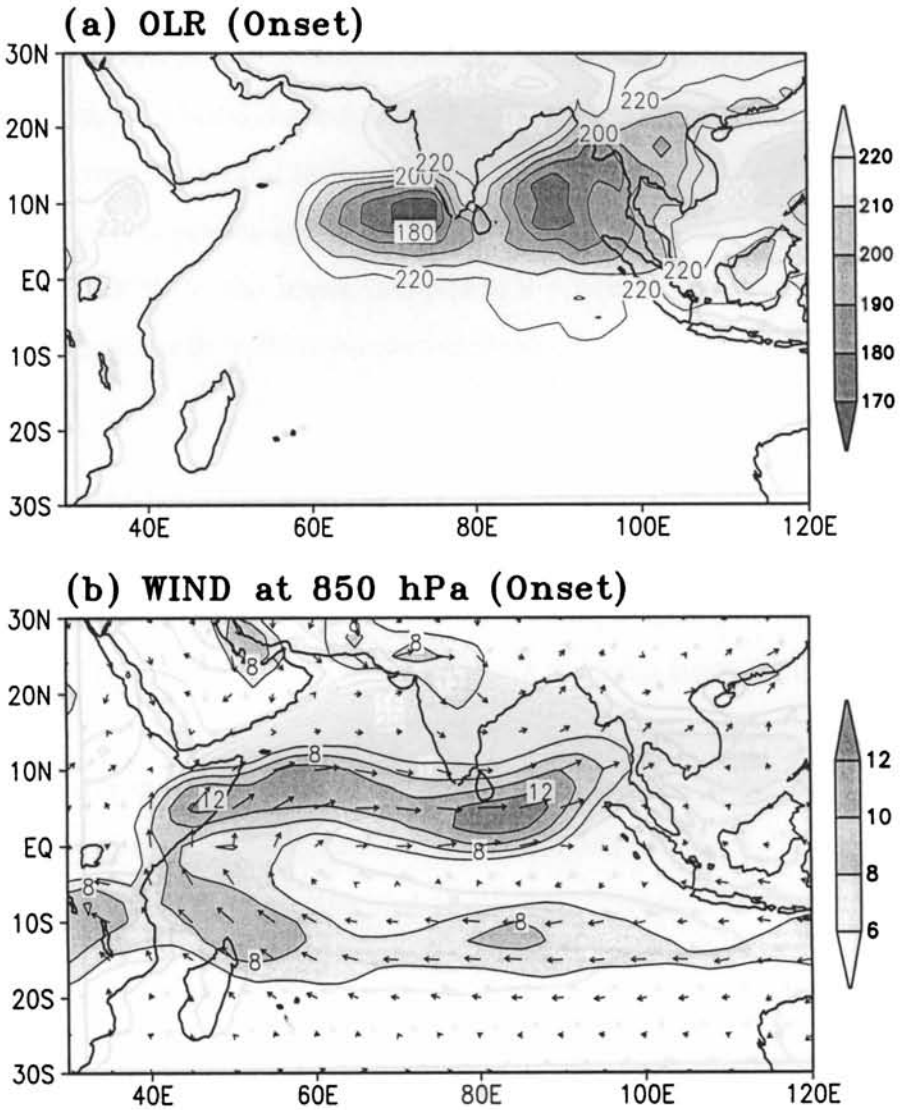

Figure 4.1: Composites for the onset pentad (−2 to +2 days around day of monsoon onset over Kerala) of 12 years 1979–1990 in (a) OLR (b) 850 hPa wind.

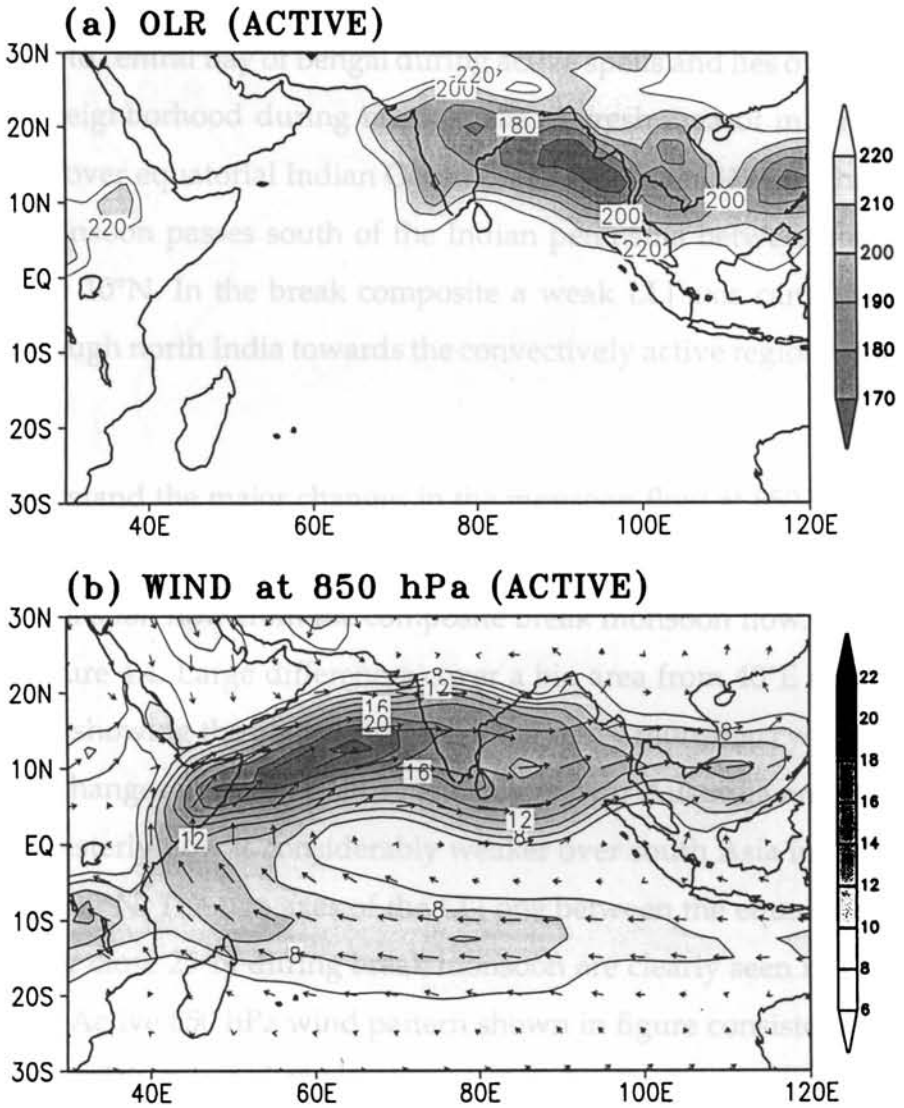

Figure 4.2: Composites for active monsoon days in June to August of 1979–1990. (a) OLR and (b) 850 hPa wind.

Composite pentad analysis of OLR and wind at 850 hPa for break monsoon spells during July and August are presented in Figures 4.3 (a–b). Details of the break monsoon spells of July and August of 1979-1990 are listed in Table 2.2. The OLR minimum area located at low latitudes at the time of MOK has moved northwards to central Bay of Bengal during active spells and lies over north east India and neighborhood during break spells. A fresh area of minimum OLR has formed over equatorial Indian Ocean (*Sikka and Gadgil*, 1980). The LLJ axis of break monsoon passes south of the Indian peninsula between the equator and latitude 10°N. In the break composite a weak LLJ axis can also be seen passing through north India towards the convectively active region over north–east India.

To understand the major changes in the monsoon flow at 850 hPa between the composites of active and break monsoon spells, we subtracted the composite active monsoon flow from the composite break monsoon flow. The result is given in Figure 4.4. Large differences cover a big area from 40°E to 170°E and 10°S to 35°N showing the planetary scale of the active monsoon cycle. There are some large changes in the southern hemisphere over Australia and to its east. Monsoon westerly flow is considerably weaker over south Asia in the latitude belt 10°N to 20°N. The two axes of the LLJ one between the equator and 10°N and the other close 25°N during break monsoon are clearly seen in Figure 4.4. Break *minus* Active 850 hPa wind pattern shown in figure consistent with pattern shown by *Webster et al.* (1998). They pointed out a strong cross equatorial flow in the western Indian Ocean during active phase. *Goswami and Ajayamohan* (2001) have shown the large zonal scale circulation changes associated with active (break) phases of Indian monsoon extending from about 50°E to 120°E from the composite active (break) phases for 20 years (1978-1992).

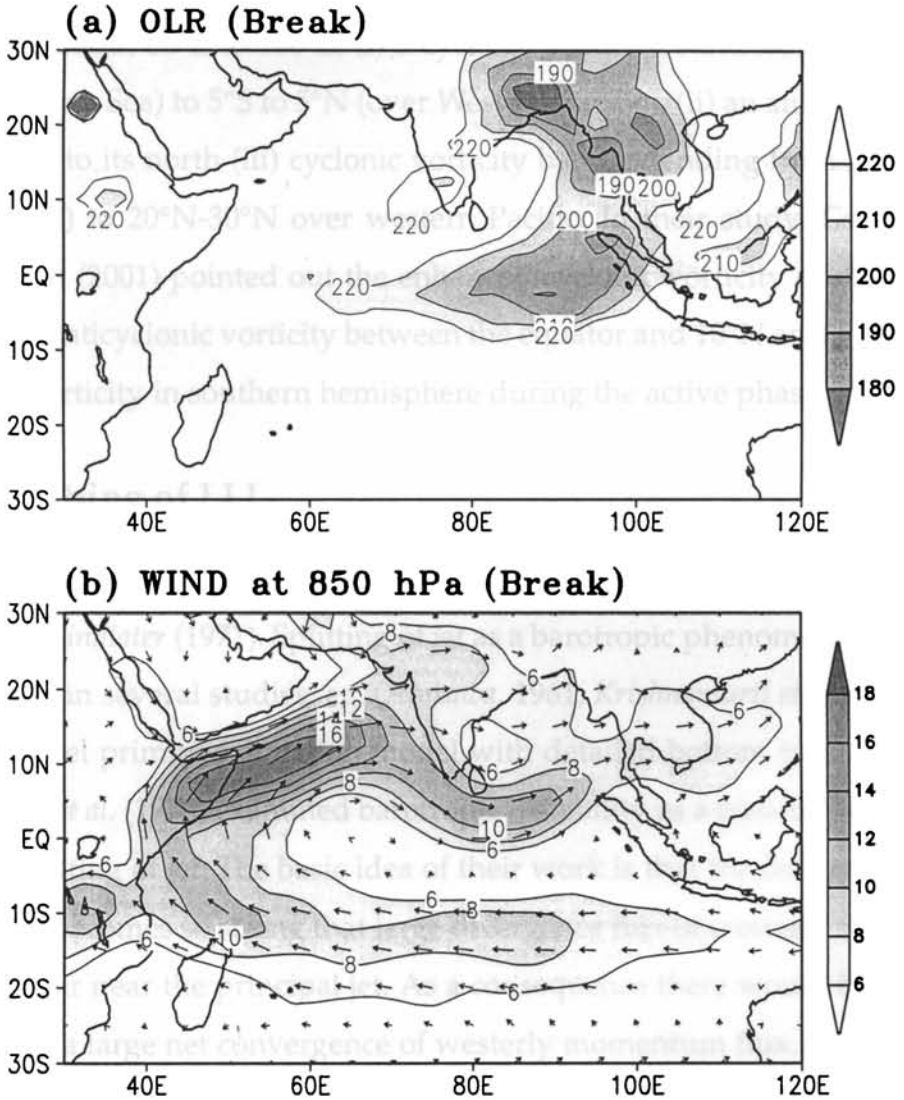

Figure 4.3: Composites for break monsoon days in July and August of 1979–1990. (a) OLR and (b) 850 hPa wind. .

The vorticity field corresponding to the horizontal wind field (Figure 4.4 (a)) is given in Figure 4.4 (b). The two strong convective areas during breaks, one to the south of India and the other over north–east India and neighborhood, are characterised by strong cyclonic vorticity at 850 hPa. In break monsoon spells, vorticity is arranged in three latitudinal bands each band covering a big longitude zone about 60°E to 160°E; (i) a cyclonic vorticity band from 5°S to 10°N (over Arabian Sea) to 5°S to 5°N (over Western Pacific), (ii) an anticyclonic vorticity band to its north (iii) cyclonic vorticity band extending from 25°N-35°N (over India) to 20°N-30°N over western Pacific. In their study, *Goswami and Ajayamohan* (2001) pointed out the enhanced cyclonic vorticity north of 10°N, enhanced anticyclonic vorticity between the equator and 10°N and a weakened cyclonic vorticity in southern hemisphere during the active phase.

4.2 Splitting of LLJ

The splitting of Low Level Jetstream in to two branches over Arabian Sea is shown by *Findlater* (1971). Splitting of jet as a barotropic phenomenon has been mentioned in several studies, eg. (*Arakawa*, 1961; *Krishnamurti et al.*, 1976). Using one level primitive equation model with detailed bottom topography *Krishnamurti et al.* (1976) examined barotropic instability as a possible mechanism for the splitting of jet. The basic idea of their work is that the flow near the Somali coast becomes so strong that large divergence flux of westerly momentum would occur near the principal jet. As a consequence there would be other regions with a large net convergence of westerly momentum flux. The parent jet would weaken as consequence of the divergence of flux and a new jet would form somewhere near in the vicinity due to the convergence of momentum flux. A split jet phenomenon may be observed when such a mechanism is operating, according to them.

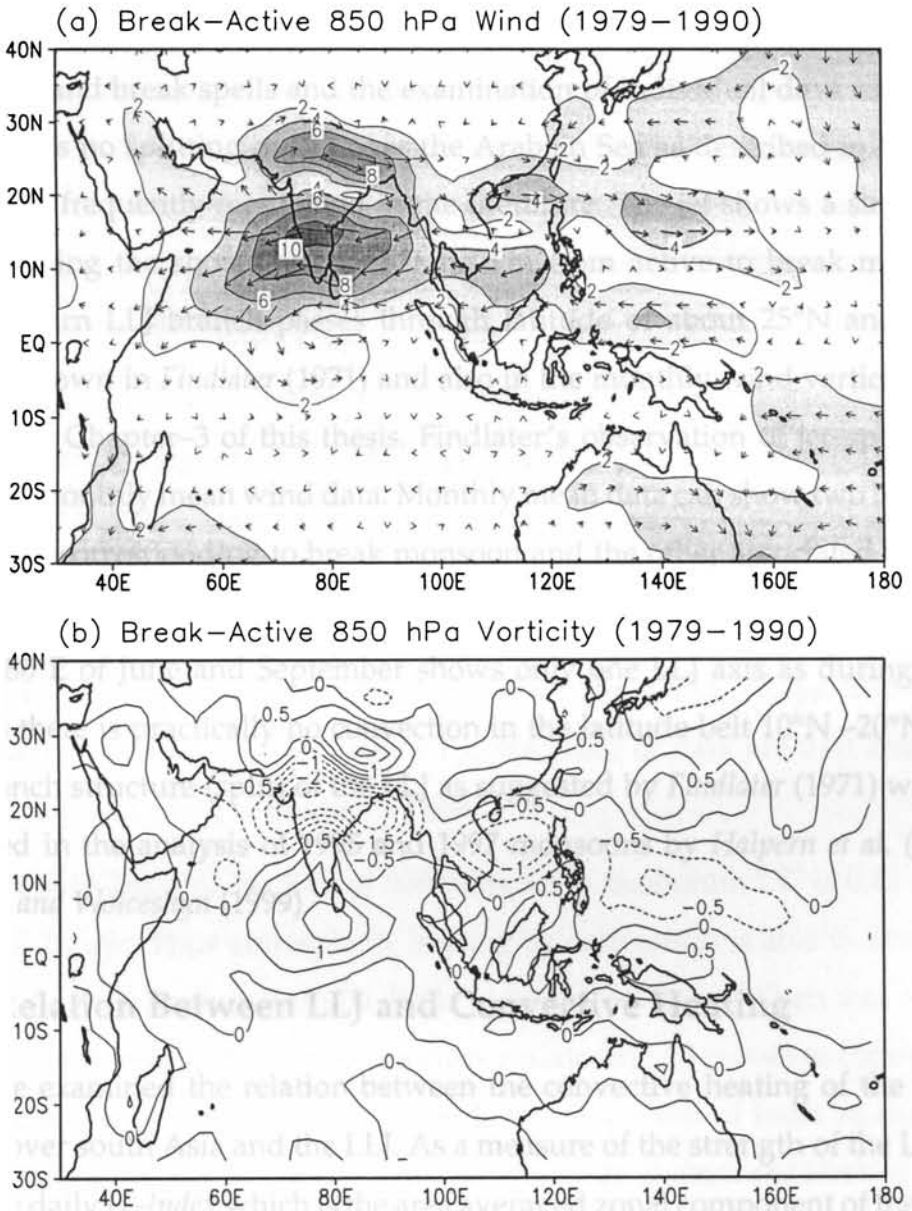

Figure 4.4: (a) Difference between the 850 hPa wind composites, Break Monsoon (Figure 4.3) *minus* Active Monsoon (Figure 4.2). (b) Vorticity of the difference wind field, positive vorticity (cyclonic in northern hemisphere) by continuous lines and negative vorticity by broken lines multiplied by 10^5 at intervals of 0.5 s^{-1}.

It is interesting to note that the present study based on daily NCEP/NCAR reanalysis data did not support the splitting of LLJ over the Arabian Sea as suggested by *Findlater* (1971). Study of the 12 year composites of monsoon onset, active and break spells and the examination of individual days confirmed that there is no splitting of LLJ over the Arabian Sea as described in *Findlater* (1971) and frequently mentioned in the literature. The jet shows a single axis except during the short period of transition from active to break monsoon. The northern LLJ branch passes through latitude of about 25°N and not at 17°N as shown in *Findlater* (1971) and also in the monthly wind vertical cross-sections of Chapter–3 of this thesis. Findlater's observation of jet–splitting is based on monthly mean wind data. Monthly mean data can show two branches of LLJ one corresponding to break monsoon and the other associated with active monsoon . The monthly mean vertical sections of zonal wind through longitude 80°E of June and September shows only one LLJ axis as during these months there is practically no convection in the latitude belt 10°N –20°N. The two branch structure (split) of the LLJ as suggested by *Findlater* (1971) was not observed in the analysis of 1995 and 1997 monsoons by *Halpern et al.* (1998); *Halpern and Woiceshyn* (1999)

4.3 Relation Between LLJ and Convective Heating

We have examined the relation between the convective heating of the atmosphere over south Asia and the LLJ. As a measure of the strength of the LLJ we used the daily *U–Index* which is the area averaged zonal component of the wind at 850 hPa in (a) the peninsular box bounded by 10°N and 20°N and 70°E and 80°E and (b) the Bay of Bengal box bounded between 10°N and 20°N and 80°E and 100°E as averages of 00z and 12z observations. For the strength of the convective heating we have used the daily *OLR–Index* which is the area averaged OLR in the box 10°N–20°N and 80°E–100°E (the Bay of Bengal box). The *OLR–*

Index chosen is representative of the large scale convection in the monsoon. According to *Sikka and Gadgil* (1980) a Maximum Cloud Zone (MCZ) of deep convective clouds form in the low latitude regions south of India and moves north to the Himalayas through Bay of Bengal and this process is repeated with a periodicity of 30–50 days during the monsoon season June to September. It is observed that LLJ is strong through peninsular India when MCZ passes through the Bay of Bengal (active monsoon). LLJ then reaches strength of 40 to 60 knots at 850 hPa (*Joseph and Raman,* 1966).

The linear correlation coefficient (CC) between the daily *OLR–Index* and the daily *U–Index* for lags of -5 days to $+5$ days is given in Figure 4.5. CC increases with lag for both the boxes of wind and reaches a maximum and then decreases. Maximum CC is -0.51 between the daily *OLR–Index* and the daily *U–Index* of the peninsular box (for 744 pairs of the indices during July and August months of 1979 to 1990) for *OLR–Index* leading *U–Index* by 2 and 3 days. The CC for significance at levels 99% and 99.9% for 744 pairs of data are 0.08 and 0.115 respectively according to Student's t test.

For the *U–Index* of the Bay of Bengal box the maximum CC is 0.41 at lags of 1 and 2 days. Thus atmospheric heating by convection is able to accelerate the LLJ flow through peninsular India in about 2-3 days. When this heating between 10°N and 20°N is weak the cross equatorial LLJ moves to central Arabian Sea and then moves southeastwards to areas south of India as shown in the modelling studies by *Hoskins and Rodwell* (1995); *Rodwell and Hoskins* (1995). It was seen in section 1 of this chapter that in break monsoon spells, when the active monsoon convection has moved to northeast India from the Bay of Bengal, there is a branch of LLJ through north India (about 25°N) carrying moisture to this area from the Indian Ocean. Thus we may infer that the MCZ of *Sikka and Gadgil* (1980) is closely associated with the cross–equatorial LLJ (*Findlater,*

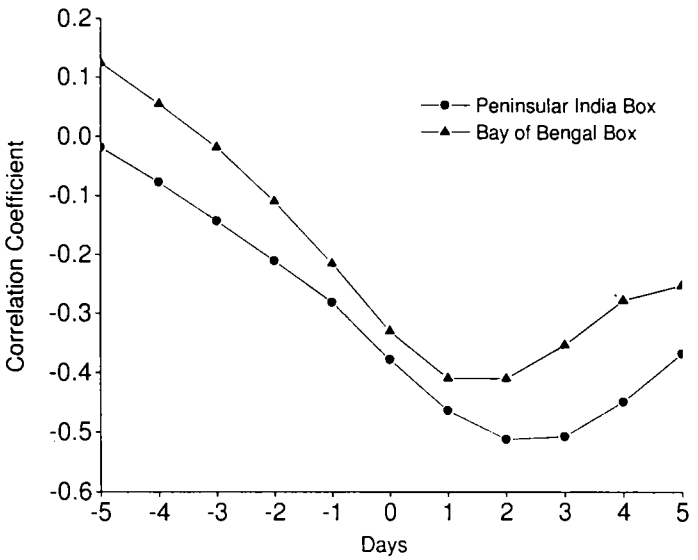

Figure 4.5: Linear correlation coefficient (CC) between the daily *OLR–Index* for the Bay of Bengal (area 10°N-20°N and 80°E-100°E) and the daily *U–Index* (a) for Bay of Bengal (area same as for OLR) and (b) for peninsular India (area 10°N-20°N and 70°E-80°E) for lags of -5 days to $+5$ days. Line (a) is with triangles and line (b) is with dots.

1969b) over south Asia. While the LLJ crosses the equator in a geographically fixed and narrow longitude band, the latitude of the core of the LLJ over peninsular India moves from low latitudes to almost 25°N along with the northward movement of the MCZ in its 30–50 day cycles.

4.4 Case Study of ISO of LLJ in Monsoon 1979

Monsoon of 1979 had strong intra-seasonal oscillation and pronounced active–break cycles as studied by *Krishnamurti* (1985). Figure 4.6 (a) shows the Hovmoller diagram of the mean OLR between longitudes 80°E and 100°E from latitudes 10°S to 30°N of the period 1 June to 31 August 1979 smoothed by a 5 day moving average. After an active monsoon spell in the second half of June, convection in the 10°N–20°N belt weakens. By mid–July two zones of convec-

tion are found over 80°E–100°E zone, one around latitude 25°N and the other just south of the equator. A second active monsoon spell is observed during the first half of August when convection is again active in the 10°N–20°N latitude belt. This is followed by a long break monsoon spell (see Table 2.2) when the main areas of convection are just south of the equator and around 25°N.

Figure 4.6 (b) shows the Hovmoller diagram of the 850 hPa zonal wind (u) averaged over the longitudes 80°E to 100°E from latitudes 10°S to 30°N of the period 1 June to 31 August smoothed as in the case of the OLR by a 5 day moving average. The two active spells are seen as maxima of zonal wind in the 10°N–20°N region. These wind maxima are found to lag in time behind the OLR maxima by a few days in agreement with the findings of the previous section. The zone of maximum convection is on the cyclonic u–shear vorticity zone of the LLJ where the frictional convergence in the boundary layer produces upward motion to generate cumulonimbus cloud heating in the conditionally unstable tropical atmosphere. It is speculated that the dynamics (cyclonic vorticity and the consequent frictional convergence producing Ekman pumping of the moist boundary layer air) and the thermodynamics (the convective heating of the atmosphere and the consequent lowering of atmospheric pressure below) co–operate to increase convection and strengthen the LLJ, step by step. Since for continuity the whole LLJ has to strengthen, LLJ intensification has to lag behind the convection by a few days. This is a kind of instability in which a planetary scale system (LLJ) cooperates with the convection in the cloud cluster over the Bay of Bengal and both intensifies. This phenomenon is similar to the Conditional Instability of the Second Kind (CISK) in the case of a synoptic scale system like the tropical cyclone. In synoptic scale systems, since space scales are small, the increase in convèction and the corresponding increase in wind field take place in a few hours and not in a few days as in the case of the LLJ.

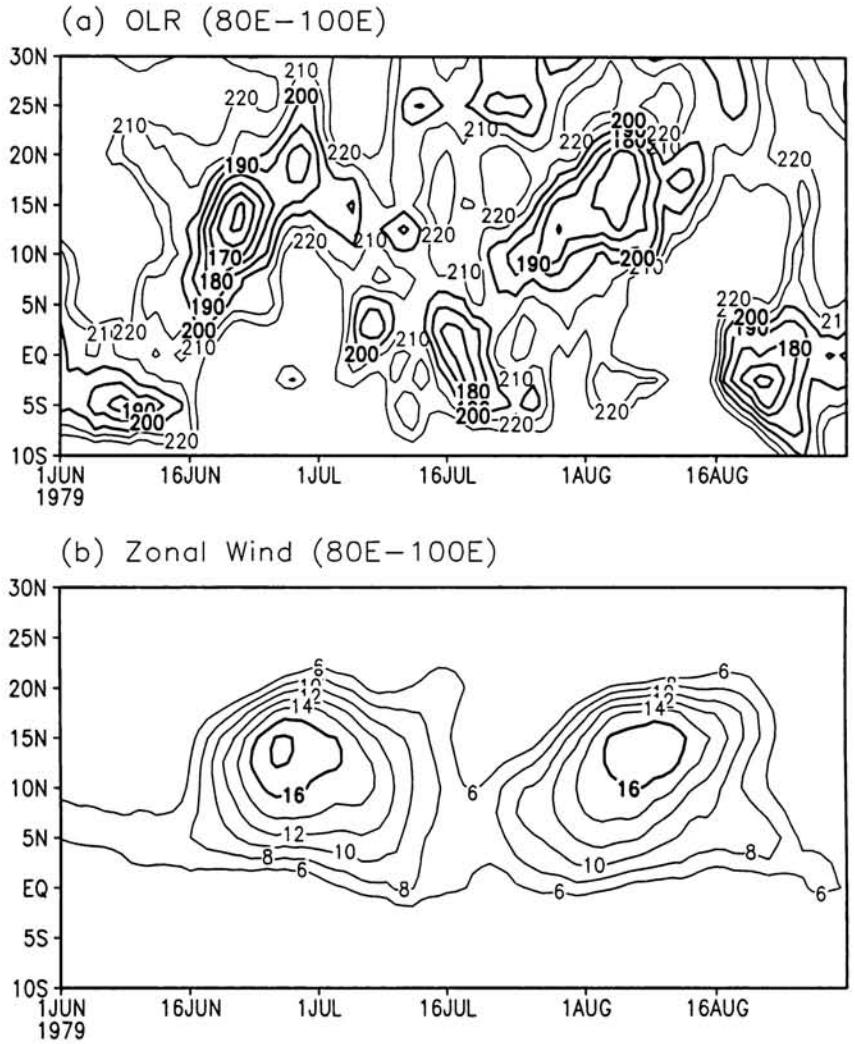

Figure 4.6: Hovmoller diagram showing evolution of (a) convection (OLR) and (b) 850 hPa zonal wind speed from 1 June to 31 August 1979. Averaging is done for the longitude band 80°E to 100°E and a five day moving average is applied as a smoother. OLR contours 220 Wm^{-2} and lower at intervals of 10 Wm^{-2} and wind speed contours more than 6 ms^{-1} at intervals of 2 ms^{-1}.

Figure 4.7 (a) shows the Hovmoller diagram of zonal wind (u) of 850 hPa averaged over the longitude band 62.5°E-67.5°E and smoothed by a five day moving average. Active monsoon spells are characterised by strong cores of u, but what is important is that whether it is active or break monsoon the strongest u is at one 15°N only. The intra–seasonal oscillation at this longitude (65°E) is the weakening and strengthening of the LLJ core without north–south movement. On the other hand a similar section through longitude 80°E (77.5°E-82.5°E) shows that after the active monsoon spell of the second half of June, LLJ appears as two axes, one moving to latitude 25°N and the other towards the equator (see Figure 4.7 (b)). The movement of the jet core towards 25°N is in response to the northward movement of the area of active convection. The other axis moves towards equator verifying the mechanism suggested by *Rodwell and Hoskins* (1995) that in the absence of heat sources in the 10°N–20°N latitude belt, LLJ moves south–eastwards from central Arabian Sea conserving its potential vorticity.

It is speculated that when this axis of LLJ reaches near the equator a zone of strong u–shear with cyclonic vorticity forms just south of the equator (as shown in Figure 4.8 (a)) that leads to frictional convergence in the boundary layer and the generation of an east–west band of convection there. It may be noted that Ekman pumping is very effective in low latitudes, more so in equatorial latitudes (*Holton*, 1992). This convective band will then strengthen the LLJ and a zone of strong cyclonic shear vorticity appears north of the equator that generates an east–west band of convection north of the equator which then moves north (Figure 4.8 (b)). In this process the area very close to the equator remains with very little convection as may be noticed in Figure 4.6 (a) around 16 June and 23 July.

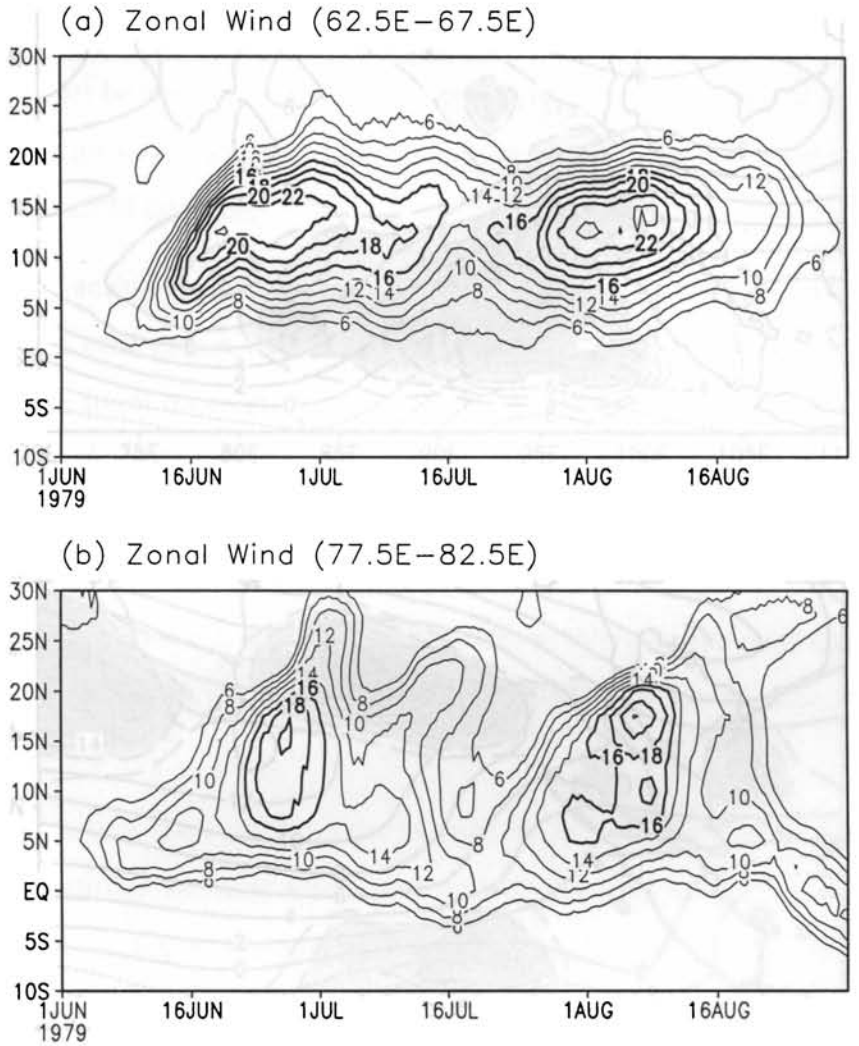

Figure 4.7: Hovmoller diagram showing evolution of 850 hPa zonal wind speed from 1 June to 31 August 1979. Averaging is done (a) for the longitude band 62.5°E to 67.5°E and (b) for the longitude band 77.5°E to 82.5°E and a five day moving average is applied as a smoother. Wind speed contours more than 6 ms^{-1} at intervals of 2 ms^{-1}.

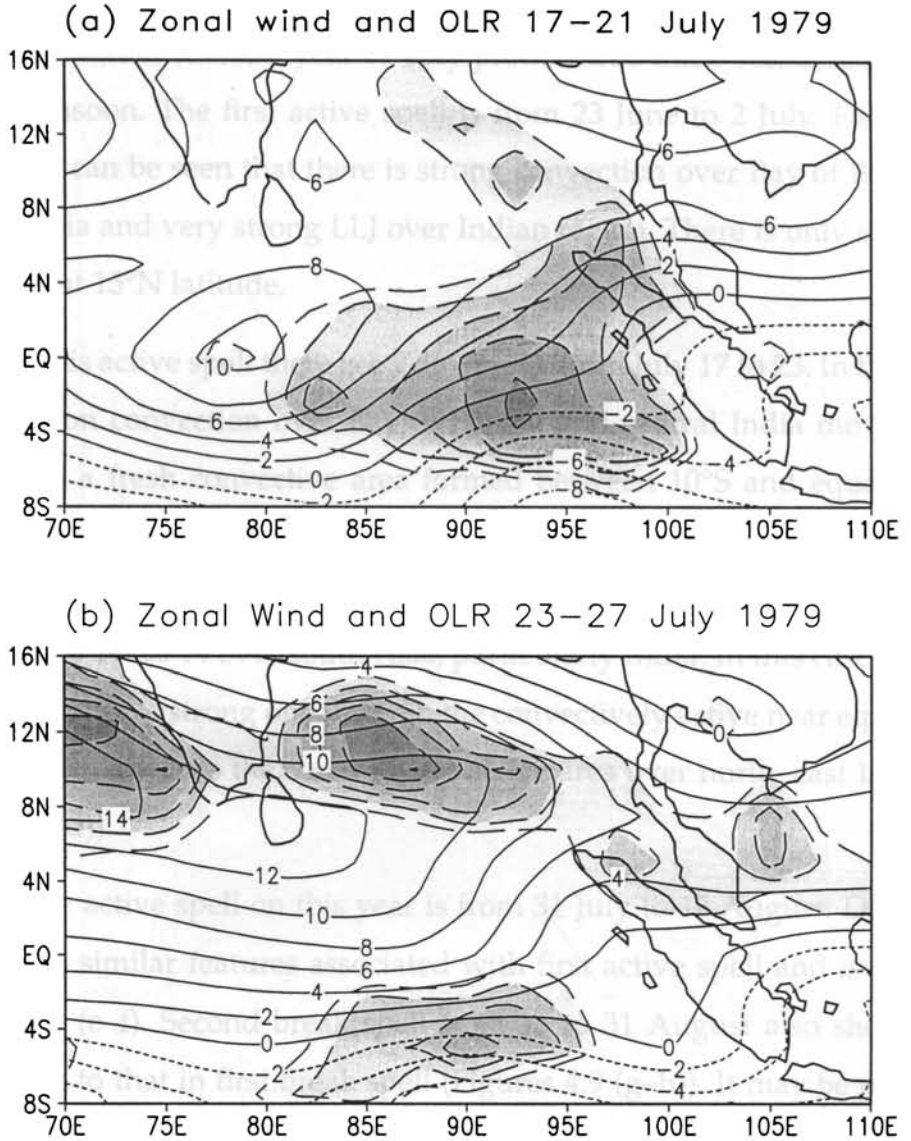

Figure 4.8: Five day averaged 850 hPa zonal wind (Westerly as continuous lines and easterly as dotted lines) and OLR (shaded area with broken line boundary) for the periods (a) 17 to 21 July 1979 and (b) 23 to 27 July 1979. Zonal wind at intervals of 2 ms^{-1} and OLR 200 Wm^{-2} and less at intervals of 10 Wm^{-2}.

Figure 4.9 (a–h) gives the mean OLR and 850hPa wind fields corresponding to the two active and break spells during June to August 1979. In this year the active and break spells are very long as may be seen from Table 2.2. As mentioned earlier it was a year of very pronounced intra–seasonal oscillation in the monsoon. The first active spell is from 23 June to 2 July. From Figure 4.9 (a–b) it can be seen that there is strong convection over Bay of Bengal and central India and very strong LLJ over Indian region. There is only one axis of LLJ at about 15°N latitude.

After this active spell there is a 7 day break from July 17 to 23. In this period the monsoon convection over Bay of Bengal and central India moves northwards and a fresh convective area formed between 10°S and equator. Thus there are two active areas of convection, one from the equator to latitude 10°S and the other around northeast India. There is very little convection in the latitude belt 10°N–20°N over south Asia, particularly India. In this case there can be two LLJ axes, a strong one through the convectively active near equator and a weaker one towards the convectively active area over north–east India (Figures 4.9 (c–d)).

Another active spell on this year is from 31 July to 12 August. During this period also similar features associated with first active spell and is shown in Figures 4.9 (e–f). Second break spell from 15 to 31 August also shows similar features to that in first break spell (Figures 4.9 (g–h)). It may be noted that the space scale of active–break phenomena covers practically the whole of the monsoon area of Asia.

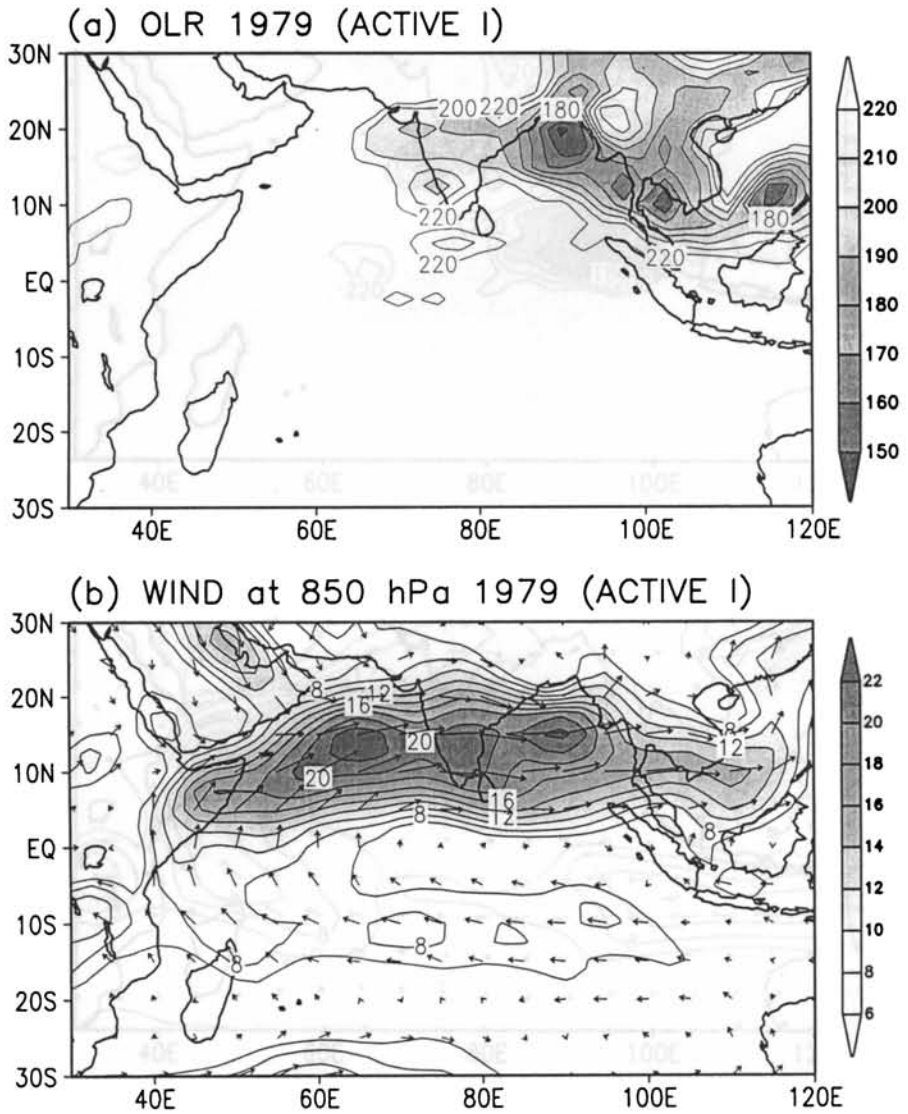

Figure 4.9: Average of (a) OLR and (b) 850 hPa zonal wind averaged for the first active monsoon spell of 1979 (23 June to 02 July).

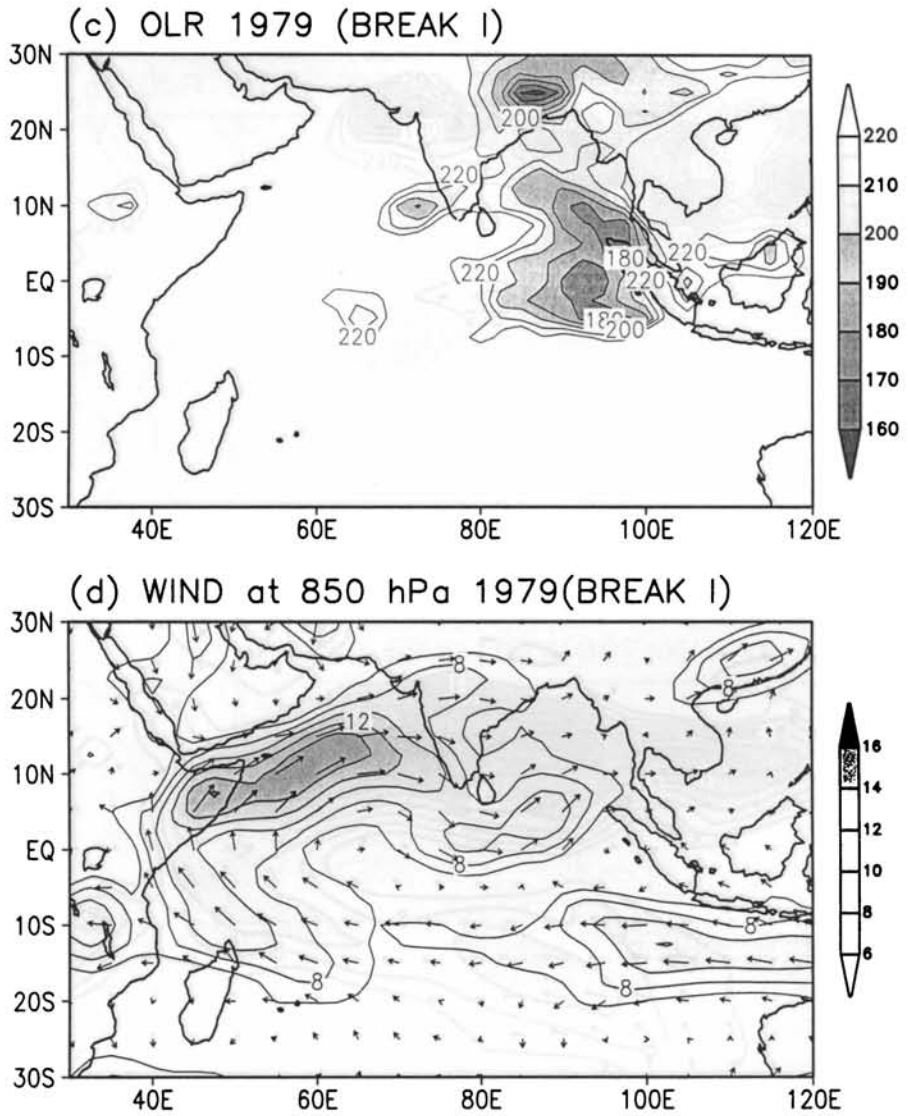

Figure 4.9: (contd) Average of (c) OLR and (d) 850 hPa zonal wind averaged for the first break monsoon spell of 1979 (17July to 23 July).

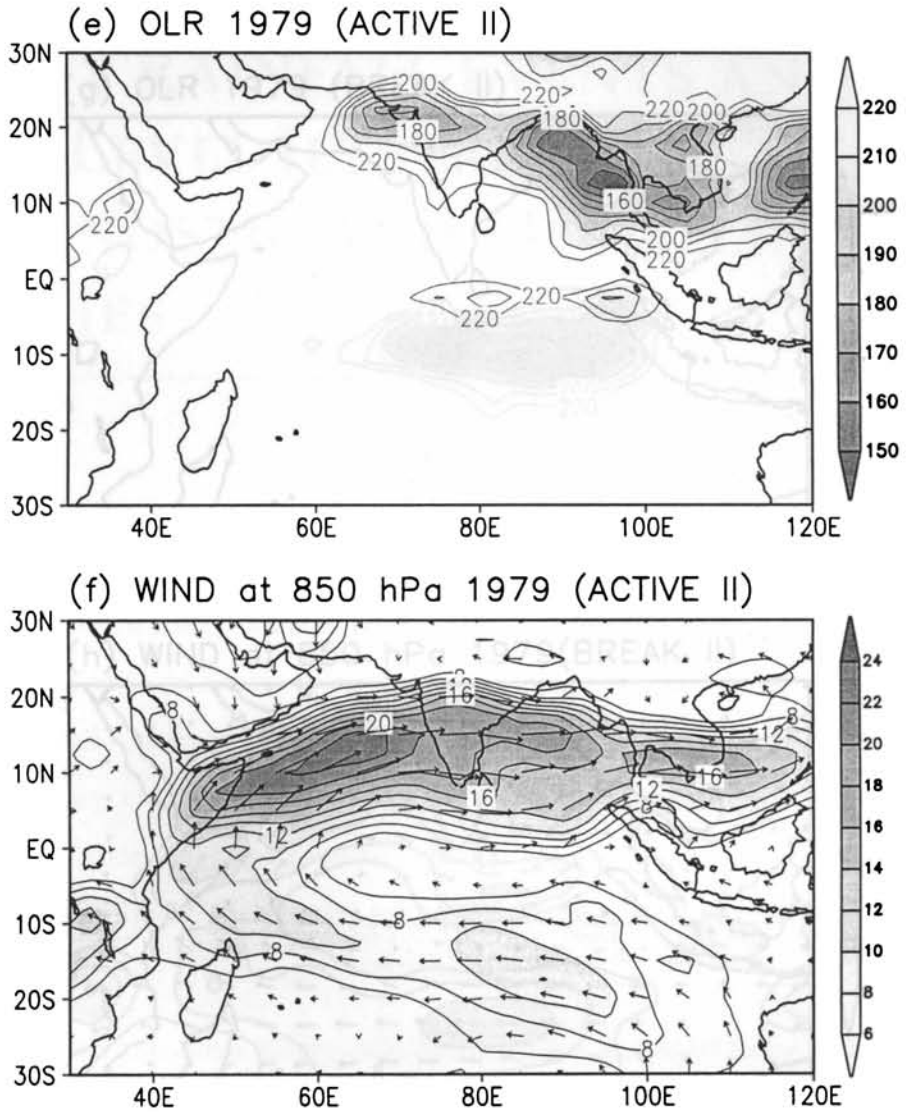

Figure 4.9: (contd) Average of (e) OLR and (f) 850 hPa zonal wind averaged for the second active monsoon spell of 1979 (31 July to 12 August).

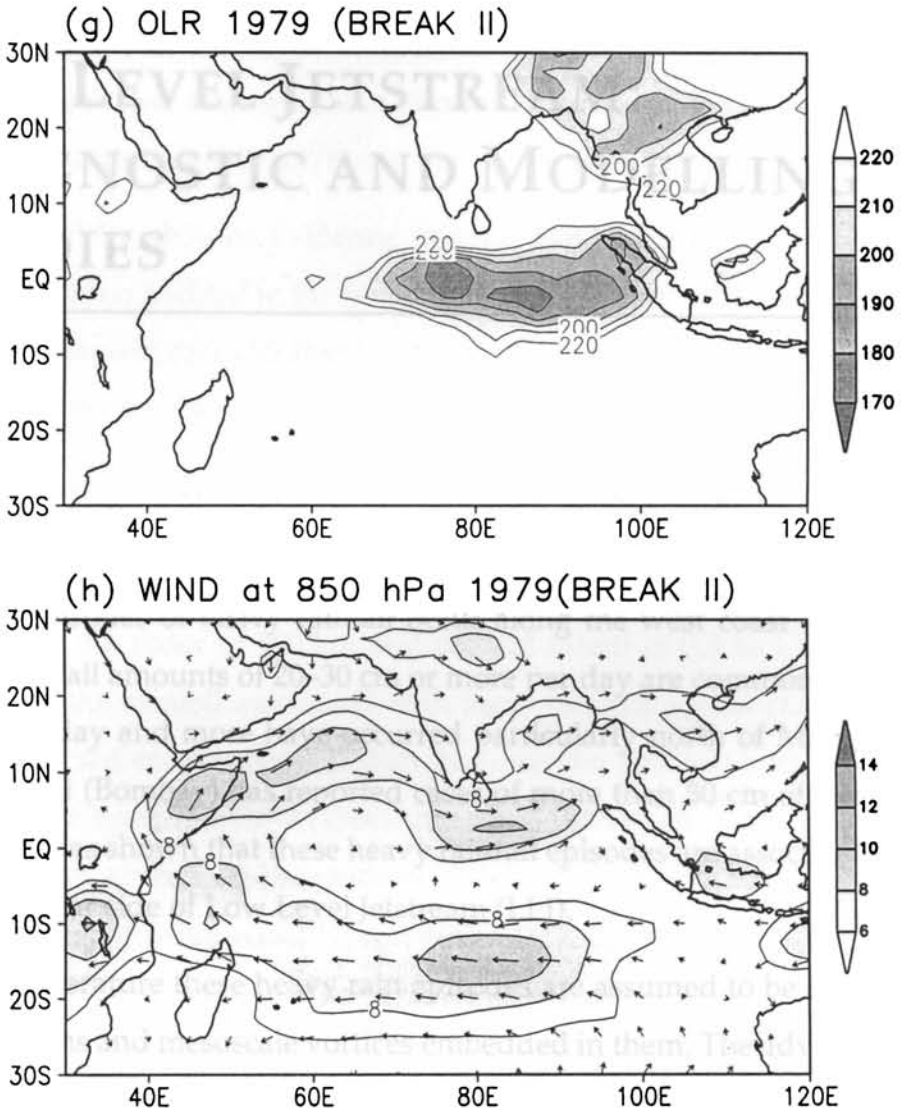

Figure 4.9: (contd) Average of (g) OLR and (h) 850 hPa zonal wind averaged for the second break monsoon spell of 1979 (15 August to 31 August).

CHAPTER 5

HEAVY RAINFALL EVENTS AND LOW LEVEL JETSTREAM: DIAGNOSTIC AND MODELLING STUDIES

During the monsoon season, particularly during the period mid June to mid August, episodes of heavy rainfall occur along the west coast of India (*Rao*, 1976). Rainfall amounts of 20–30 cm or more per day are common. Episodes of 40 cm per day and more have occurred particularly north of Mangalore (13° N). Mumbai (Bombay) has reported cases of more than 50 cm of rain per day. Our study has shown that these heavy rainfall episodes are associated with the cyclonic shear side of Low Level Jetstream (LLJ).

In the literature these heavy rain episodes are assumed to be caused by off shore troughs and mesoscale vortices embedded in them. The advance of monsoon into Kerala is often associated with a weak trough in the low level westerlies along and off Kerala coast. This type of system quite frequently develops off the west coast of India, anywhere from north Kerala to south Gujarat, dur-

ing the south west monsoon season (*Rao*, 1976). The troughs form often near coastal Karnataka and slowly shift about 2° latitude per day northward, though they may also appear and disappear *in situ* over any area. Usually the southern portion of a trough off coastal Karnataka extends to north Kerala, but not further south. Nearly half the number of active to vigorous monsoon situations in Konkan and three quarters of such occasions in coastal Karnataka are found to be with troughs off the west coast. Heavy rainfall is generally in the southern portion of the trough (*Rao*, 1976).

George (1956) showed evidence, though feeble, for the formation of offshore vortices embedded in the trough off the west coast of India which according to him caused concentrated heavy rainfall over the coastal areas. *Mukherjee et al.* (1978) documented these vortices for the month of July for the three year period of 1974–1976. They came to the conclusion that these vortices form just south of Goa and move northwards, sometimes northwest, with a speed of about 100 km per day, producing heavy rainfall over the coast. They have diameter of the order of 100 km and vertical extent of 0.3 to 1.5 km. The peculiarity of the rainfall associated with these troughs and vortices is that the rainfall over the coast is heavier than that over the hills just a few tens of kilometers to the east. *Mukherjee* (1980) studied the structure of an offshore vortex from research aircraft dropinsonde of 20 June 1979 during the MONEX. They found that the dimension of a typical vortex is on the mesoscale. They obtained the values of the convergence and vorticity associated with it.

Another reason for the heavy rainfall along the west coast is orographically forced lifting in the immediate vicinity of the Western Ghats (*Rao*, 1976). The problem of orographically forced rainfall in the immediate vicinity of the Ghats has been studied extensively by *Sarker* (1966, 1967). *Smith* (1979) suggested that the destabilisation of mid–tropospheric air, produced by air lifted up wind of a

mountain barrier, could be an important factor in the generation of orographic precipitation. *Grossman and Durran* (1984) studied the effect of the orography on the low level flow, using the data of MONEX on 24 June 1979 and concluded that the Western Ghats are capable of producing deep convection well offshore (50–200 km) by gently lifting potentially unstable air as it approaches the coast. *Smith and Lin* (1983) showed that the latent heat induces upward motion in and downstream of the heating area and strengthens the orographic lifting of potentially unstable air. In order to study the physics of the orographic–convective precipitation over the west coast of India, *Ogura and Yoshizaki* (1988) used a two dimensional compressible moist cloud model. The model is in terrain following co–ordinates and includes Coriolis force and a planetary boundary layer parameterisation. They considered six cases with and without vertical shear in the wind and including and omitting heat and moisture fluxes from the ocean. They concluded that the strongly sheared environment and fluxes of latent and sensible heat from the ocean are essential for realistic simulation of rainfall distribution.

We have examined daily rainfall data (rain during the 24 hr period ending at 03 UTC – 0830 IST – of a day) of 5 stations Kozhikode (11.2°N, 75.7°E), Honavar (14.2°N, 74.4°E), Goa (15.3°N, 73.8°E), Ratnagiri (16.9°N, 73.3°E) and Mumbai (19°N, 72.9°E) along west coast of India (see Figure 5.1) for the monsoon months (June to September) for the years 1975 to 1990. The rainfall data is taken from India Meteorological Department (IMD) sources. Rainfall data of 15 cm per day and more are considered for the present study. Tables 5.2 to 5.6 give the rainfall data of each stations. The following section describe the relation between LLJ and heavy rainfall events.

5.1 Analysis of Heavy Rainfall Events

It is well known that large amount of convection prevails over the eastern Arabian Sea and west coast of India (windward side of Western Ghats) during the summer monsoon season. When the southwest monsoon wind prevails across the Arabian sea in the summer season, convective clouds develop offshore near the Indian coast, bringing intense precipitation there. A cause for intense convection and heavy rainfall could be the large cyclonic vorticity in the atmospheric boundary layer associated with the LLJ. Boundary layer friction induces vertical motion in the presence of cyclonic vorticity (Ekman pumping) in the monsoon air carrying huge amounts of moisture. This aspect is examined in the following.

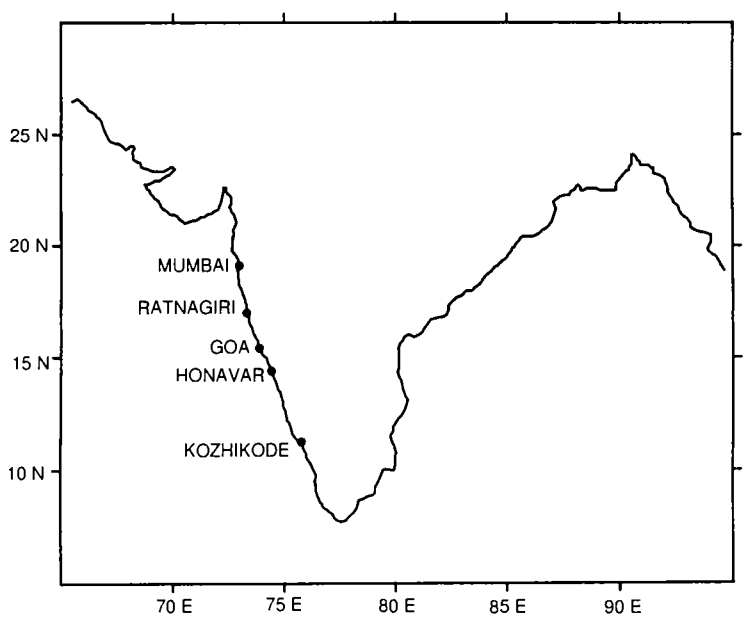

Figure 5.1: Stations selected for Study.

5.1.1 Heavy Rainfall Events During June

During 1975–1990 there are three cases of heavy rain more than 15 cm per day over the station Kozhikode in June (Table 5.1). The Figure 5.2 (a) shows the composites of 850 hPa flow at 00 GMT of the day prior to the day of rainfall report (*i.e.,* when the rain is actually occurring). From the figure it is clear that the core of the LLJ is south of Kozhikode and the station is located in the strong cyclonic shear side. The composite OLR for two days before and a day before the rainfall report are shown in Figures 5.2 (b-c). One day before the period of rainfall (i.e., 2 days before the day of the rainfall reported) convection is spread over a large area. It concentrated into a small area over the station at the time of heavy rainfall.

Table 5.1: Rainfall in cm over the station Kozhikode

June		July		August		September	
Date	Amount	Date	Amount	Date	Amount	Date	Amount
21-6-75	15.78	21-7-77	15.83			10-9-75	16.68
20-6-80	19.41	15-7-80	17.83			22-9-86	23.03
08-6-88	16.81						

There are 13 cases of heavy rainfall more than 15 cm per day at Honavar in June during 1975-1990 (Table 5.2) in which 5 cases have rainfall between 20 cm and 40 cm and two cases more than 40 cm. We have omitted the case on 15 June 1978 for making composite because of the non availability of OLR data for that day. Figure 5.3 (a) shows the composite 850 hPa flow and Figures 5.3 (b–c) show the composites of OLR. There is strong horizontal shear of the LLJ (cyclonic shear) over Honavar. OLR data shows strong convection over the station during the period of the heavy rain (the day before the rainfall report).

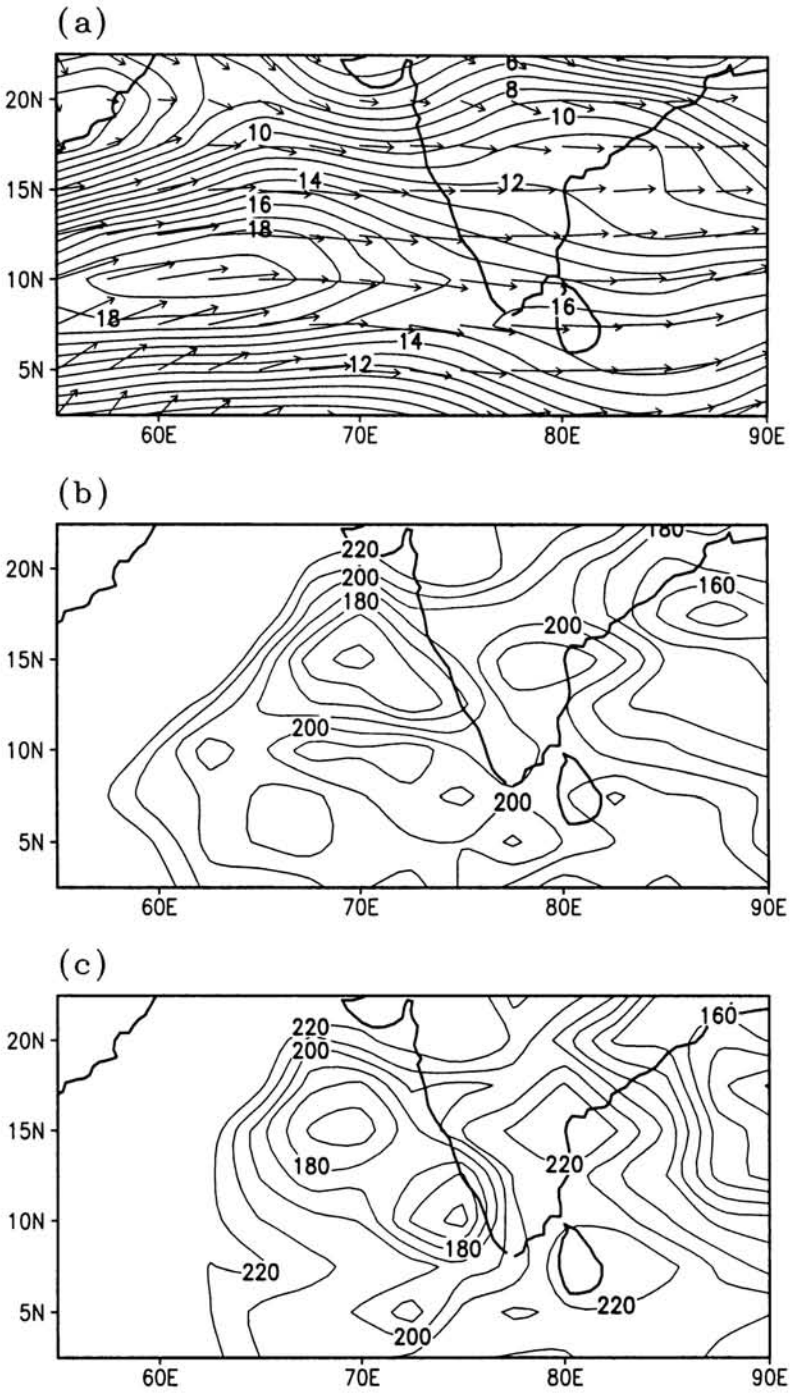

Figure 5.2: Composites of 850 hPa wind and OLR over the Station Kozhikode for June. (a) isotachs and vector of 850 hPa at 00 GMT of the day prior to the day of rainfall report, (b) OLR two days before rainfall report (c) OLR a day before the rainfall report (i.e., day of the rainfall).

Table 5.2: Rainfall in cm over the station Honavar

June		July		August		September	
Date	Amount	Date	Amount	Date	Amount	Date	Amount
22-6-75	19.95	18-7-75	17.96	12-8-80	15.04	15-9-88	16.69
23-6-75	15.23	27-7-76	17.18	3-8-82	25.92		
8-6-77	22.12	17-7-77	21.42	9-8-82	17.90		
16-6-77	25.66	19-7-77	29.44	11-8-83	18.33		
15-6-78	18.00	13-7-78	17.08	12-8-83	15.67		
21-6-80	18.26	17-7-78	15.47	1-8-85	16.22		
18-6-81	15.34	15-7-79	20.64	5-8-86	22.87		
25-6-81	16.55	22-7-82	14.99	17-8-88	16.94		
23-6-82	21.27	18-7-84	15.96				
26-6-85	21.00						
16-6-86	30.38						
13-6-88	46.63						
7-6-89	43.22						

Goa has 11 cases of heavy rainfall more than 15 cm per day in June during the study period in which three cases are above 20 cm (Table 5.3). Figure 5.4 (a)

Table 5.3: Rainfall in cm over the station Goa

June		July		August		September	
Date	Amount	Date	Amount	Date	Amount	Date	Amount
22-6-75	18.71	27-7-79	15.12	1-8-81	21.34		
4-6-81	21.00	31-7-81	23.02	7-8-83	16.88		
13-6-81	18.00	16-7-84	18.50	8-8-83	19.80		
19-6-81	15.38	1-7-87	19.60	9-8-83	17.44		
22-6-82	29.10			11-8-83	28.08		
26-6-83	19.90						
28-6-83	16.30						
30-6-84	18.33						
19-6-85	20.00						
25-6-85	18.00						
30-6-87	18.90						

shows the composite 850 hPa wind flow and Figures 5.4 (b–c) show the OLR composite. The core of LLJ is located relatively north than in the previous cases and there is strong horizontal shear (cyclonic) of the LLJ over Goa. OLR data shows similar features as described in the previous cases.

Ratnagiri has 11 cases of heavy rainfall in June during the study period. Two cases of heavy rainfall during 1978 are omitted for making composites because of the nonavailability of OLR data. There are eight cases of rainfall above 20 cm during the period (Table 5.4). Composite 850 hPa wind shows strong cyclonic

Table 5.4: Rainfall in cm over the station Ratnagiri

June		July		August		September	
Date	Amount	Date	Amount	Date	Amount	Date	Amount
19-6-75	24.20	23-7-77	19.34	14-8-82	15.12	2-9-75	16.33
15-6-78	23.07	7-7-78	24.69	16-8-83	15.31		
16-6-78	15.57	14-7-78	19.87	7-8-86	16.25		
24-6-79	15.90	2-7-80	15.54	17-8-90	27.99		
23-6-82	15.82	31-7-81	18.44				
27-6-83	20.04	29-7-82	17.24				
30-6-84	19.52	21-7-83	16.43				
18-6-86	15.45	1-7-87	16.36				
17-6-87	22.46	25-7-88	17.81				
22-6-89	24.84	22-7-89	15.83				
28-6-89	15.79	23-7-89	19.59				
		24-7-89	19.59				

shear north of 15°N (Figure 5.5 (a)). Ratnagiri is in the cyclonic shear side of LLJ and shear vorticity is large around the station Figures 5.5 (b–c) show the composite of OLR. OLR data shows that 1–day before the period of rainfall, the convection is not organised over the station, but on the day of heavy rainfall we can see an area of intense convection over and around Ratnagiri.

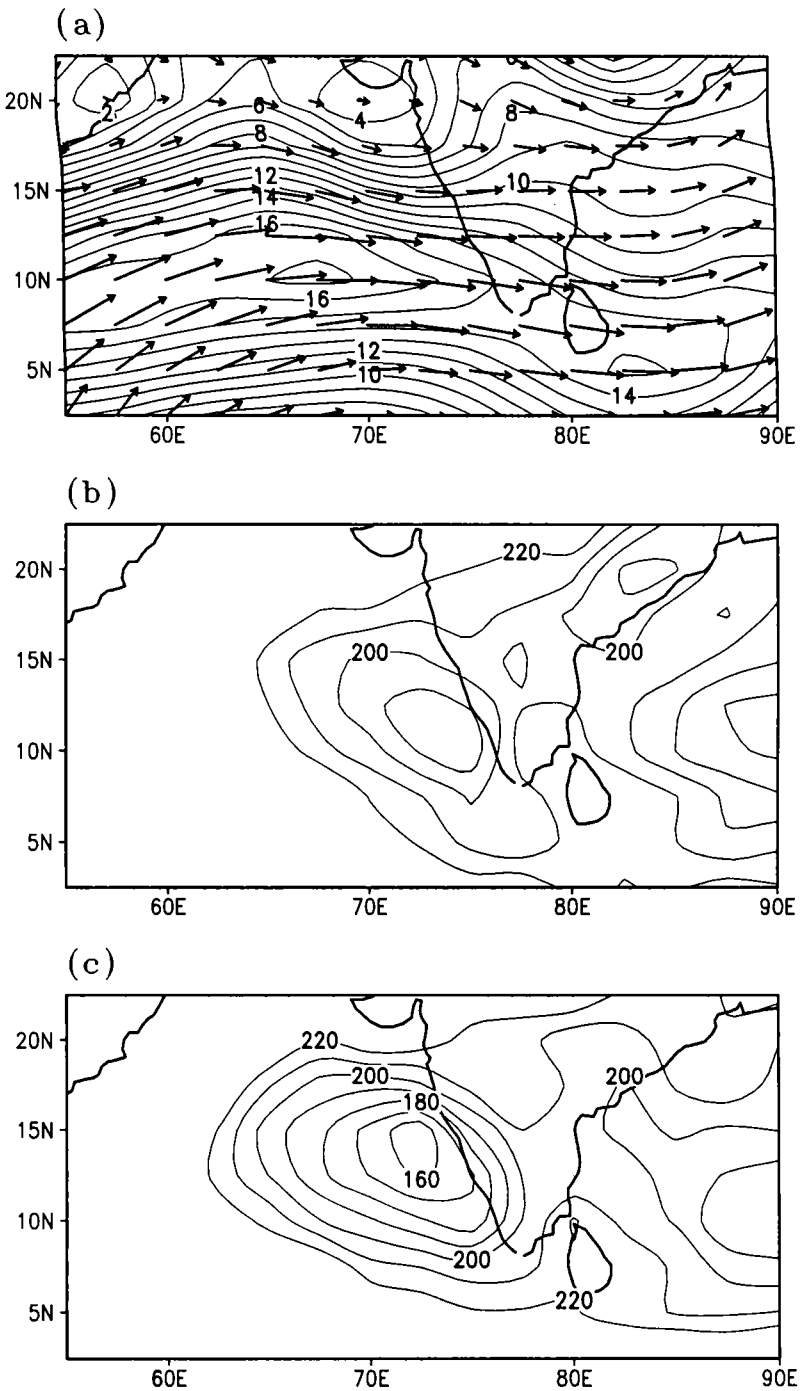

Figure 5.3: Composites of 850 hPa wind and OLR over the Station Honavar for June. (a) isotachs and vector of 850 hPa at 00 GMT of the day prior to the day of rainfall report, (b) OLR two days before rainfall report (c) OLR a day before the rainfall report (i.e., day of the rainfall).

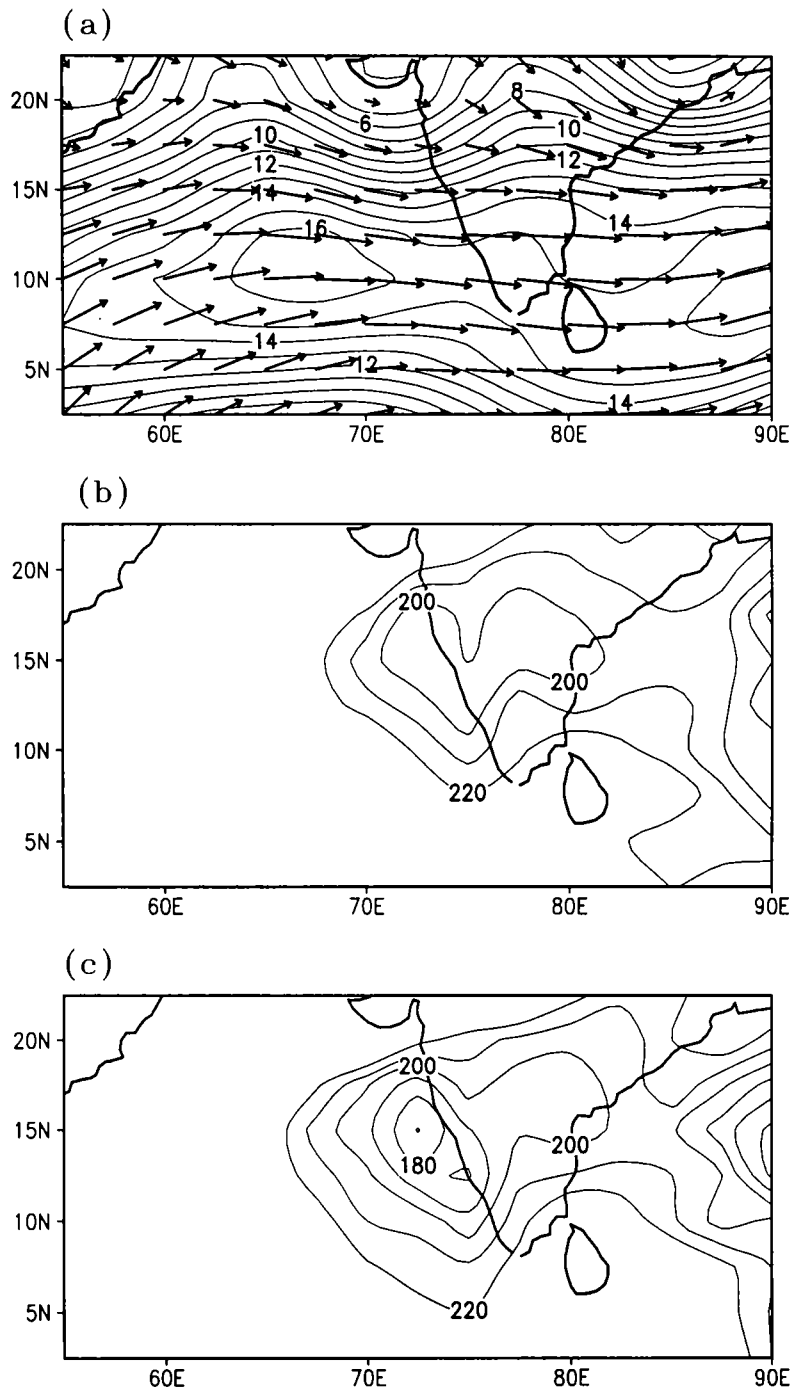

Figure 5.4: Composites of 850 hPa wind and OLR over the Station Goa for June. (a) isotachs and vector of 850 hPa at 00 GMT of the day prior to the day of rainfall report, (b) OLR two days before rainfall report (c) OLR a day before the rainfall report (i.e., day of the rainfall).

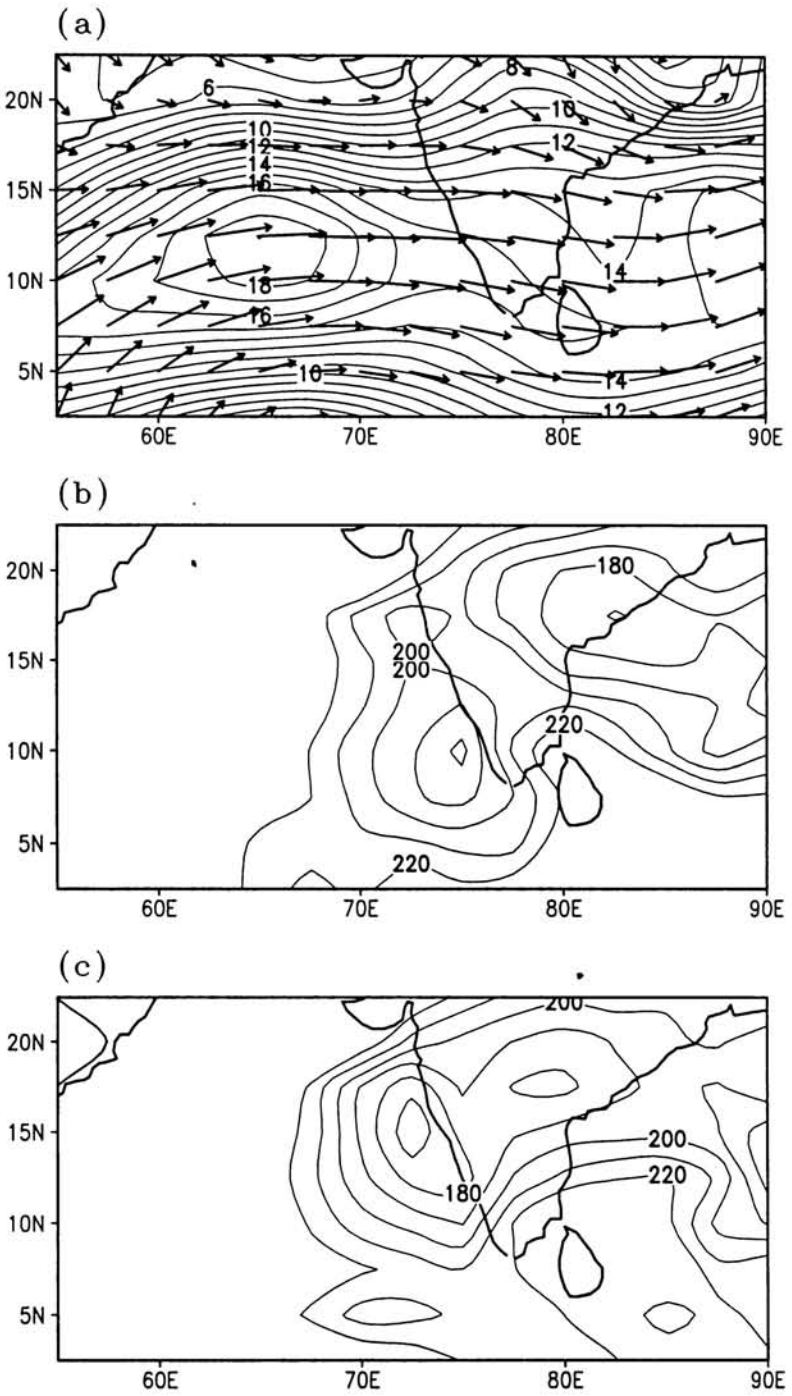

Figure 5.5: Composites of 850 hPa wind and OLR over the Station Ratnagiri for June. (a) isotachs and vector of 850 hPa at 00 GMT of the day prior to the day of rainfall report, (b) OLR two days before rainfall report (c) OLR a day before the rainfall report (i.e., day of the rainfall).

There are 5 cases of heavy rainfall in June for Mumbai in which two cases are more than 30 cm per day and one is more than 40 cm per day (Table 5.5). The composite 850 hPa flow is shown in Figure 5.6 (a) and Figures 5.6 (b–c)

Table 5.5: Rainfall in cm over the station Bombay

June		July		August		September	
Date	Amount	Date	Amount	Date	Amount	Date	Amount
16-6-78	17.57	9-7-75	16.40	1-8-79	20.62	2-9-75	17.53
19-6-82	18.09	31-7-75	41.72	13-8-83	17.34	3-9-77	18.19
25-6-85	30.93	23-7-77	18.44	15-8-83	15.04	23-9-81	24.16
25-6-85	30.93	2-7-84	54.42	15-8-90	25.90	24-9-81	17.19
16-6-90	42.12	1-7-87	15.39				
		24-7-89	18.33				

show the composite of OLR. The core of LLJ in this case is south of Mumbai and there is strong horizontal shear (cyclonic) over Mumbai. OLR data shows similar features as described in the previous cases.

5.1.2 Heavy Rainfall Events at Mumbai

During all four months of the summer monsoon season (June to September) Mumbai experiences a number of days of heavy rainfall more than 15 cm per day (see Table 5.5). There are 5 cases in June (already discussed) 6 cases in July, 4 in August and 5 in September during the period 1975-1990. Figures 5.7 (a–c) show the composite of 850 hPa wind for July, August and September. From this figure it is evident that the heavy rainfall events during the summer monsoon months are generally associated with the large cyclonic shear of the LLJ near Mumbai. Figures 5.8(a–c) give OLR maps for the heavy rainfall day.

From these analysis it is seen that Mumbai and surroundings have strong cyclonic vorticity associated with LLJ at 850 hPa level (just above the boundary

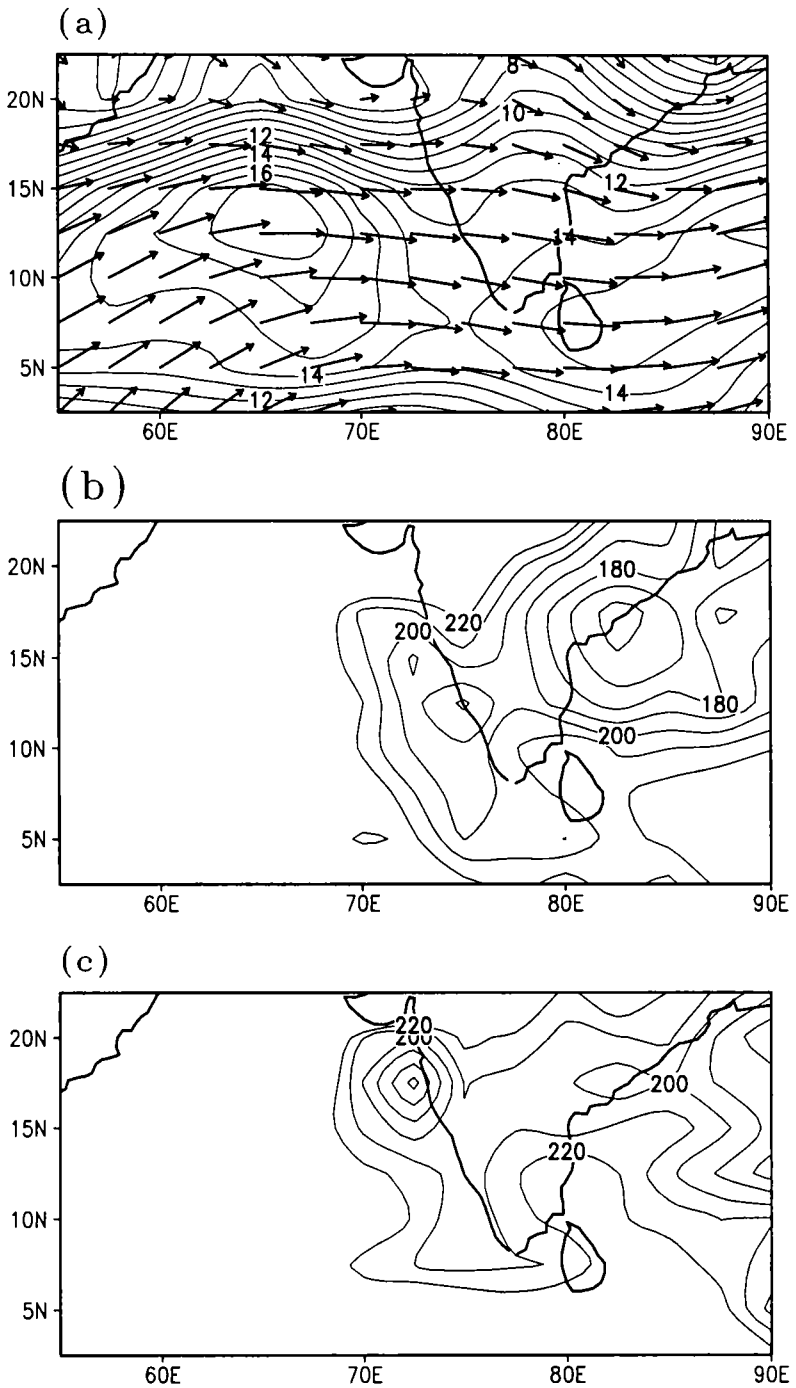

Figure 5.6: Composites of 850 hPa wind and OLR over the Station Mumbai for the June. (a) isotachs and vector of 850 hPa at 00 GMT of the day prior to the day of rainfall report, (b) OLR two days before rainfall report (c) OLR a day before the rainfall report (i.e., day of the rainfall).

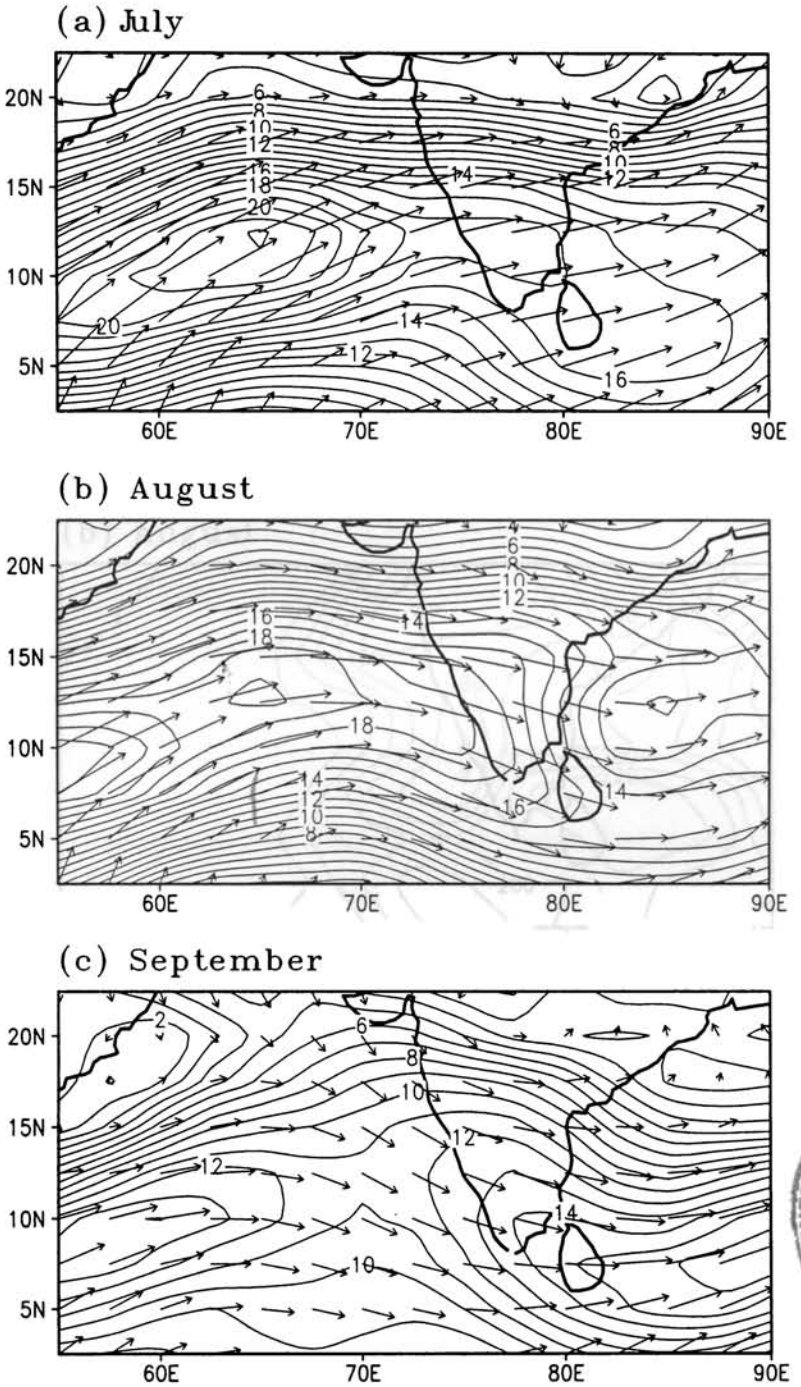

Figure 5.7: Composites of 850 hPa wind 00 GMT of the day prior to the day of rainfall report over the Station Mumbai for (a) July (b) August and (c) September.

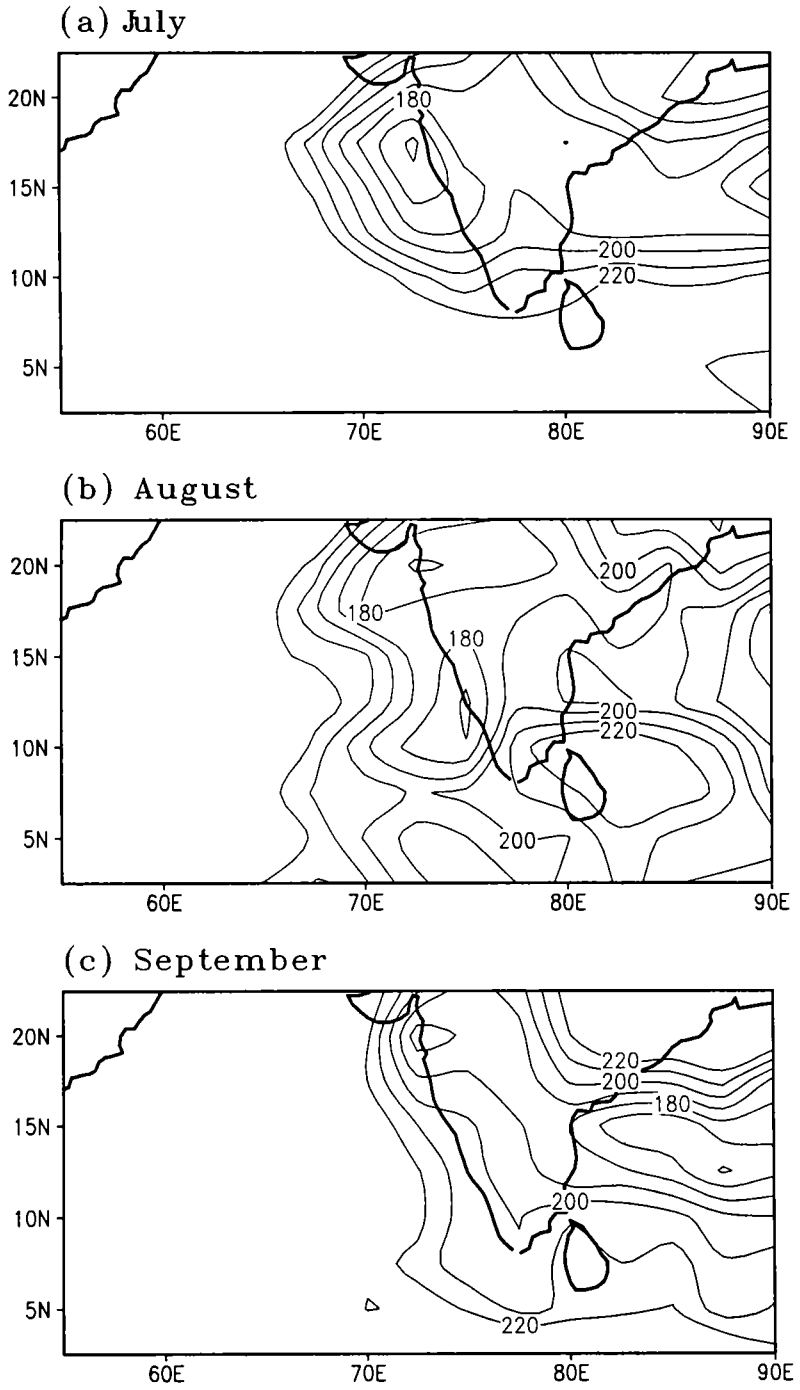

Figure 5.8: Composites of OLR a day before the rainfall report (i.e., day of the rainfall) over the Station Mumbai for (a) July, (b) August and (c) September.

layer). It is also seen that low OLR region shrinks to a small area at the time of the station experiences heavy rainfall. Thus it is clear that one of the most important condition for heavy monsoon rainfall along the west coast of India is the presence of strong cyclonic shear vorticity around the station associated with LLJ. From OLR data it can be inferred that at the time of heavy rainfall the cyclonic vorticity gets concentrated over a small area near the coast. In order to search whether the above observational evidence is an indication of the formation of a mesoscale vortex due to the concentration of the cyclonic vorticity of the LLJ, a mesoscale modelling study has been attempted in this work. To understand the mechanisms for the heavy rainfall and to verify the existence of mesoscale vortices, Govt. of India (DST) has organised a field experiment in Arabian Sea, known as ARMEX.

5.2 Simulation using Mesoscale Model

From the analysis done so far in this section, it is seen that one of the conditions associated with heavy rain at west coast stations during southwest monsoon is the presence of the core (axis) of the LLJ at 850 hPa close to and south of the station. This ensures strong cyclonic shear vorticity at the station in the boundary layer which generates Ekman pumping up of the moisture rich monsoon air mass. OLR analysis has shown that on the day of heavy rainfall, the area of precipitation shrinks and becomes intense (very low OLR) just in a small area around the station. One inference from these is that on the day of heavy rain the vorticity in the cyclonic shear side of the LLJ is enhanced in the boundary layer (levels below 850 hPa) in a limited area around the station. As given in the literature this may be due to the flow getting organised into an off–shore trough or a meso scale vortex. Till date there is no clear evidence from data for the formation of a mesoscale vortex of the west coast of India.

To see whether starting from a strong LLJ (shear vorticity) background an off shore trough or a mesoscale vortex gets developed, a modelling experiment was performed using PSU/NCAR mesoscale model MM5. Details of model structure are described in Chapter 2. Input data and physics options used for simulation are described in the following section.

5.2.1 Model Domain and Orography

We have selected three nested domains with grid resolutions 90 km, 30 km and 10 km for integration. These domains are shown in Figure 5.9. Mercator type map projection is used for these domains. Terrain height data with 30 min, 10 min and 5 min resolutions are used as input for these 3 domains. All these data are created from United States Geological Survey (USGS) elevation data at 30 sec resolution. Input for vegetation/Land–use are also taken from USGS. Overlapping parabolic interpolation with 2 pass smoother is used to construct mesoscale grid for orography and vegetation/Land–use data.

5.2.2 Physics options

Cumulus parameterisation

We have used Betts–Miller scheme for cumulus parameterization (*Betts and Miller*, 1993). The original Betts–Miller scheme was designed to adjust the atmospheric temperature and moisture structure back toward a reference quasi-equilibrium thermodynamic structure in the presence of large-scale radiative and advective processes. Two distinct reference thermodynamic structures (which are partly specified and partly internally determined) are used for shallow and deep convection . Later the scheme was modified to explicitly introduce the low–level cooling and drying by a downdraft mass flux.

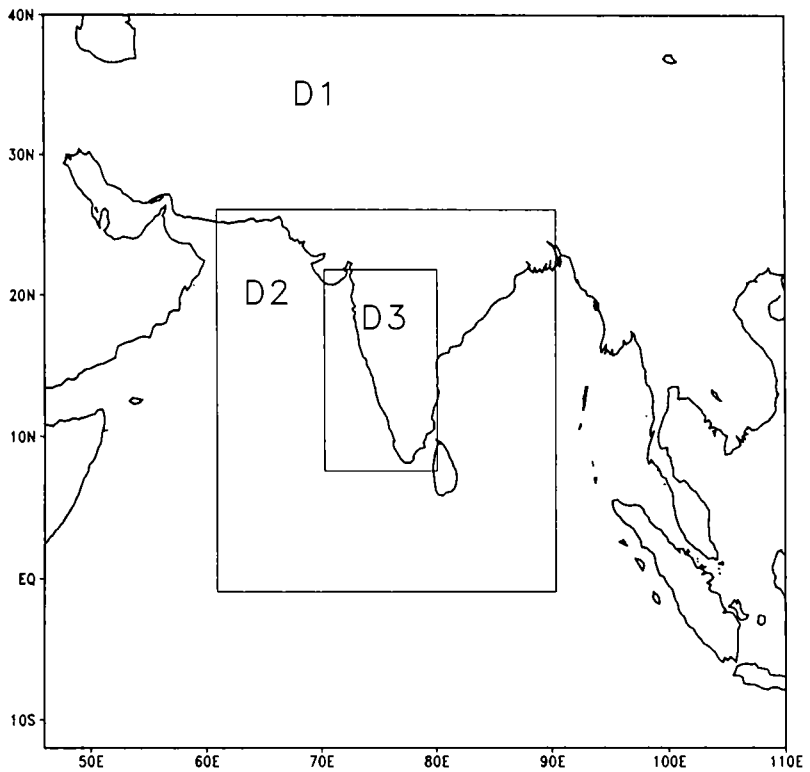

Figure 5.9: Domain selected for simulation. D1: 90 km, D2: 30 km, and D3: 10 km.

PBL scheme

Mellor–Yamada PBL scheme as used in the Eta model is used for the present study. It predicts turbulent kinetic energy and local vertical mixing (*Janjic*, 1994)

Moisture Scheme

Moisture scheme is Simple Ice (*Dudhia*, 1993). In this scheme cloud and rain water fields are predicted explicitly with microphysical processes. Ice phase processes adds to above processes without adding memory. There is no super-cooled water and immediate melting of snow below freezing level.

Radiative scheme

The radiation effects due to cloud are considered and are sophisticated enough to account for longwave and shortwave interaction (Cloud-radiation scheme). All the above details are taken from MM5 Document.

5.2.3 Numerical Simulations

For the present study we have taken six cases of heavy rainfall events during the period 1984-1990. In all these cases the observed rainfall is more than 30 cm. Three cases are for Honavar and three for Mumbai (Table 5.6). No depression or cyclone existed in Arabian Sea during these rainfall episodes as obtained from *IMD* (1996). The input data used for the simulation is from NCEP/NCAR

Table 5.6: Rainfall cases selected for Numerical Simulation

	Station	Date	Amount (cm)
Case 1	Honavar	07 June 1989	43.2
Case 2	Honavar	14 June 1986	30.4
Case 3	Honavar	13 June 1988	46.6
Case 4	Bombay	02 July 1984	54.4
Case 5	Bombay	17 June 1985	34.5
Case 6	Bombay	16 June 1990	46.1

Reanalysis Project (NNRP). These data are on $2.5° \times 2.5°$ latitude–longitude grid with 17 vertical levels. This data were interpolated by the MM5 model to the desired grid size for running the model. The simulation started 48 hrs before the day of rainfall report and model is run for the following 48 hours with time steps of 360 sec. The model output is taken every six hours. The integration has been performed (a) with the model orography (O–Run) and with (b) a flat terrain at altitude 1 m above mean sea level or without orography (NO–Run) in the innermost domain to study the role of Western Ghats.

On 7 June 1989 at 0830 IST Honavar reported 43.2 cm rain during the previous 24 hours (Case 1). Figure 5.10 shows the 850 hPa wind analysis at 00GMT of 5 June 1989. There is strong horizontal wind shear of LLJ around Honavar and the core of LLJ is located south of Honavar. The O–Run for this case starts from 00 GMT of 5 June 1989. Figure 5.11 shows 950 hPa wind vector in the fine mesh (10 km grid). A marked change in the wind field can be seen at 950 hPa after 18 hours of integration. It has been seen that the westerlies are veered into north westerlies. To the west of that area at 24 hours a small vortex forms centered at about 15°N and 71°E. This vortex slowly intensified and moved in an easterly direction and approached close to Honavar after 48 hours of integration. Thus during the duration of heavy rain Honavar was under the influence of this meso–scale vortex. These types of circulation are seen in 925 hPa and 900 hPa levels. At 850 hPa level the vortex is weak and thereafter it become very feeble (figure not shown).

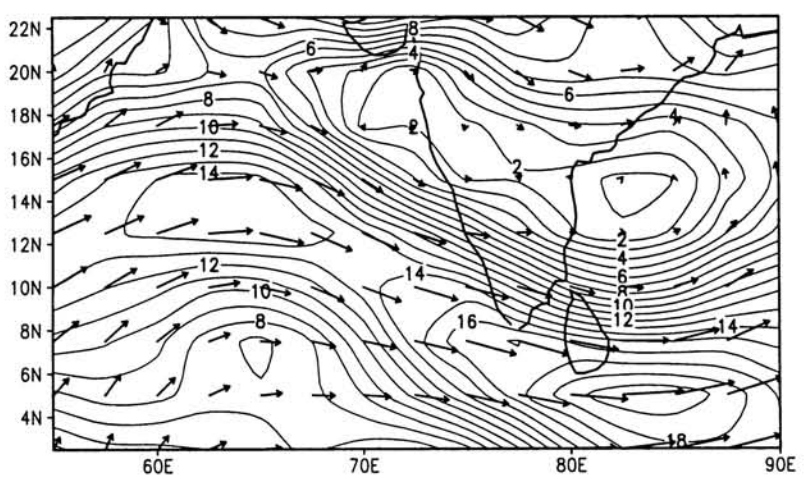

Figure 5.10: 850 hPa isotachs and vector wind at 00 GMT 5 June 1989.

Figure 5.12 shows the NO–Run simulation of 7 June 1989 rainfall event. A vortex circulation formed after 30 hours of integration similar to that with model orography but the vortex is slightly weaker compared to case 1, O–Run.

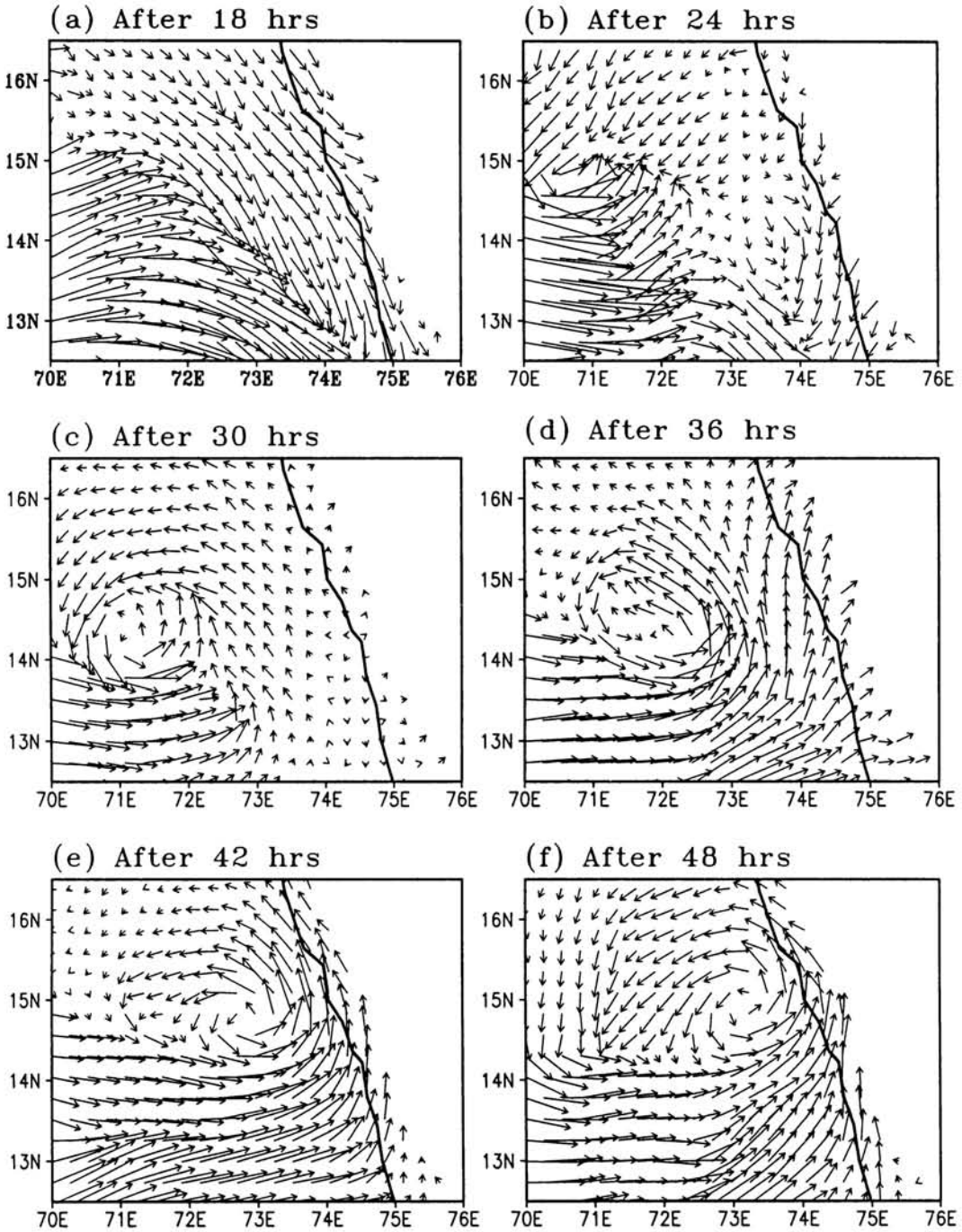

Figure 5.11: Simulated 950 hPa wind vector for simulation that starts from 00 GMT 5 June 1989 with model orography (Case I O–Run). (a) after 18 hrs of integration to (f) 48 hrs in 6 hrs interval.

This indicates that role of Western Ghats in formation of the vortex and concentration of vorticity is not a major factor as compared to the cyclonic shear due to the LLJ.

Cases 2 and 3 are the heavy rainfall events on 16 June 1986 and on 13 June 1988 at Honavar. On 16 June 1986, Honavar reported 30.3 cm rainfall and on 13 June 1988 the rainfall is 46.6 cm. Model integration starts at 00 GMT 14 June 1986 and 00 GMT 11 June 1988, respectively for these two cases. Figures 5.13 and 5.14 show 850 hPa wind analysis for 00 GMT 14 June 1986 and 00 GMT 11 June 1988, respectively. In Figure 5.13 the axis of LLJ is on the southern tip of India and there is strong horizontal wind shear between 10° N and 15° N over the west coast of India. But in Figure 5.14 the axis of LLJ is near 12° N and there is strong wind shear between 13° N and 18° N. In both cases Honavar is on the cyclonic shear side of the LLJ.

Figure 5.15 shows the 950 hPa wind vector for Case 2 (O–Run). After 18 hours of integration a change in the wind field can be seen. A closed circulation has formed after 24 hours around 12° N and it moved eastwards in another six hours. A new circulation developed to the north of 12° N and to the west of the first circulation during this time. This secondary circulation strengthened after 36 hours of integration and the first one weakened. After 42 hours, the second circulation moved eastwards and it weakened in the next 6 hours. Both these the circulations are formed at latitudes south of Honavar. From figure 5.13 we can see that the strong horizontal wind shear at 850 hPa was also more south than in Case 1. This may be a reason for the formation of the circulation in more southern latitudes. The simulation with flat terrain (NO–Run) also shows similar results but the vortex is relatively weaker.

Wind vectors at 950 hPa for the simulation for Case 3 (O–Run) in Figure 5.16. After 12 hours of integration, a small scale circulation has formed at a lat-

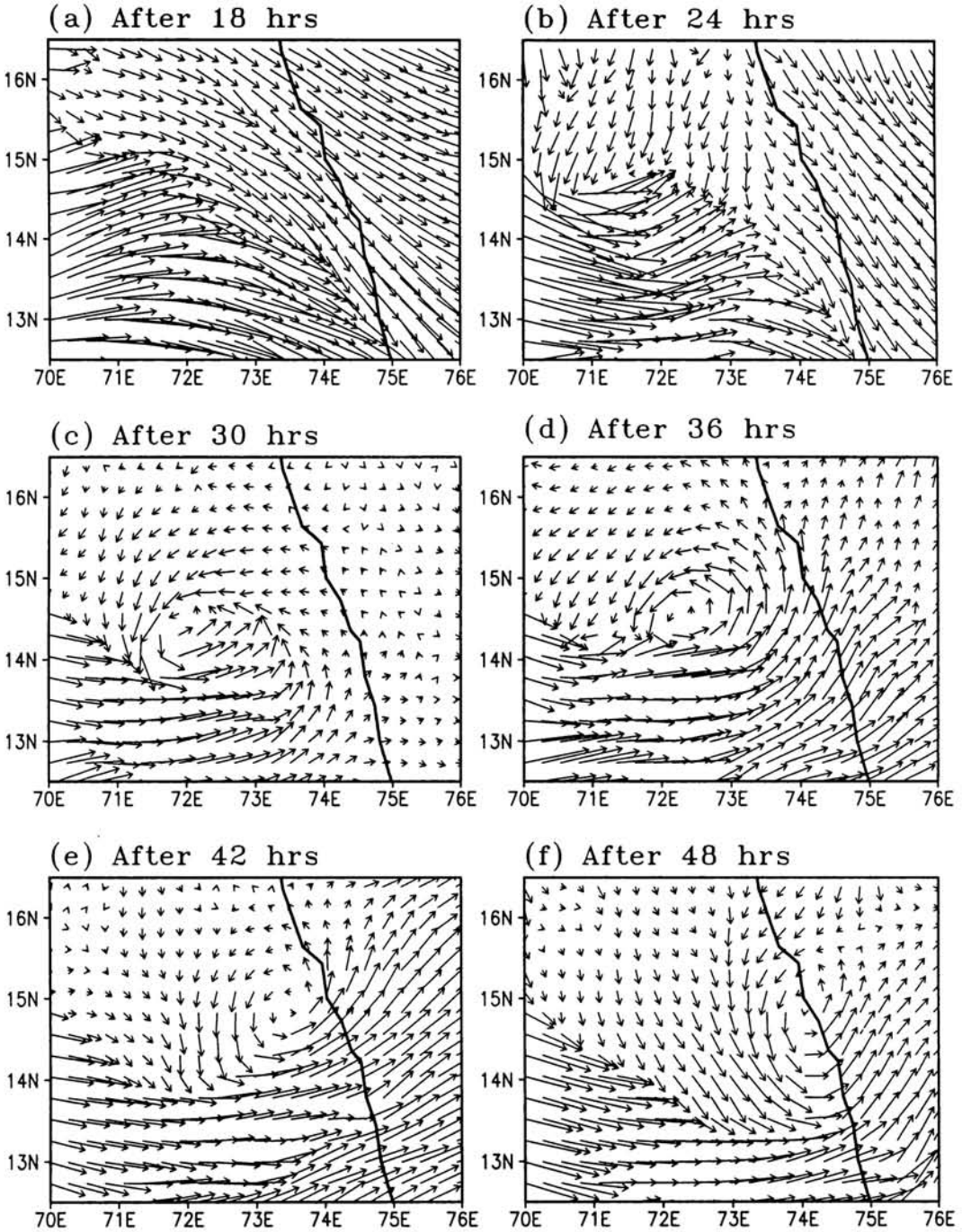

Figure 5.12: Simulated 950 hPa wind vector for simulation that starts from 00 GMT 5 June 1989 with flat terrain (Case I NO–Run). (a) after 18 hrs of integration to (f) 48 hrs in 6 hrs interval.

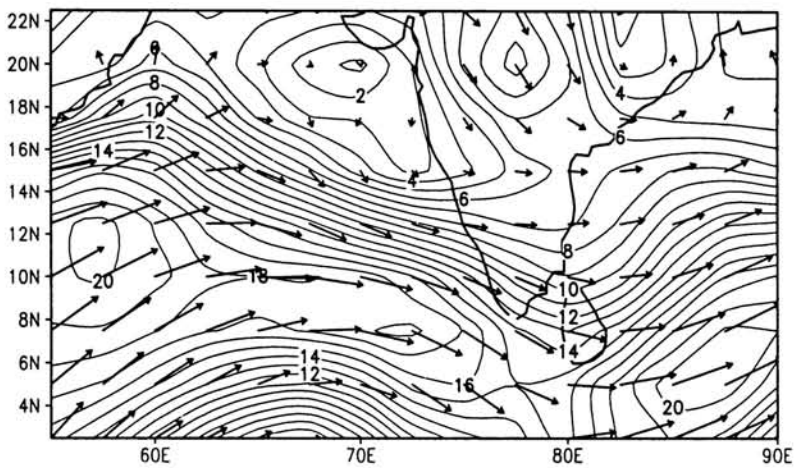

Figure 5.13: 850 hPa isotachs and vector wind at 00 GMT 12 June 1986.

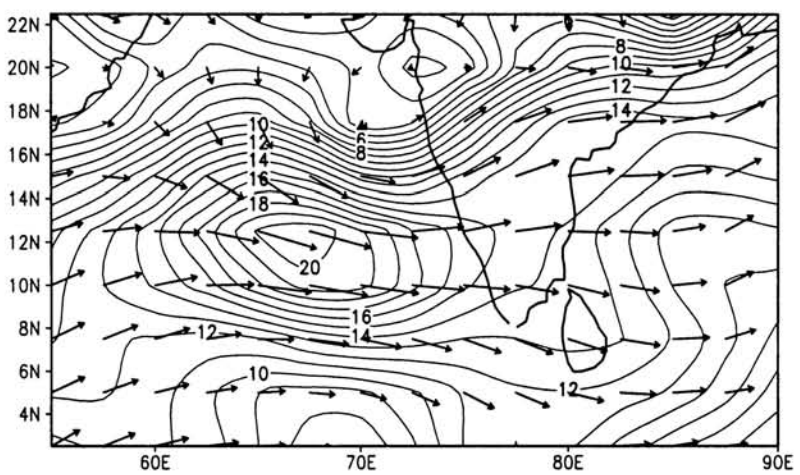

Figure 5.14: 850 hPa isotachs and vector wind at 00 GMT 11 June 1988.

itude north of Honavar. It intensified further and moved northwards. In figure 5.14 the 850 hPa analysis shows strong wind shear north of 12.5° N and the circulation is formed around 14.5° N. The simulation with flat terrain (NO–Run) also shows similar result, with a weak vortex.

The other 3 cases selected for model simulation are the heavy rainfall events reported over Mumbai on 02 July 1984 (Case 4), 17 Jun 1985 (Case 5) and 16 June

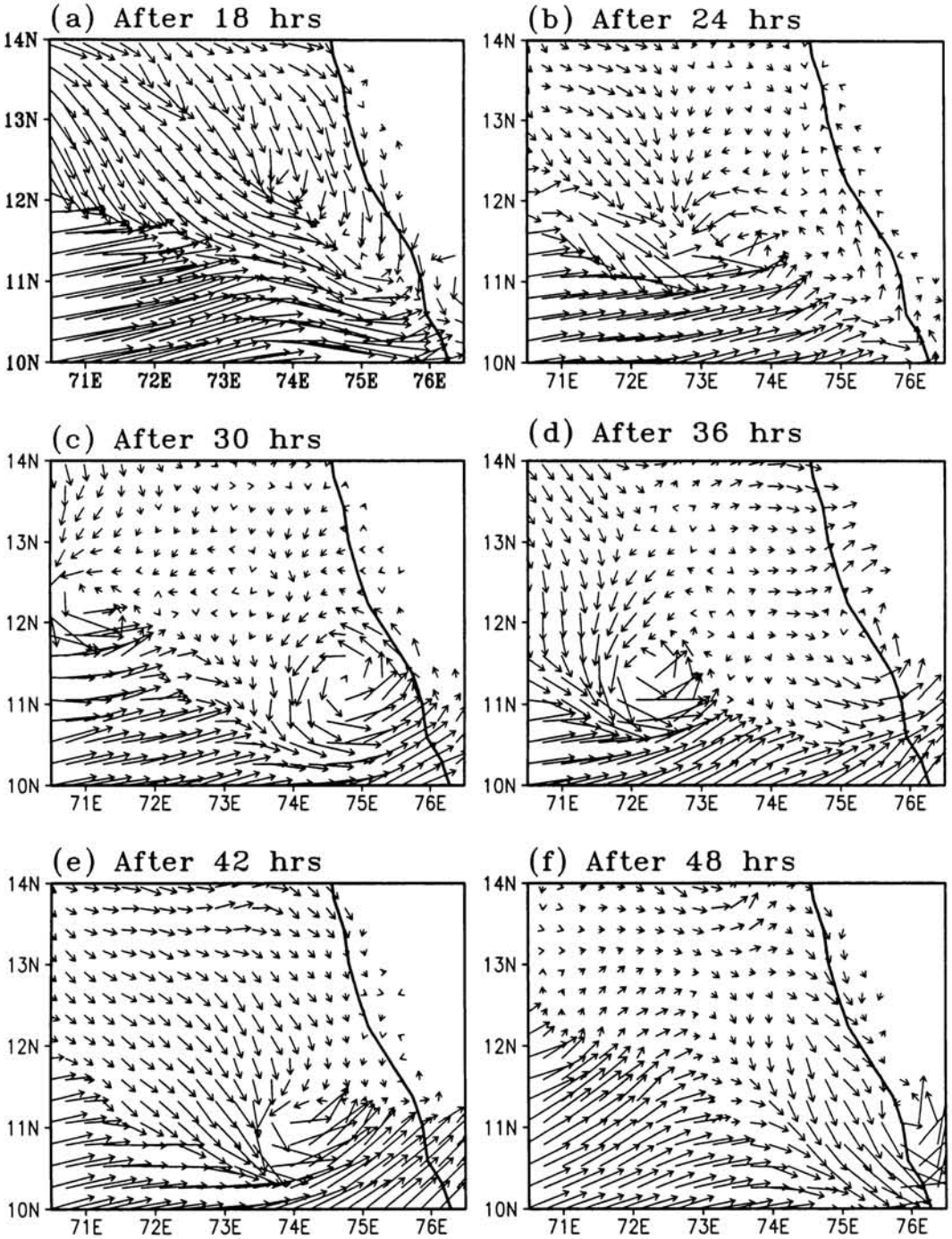

Figure 5.15: Simulated 950 hPa wind vector for simulation that starts from 00 GMT 12 June 1986 with model orography (Case II O–Run). (a) after 18 hrs of integration to (f) 48 hrs in 6 hrs interval.

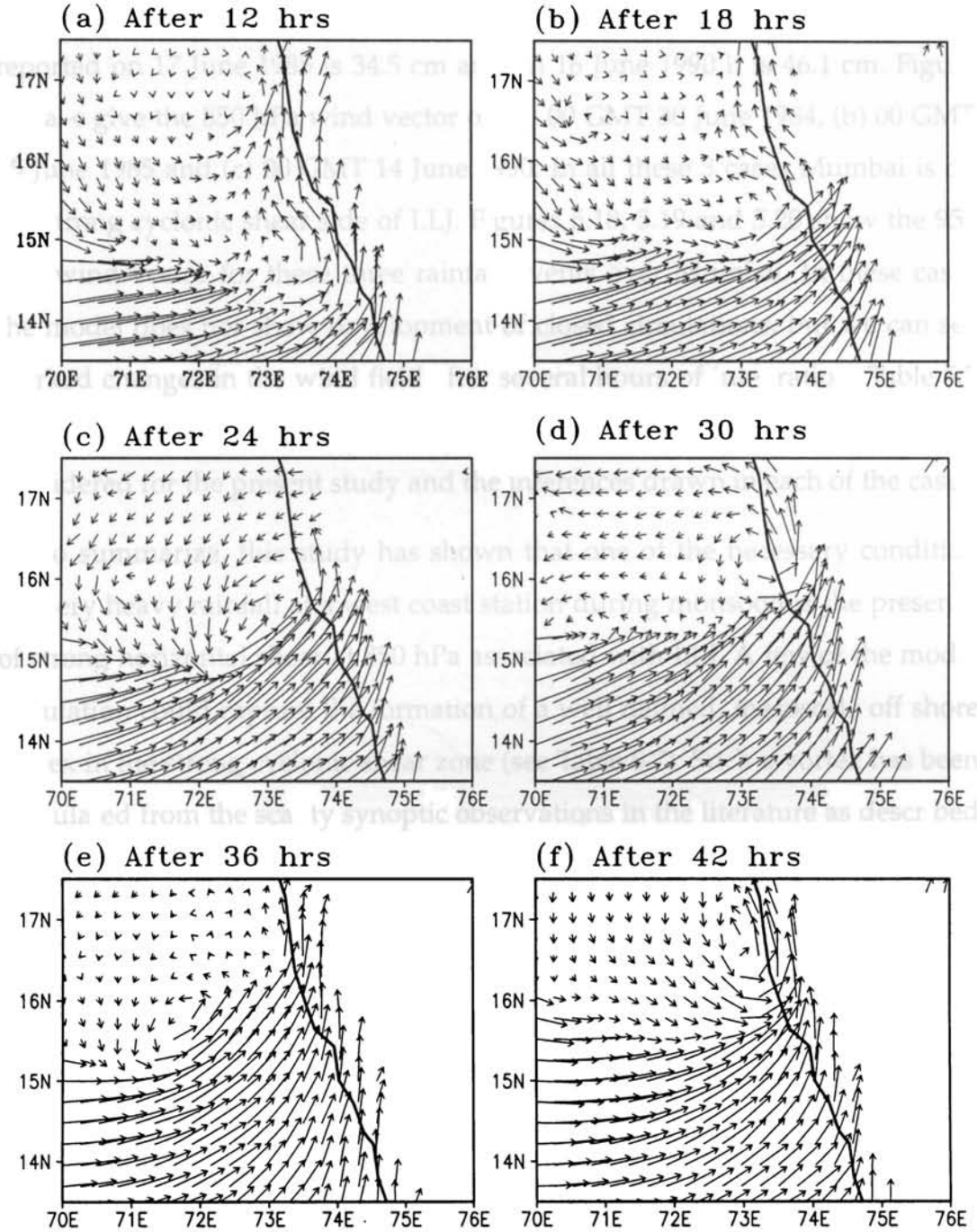

Figure 5.16: Simulated 950 hPa wind vector for simulation that starts from 00 GMT 11 June 1988 with model orography (Case II O–Run). (a) after 12 hrs of integration to (f) 42 hrs in 6 hrs interval.

1990 (Case 6). On 2 July 1984 Mumbai observed 54.4 cm of rain. The rainfall reported on 17 June 1985 is 34.5 cm and on 16 June 1990 it is 46.1 cm. Figure 5.17a–c give the 850 hPa wind vector on (a) 00 GMT 30 June 1984, (b) 00 GMT 15 June 1985 and (c) 00 GMT 14 June 1990. In all these 3 cases Mumbai is on the strong cyclonic shear side of LLJ. Figures 5.18, 5.19 and 5.20 show the 950 hPa wind vector for these three rainfall events over Mumbai. In these cases the model does not show development of closed circulations, but we can see marked changes in the wind field after several hours of integration. Table 5.7 illustrates the cases of heavy rainfall events selected for numerical simulation considered for the present study and the inferences drawn in each of the cases.

To summarize, this study has shown that one of the necessary condition for very heavy rainfall at a west coast station during monsoon is the presence of strong horizontal shear at 850 hPa associated with LLJ. A few of the model simulation could capture the formation of a well defined, mesoscale off shore vortex in the strong cyclonic shear zone (see Table 5.7). Such a vortex has been speculated from the scanty synoptic observations in the literature as described in this Chapter.

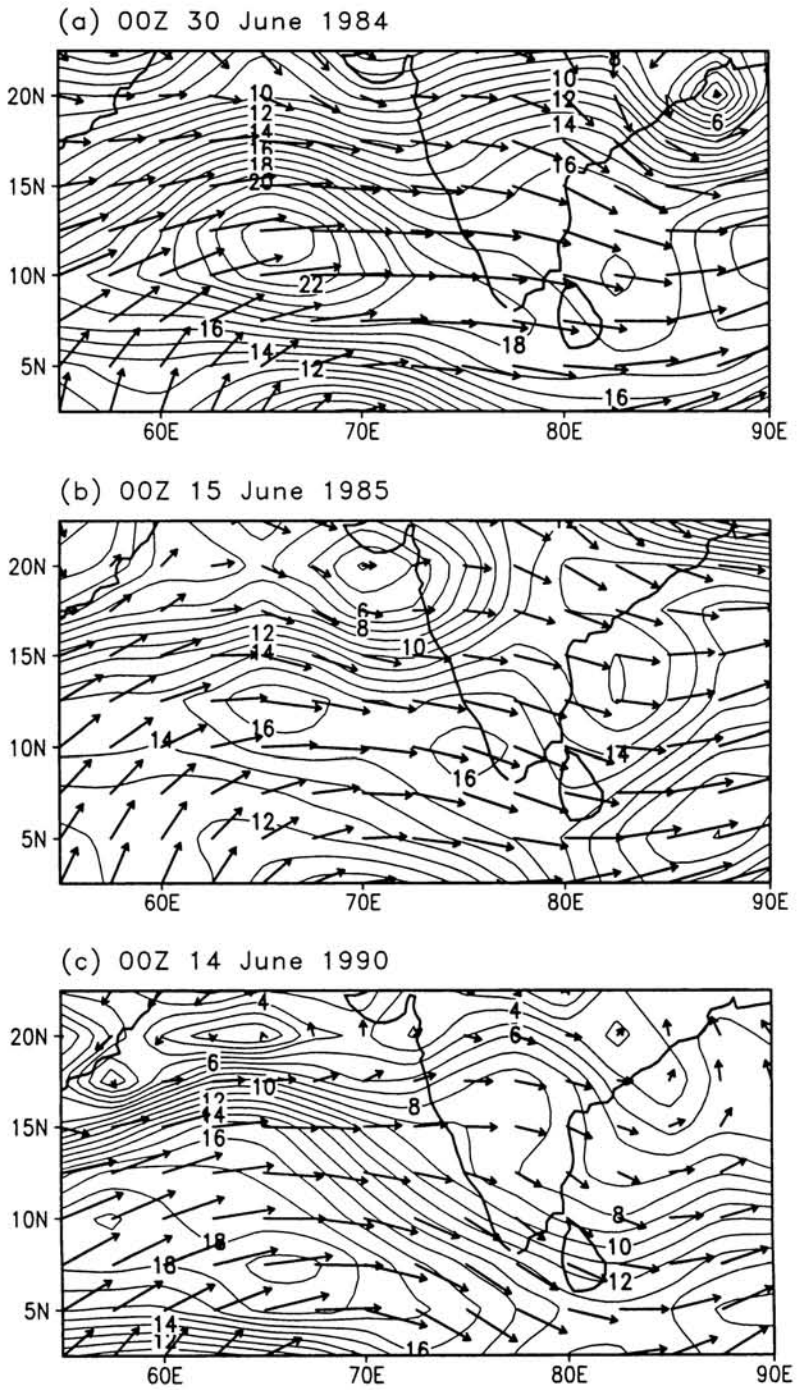

Figure 5.17: 850 hPa isotachs and vector wind at (a) 00 GMT 30 June 1984, (b) 00 GMT 15 June 1985 and (c) 00 GMT 14 June 1990

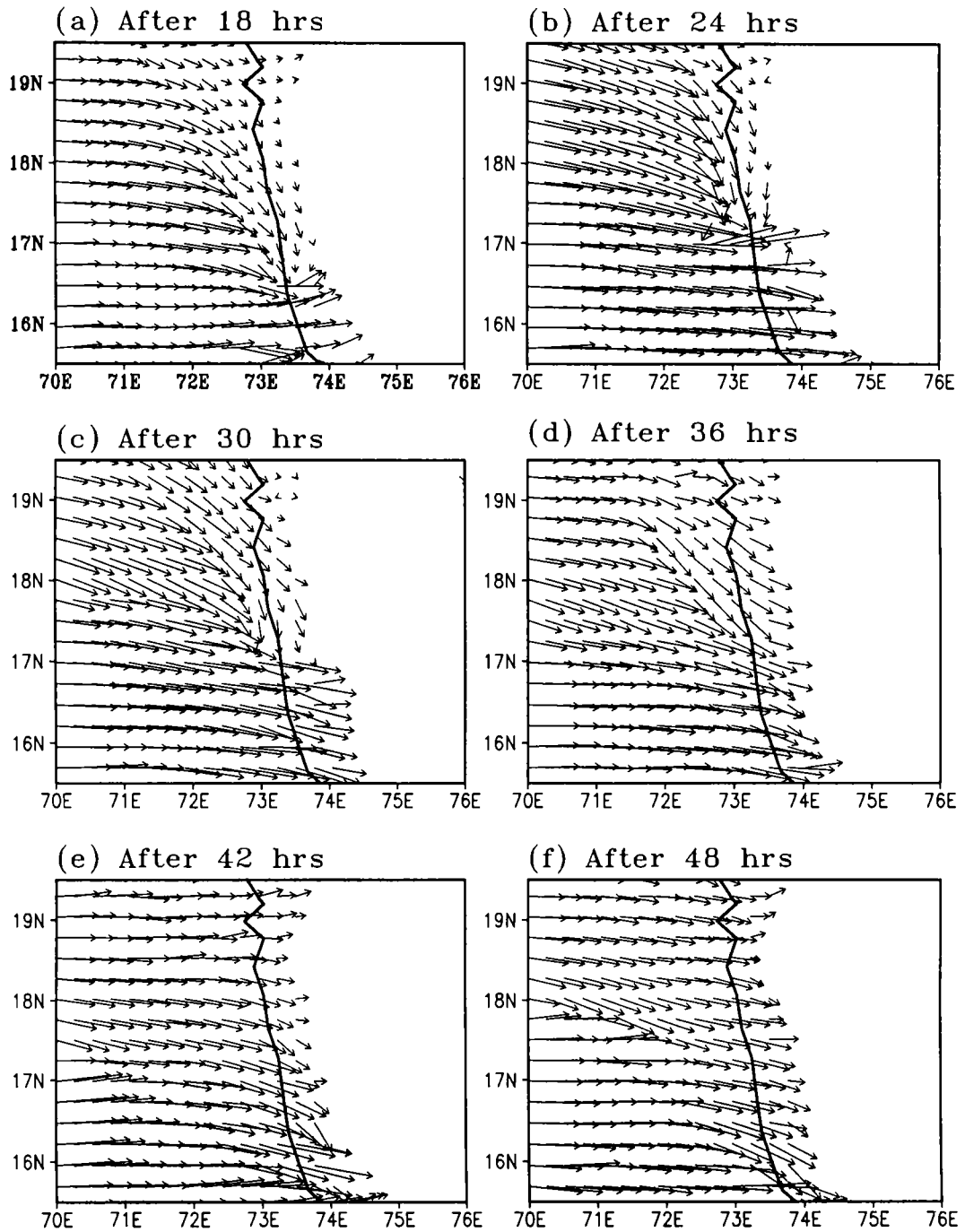

Figure 5.18: Simulated 950 hPa wind vector for simulation that starts from 00 GMT 30 June 1984 with model orography (Case IV O–Run). (a) after 18 hrs of integration to (f) 48 hrs in 6 hrs interval.

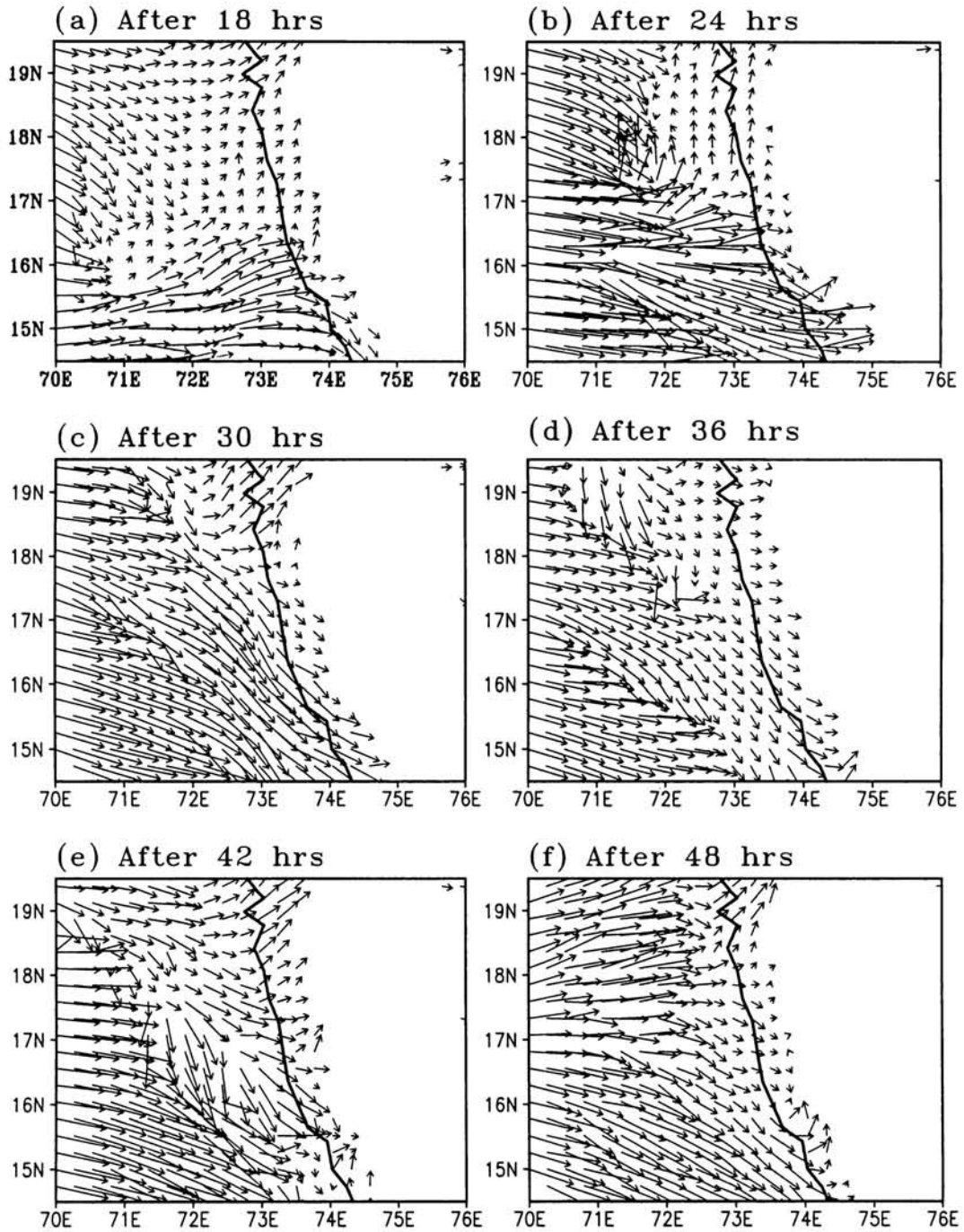

Figure 5.19: Simulated 950 hPa wind vector for simulation that starts from 00 GMT 15 June 1985 with model orography (Case V O–Run). (a) after 18 hrs of integration to (f) 48 hrs in 6 hrs interval.

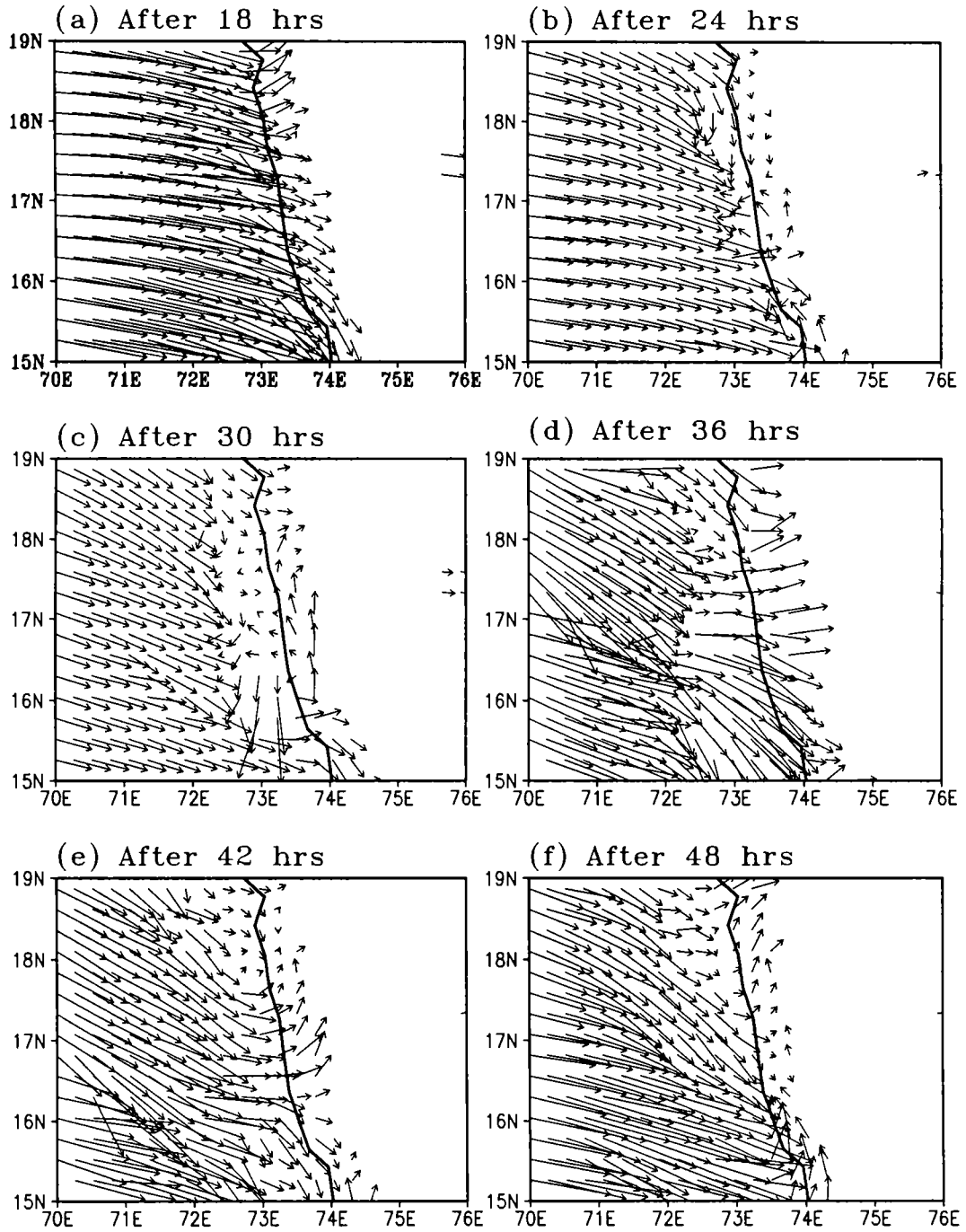

Figure 5.20: Simulated 950 hPa wind vector for simulation that starts from 00 GMT 14 June 1990 with model orography (Case VI O–Run). (a) after 18 hrs of integration to (f) 48 hrs in 6 hrs interval.

Table 5.7: Results of Numerical Simulation

	Type	Level	Inferences
Case1	O–Run	950 hPa	Vortex formed after 24 hrs
		900 hPa	same as above
		850 hPa	Vortex exist but weak
	NO–Run	950 hPa	Vortex formed after 24 hrs but weak
		900 hPa	Weak vortex
		850 hPa	Weak vortex
Case2	O–Run	950 hPa	After 24 hrs a vortex formed weakened after 30 hrs and a new one formed
		900 hPa	same as above
		850 hPa	Vortices are feeble
	NO–Run	950 hPa	same as 950 hPa level O–Run
		900 hPa	Vortices are Weak
		850 hPa	Very feeble vortices formed
Case3	O–Run	950 hPa	A feeble circulation formed after 12 hrs which intensified later
		900 hPa	same as above
		850 hPa	Weak vortex
	NO–Run	950 hPa	Vortex exists but weak
		900 hPa	Weak vortex
		850 hPa	Feeble vortex
Case4	O–Run	950 hPa	No Vortex, only marked changes in wind
		900 hPa	same as above
		850 hPa	same as above
	NO–Run	950 hPa	same as above
		900 hPa	same as above
		850 hPa	same as above
Case5	O–Run	950 hPa	Changes are sharp compared to case 4
		900 hPa	same as above
		850 hPa	Same as above
	NO–Run	950 hPa	No vortex
		900 hPa	No vortex
		850 hPa	No vortex
Case6	O–Run	950 hPa	Changes in wind
		900 hPa	same as above
		850 hPa	changes are weak compared to above
	NO–Run	950 hPa	Changes in wind vector
		900 hPa	same as above
		850 hPa	same as above

CHAPTER 6

MONSOON DEPRESSIONS AND LOW LEVEL JETSTREAM

Monsoon Depressions (MD) are synoptic scale cyclonic circulations that occur over the northern Bay of Bengal and central India during the summer monsoon season and give copious rainfall in their southwest sectors (*Rao*, 1976; *Sikka*, 1977). Usually, a prolonged spell of dry weather during the season is broken by the formation of a monsoon depression. An explanation of the intensification of low pressure systems into monsoon depression has been investigated by many workers (*Koteswaram and George*, 1958; *Sikka*, 1977; *Saha and Chang*, 1983; *Warner*, 1984). *Koteswaram and George* (1958) suggested that the intensification of the monsoon depression occurs in association with the interaction between upper tropospheric divergence and lower tropospheric convergence. According to them favourable mechanism in the upper troposphere was provided periodically by westward propagating disturbances or by the divergence in upper tropospheric strong easterly flow. These features are associated with upper level positive vorticity advection which favour upward motion and low level convergence in the north Bay of Bengal. However, synoptic experiences show that there are several cases when the development of the depressions take

place without significant changes in the upper tropospheric circulation occurring prior to the time of intensification (*Sikka*, 1977).

One of the synoptic conditions for the genesis of these depressions is the presence of strong monsoon westerlies to the south of the genesis area (*Sikka*, 1977). The intensification of the depression was accompanied with strengthening of lower tropospheric westerlies over the Peninsular India and the Gangatic valley to the north of the centre. *Saha et al.* (1981) studied the distribution of the daily changes of sea level pressure rather than the pressure itself, finding that most of the depressions that form at the head of the Bay of Bengal were associated with pressure disturbances coming from east. *Douglas* (1992a,b) suggested the importance of vertical shear for monsoon depression using the data obtained from MONEX–79. Douglas's analysis appears to substantiate the theoretical findings of *Arakawa and Moorthi* (1982), who have emphasised the importance of vertical shear and CISK in the growth of monsoon depressions. Weak easterly vertical wind shear is a characteristic feature of the flows over the north Bay of Bengal during summer monsoon months. They noted that for a reasonable easterly wind shear of the order of 20 ms^{-1}/800 hPa, large growth rates for horizontal scales of the order of 1000 to 2000 km are possible (*Krishnamurti and Surgi*, 1987). *Lindzen et al.* (1983) has examined the role of instabilities in the 200 hPa flow in the genesis of monsoon depressions.

We examined the role of LLJ in the genesis of monsoon depression. For this we made composites of 850 hPa wind field and OLR for each day from five days before (day−5) to the day of genesis of the depression (day 0) and further to 3 days after (day+3) for 12 MDs during July and August of the years 1979-1990. Westward moving monsoon depressions having life span of 3 days and more were only chosen. The tracks of these mosoon depressions are shown in Figure 6.1. Data regarding these depressions are shown in Table 2.3.

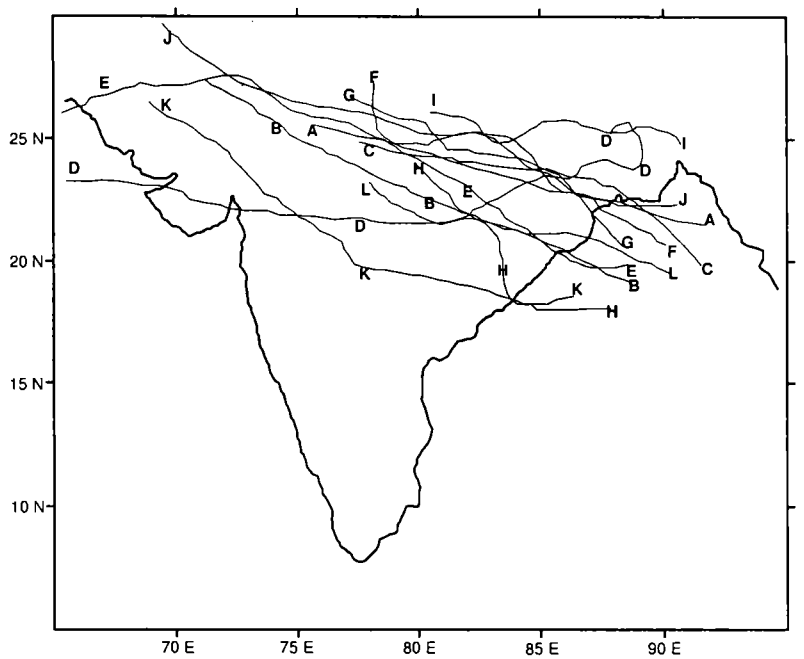

Figure 6.1: Tracks of monsoon depressions.

Composites of monsoon depressions thus made for each day from day−5 to day+3 are given in Figures 6.2 (a–i). There is an LLJ passing through the latitude belt 10°N–20°N with active convection in a long unbroken band on the cyclonic shear side of the LLJ to the east of longitude 70°E on day−5. A large cloud cluster forms in this convective band around longitude 100°E covering eastern Bay of Bengal and the Indo–China peninsula (see day−4). Convection is maximum (OLR 160 Wm^{-2}) on this day close to the coast of Myanmar. The convective cloud cluster has spread westwards on day−3 and it has expanded considerably by the next day (day−2). On day−1, this cloud cluster has covered the whole of north and central Bay of Bengal with the area of maximum convection of 150 Wm^{-2} near latitude 16°N. Day 0 denotes the day in which monsoon depression is formed with its centre over the extreme northern part of Bay of Bengal. The associated area of active convection gets concentrated to the southwest sector of the monsoon depression. It is well known that in

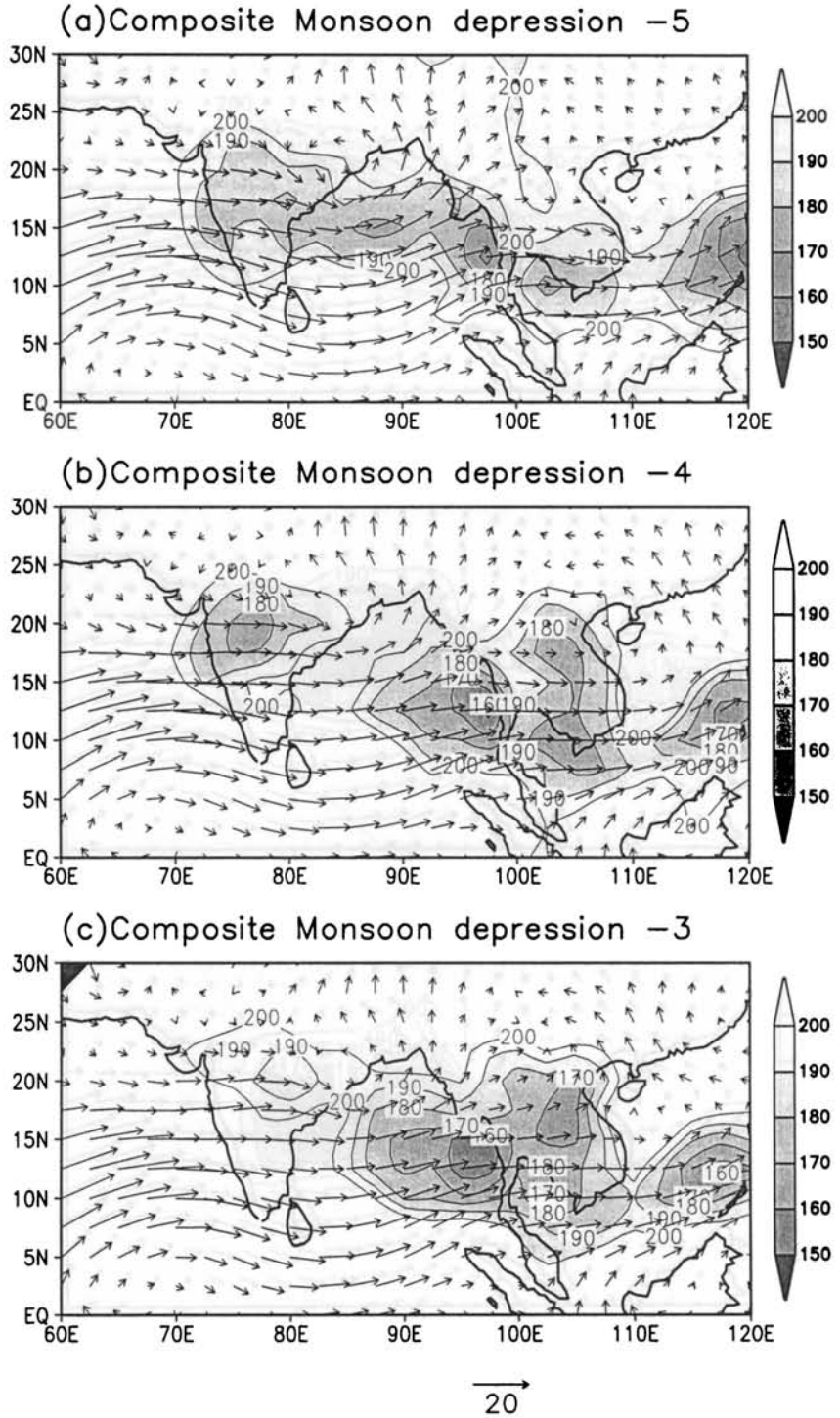

Figure 6.2: Composites of the 12 monsoon depressions (Table 2.3) in 850 hPa wind and OLR. Each composite is for a day, the first one (a) for 5 days before the day of monsoon depression genesis (day 0) to three days before (c).

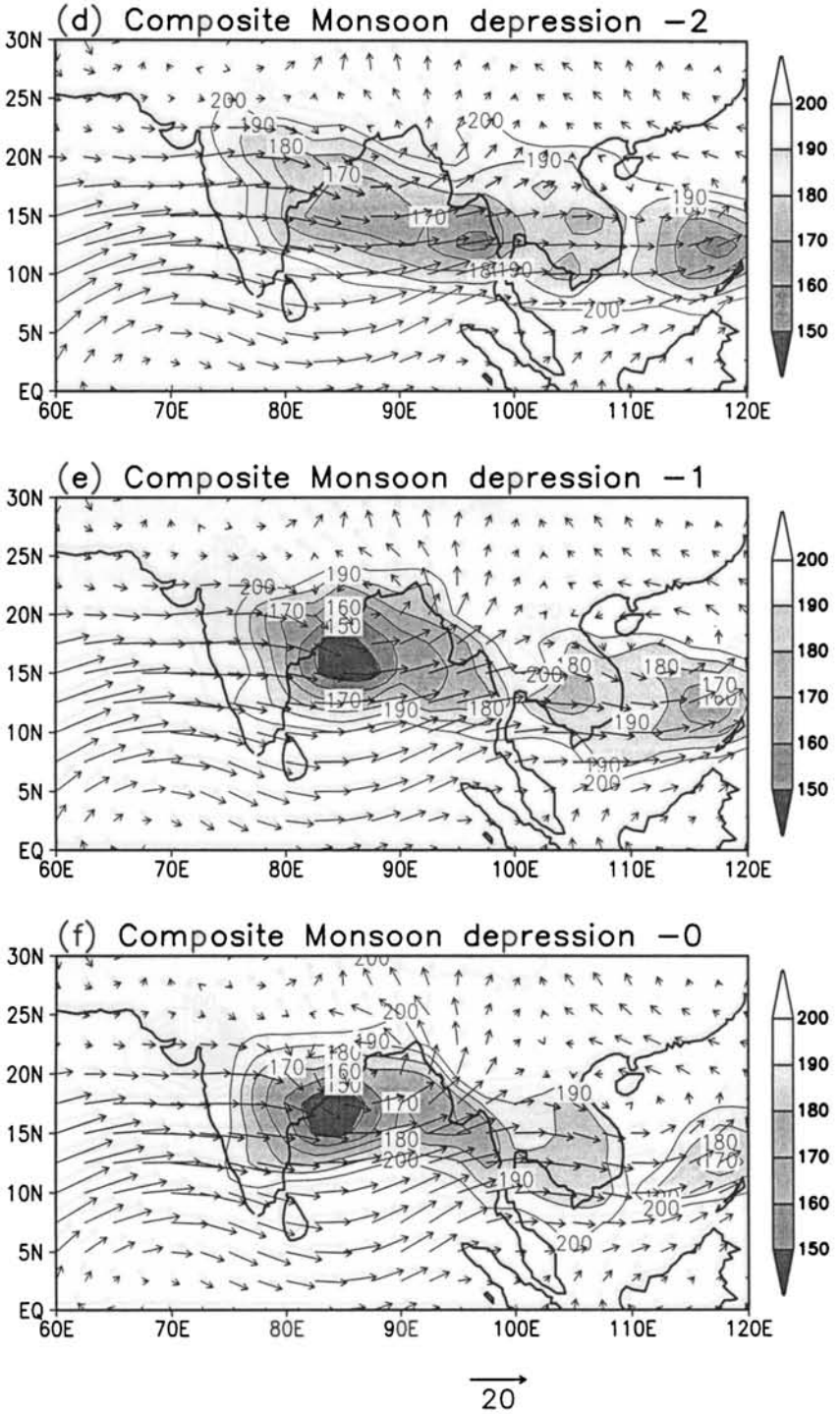

Figure 6.2: (contd) (d) for 2 days before the day of monsoon depression genesis to day of genesis (f).

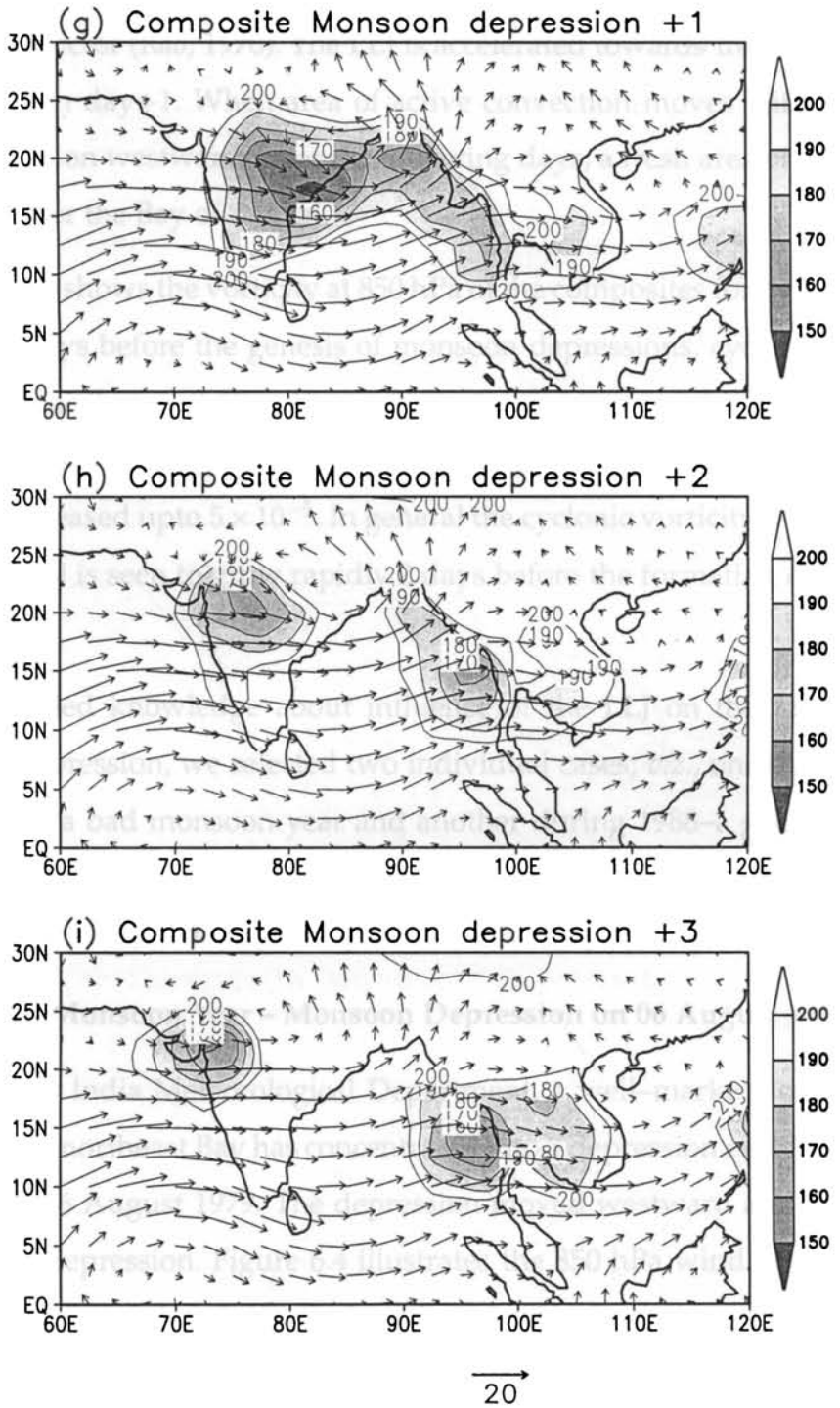

Figure 6.2: (contd) (g) for 1 day after the day of monsoon depression genesis to three day after (i).

a westward moving monsoon depression, the zone of heavy rainfall is in its south–west sector (*Rao*, 1976). The LLJ is accelerated towards the area of active convection on day+1. When area of active convection moves with the monsoon depression westwards over the following days, a fresh area of convection is formed over the Bay of Bengal.

Figure 6.3 shows the vorticity at 850 hPa of the composites for day -2 to day zero. Two days before the genesis of monsoon depressions, cyclonic vorticity concentrate at the head Bay. The vorticity intensifies rapidly of the order of 3.5×10^{-5} in day-1. The day of the genesis of monsoon depression the cyclonic vorticity increased upto 5×10^{-5}. In general the cyclonic vorticity over the head Bay of Bengal is seen to grow rapidly 2 days before the formation of monsoon depression.

For detailed knowledge about influence of the LLJ on the formation of monsoon depression, we selected two individual cases; *viz.*, one during 1979–representing a bad monsoon year and another during 1988–a good monsoon year. Horizontal wind at 850 hPa from 4 days before the genesis of monsoon depression to 3 days after are analysed.

Case 1: Bad Monsoon Year – Monsoon Depression on 06 August 1979

According to India Meteorological Department, a well–marked low pressure area over the northeast Bay has concentrated into a depression centered at 21°N and 90°E on 6 August 1979. The depression moved westward and intensified into a deep depression. Figure 6.4 illustrates the 850 hPa wind vector plotted from 2 to 9 August, i.e., 4 days before the genesis of monsoon depression to 3 days after. It can be seen that prior to the formation of monsoon depression, the LLJ become intense with strong cyclonic shear over the Bay of Bengal region. Strong LLJ is noted on the day of formation of monsoon depression. Due to the formation of monsoon depression, the region of head Bay experiences active

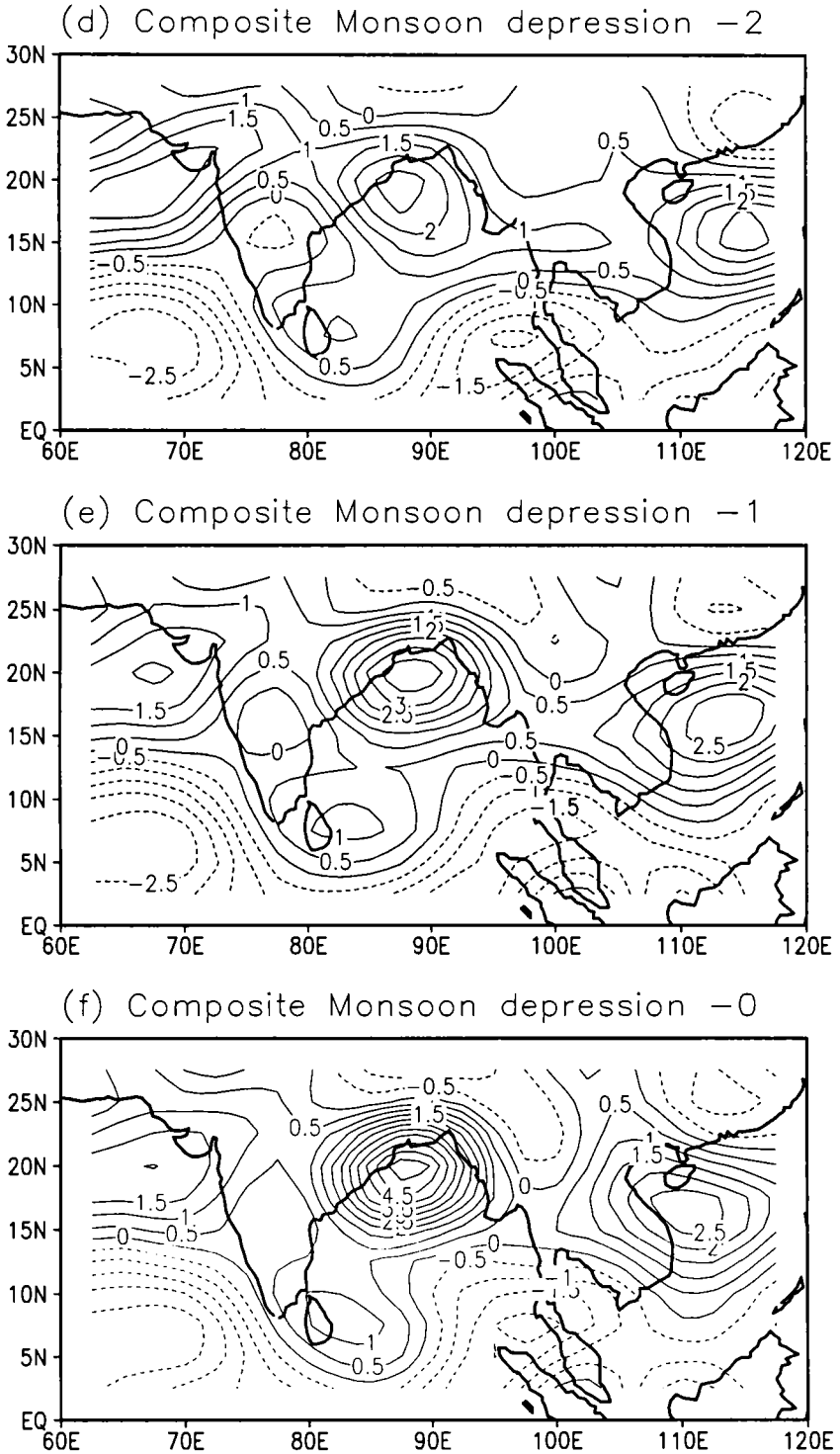

Figure 6.3: 850 hPa vorticity (multiplied by 10^5 for composites of 12 monsoon depressions. (a) for two days before monsoon depression, (b) a day before monsoon and (c) the day of monsoon depression genesis .

convection. This convection activity thus maintains the LLJ. Two days after the formation monsoon depression, the LLJ become more intense. This supports our finding reported in Chapter 4 of this thesis, that the convection leads the wind by 2–3 days.

Case 2: Good Monsoon Year – Monsoon Depression on 02 August 1988

As per the report given by India Meorological Department, a depression formed over north Bay off Bangladesh coast on 2 August 1988. After that it moved westnorthwesterly direction. It further intensified into a deep depression on 5 August over northwest of Madhya Pradesh. It further moved westwards and weakened on 7 August as a well marked low over west Rajastan. The 850 hPa wind for 4 days before the genesis of monsoon depression and 3 after are plotted in Figure 6.5. Salient features of LLJ and monsoon depressions as observed in 1979 case are also noted in this case. An intense LLJ with strong cyclonic shear can be seen before the monsoon depression genesis. After genesis the LLJ is maintained by the intense convection.

From the literature it is known that monsoon depressions do not form in break monsoon periods. During this period LLJ axis passes through south of India. In the active phase of the monsoon, the axis of LLJ passes through Bay of Bengal (~15°N) and is an important synoptic condition for depression genesis (*Sikka*, 1977). CISK is also considered as a factor in MD genesis. In active monsoon phase there is intense convection north of LLJ axis in the Bay of Bengal. It is seen from the composite that two factors are important for the genesis of monsoon depression.

1. A strong LLJ with large cyclonic shear vorticity at 850 hPa over the whole of north and adjoining central Bay of Bengal.

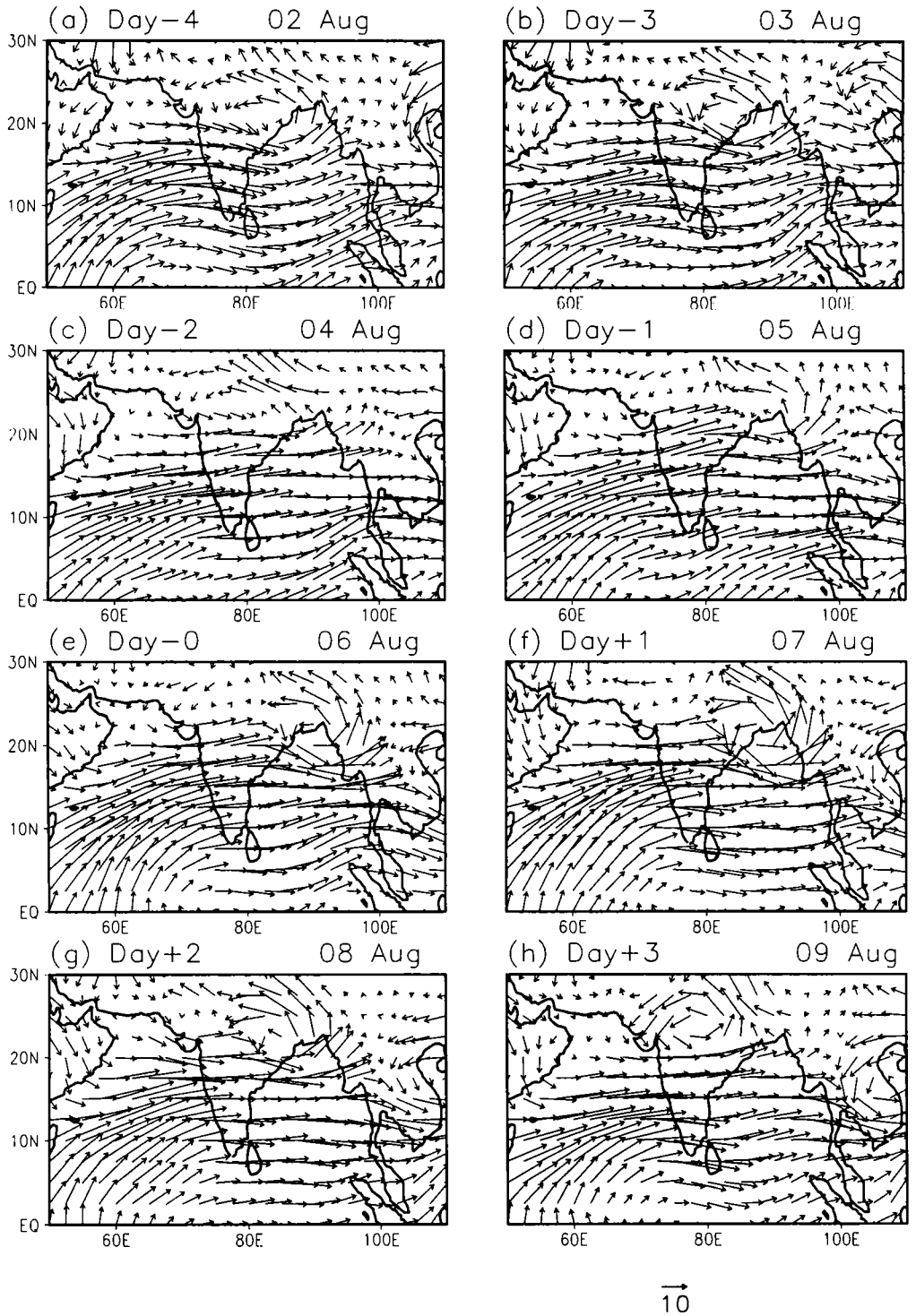

Figure 6.4: 850 hPa wind analysis for depression on 6 August 1979 (a) for 4 days before the day of monsoon depression genesis to (h) 3 days after.

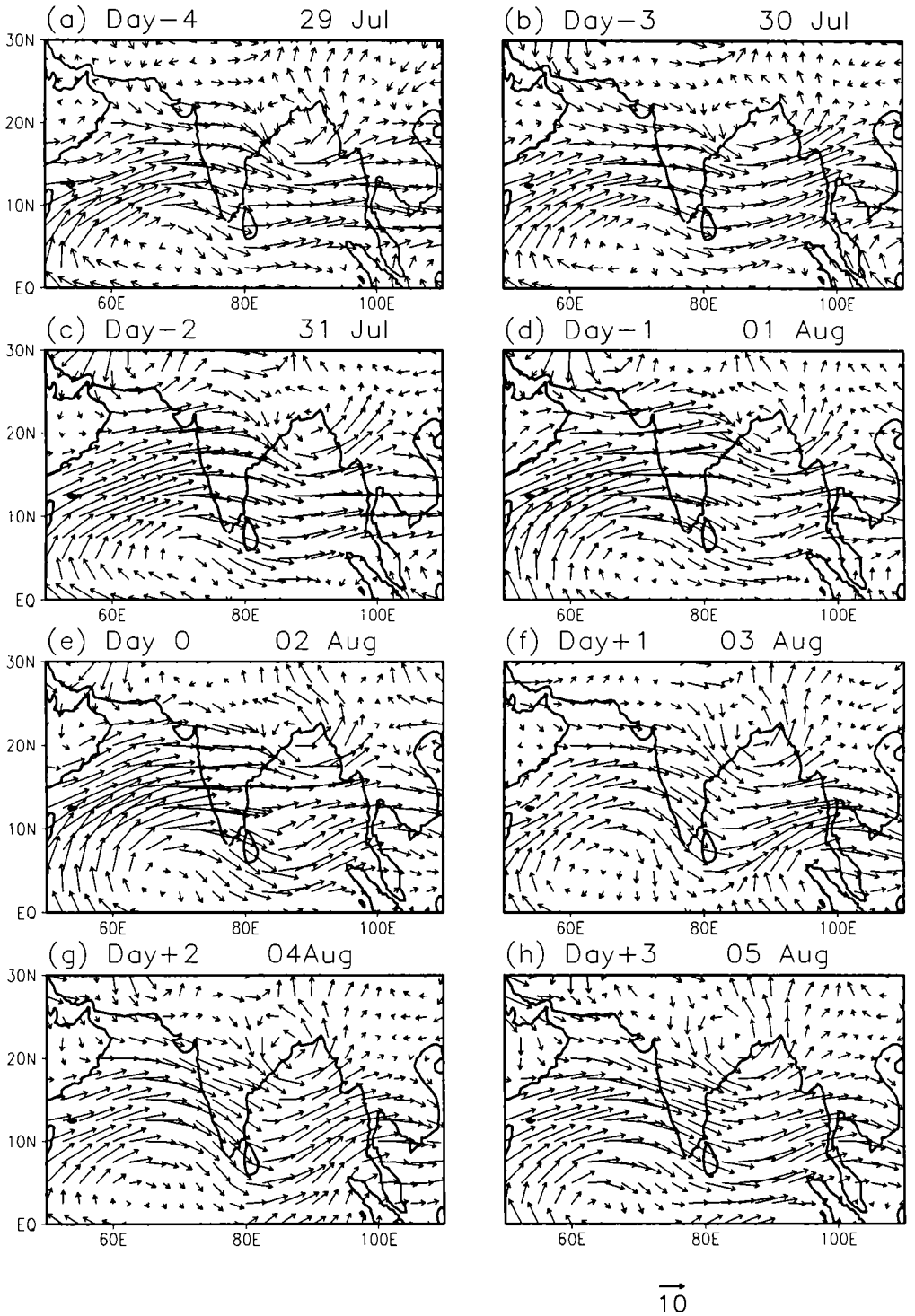

Figure 6.5: 850 hPa wind analysis for depression on 2 August 1988 (a) for 4 days before the day of monsoon depression genesis to (h) 3 days after.

2. An area of active convection in the form of a spatially large cloud cluster in this area of large cyclonic vorticity at 850 hPa.

It appears that there exists an interaction between the dynamics provided by the LLJ and the convection that is generated by the LLJ which results in the growth of both the LLJ and the convection leading to the formation of the monsoon depression as described in Chapter 4. Once the monsoon depression is formed the large area of convection shrinks and occupies a small area of intense convection in the south–west sector of the monsoon depression. Thus LLJ and associated large area of convection in the Bay of Bengal are necessary conditions for the formation of a monsoon depression. Triggering mechanism for the genesis of monsoon depression is not yet well understood.

CHAPTER 7

SUMMARY AND CONCLUSIONS

During the Asian summer monsoon season, June to September a strong cross–equatorial Low Level Jet-stream (LLJ) with core around 850 hPa exists over the Indian Ocean and south Asia. LLJ has its origin in the south Indian Ocean north of the Mascarene High as an easterly current, it crosses the equator in a narrow longitudinal belt close to the east African coast as a southerly current with speeds at times even as high as 100 knots, turns into a westerly current over the Arabian Sea and passes through India to the western Pacific Ocean. The characteristics and variability of LLJ and the assocciation of LLJ with localised heavy rainfall along the west coast of India and monsoon depressions have been studied in this thesis. The important research findings by the author are presented in the following.

The general climatology, structure and interannual variability of LLJ and also its relation with Indian Summer Monsoon Rainfall have been studied. The 30-year mean (1961-1990) monsoon flows at 850 hPa for each month from

June to September describes the monthly climatology of LLJ. During WET monsoon years westerlies extend eastwards only upto the longitude of Philippines. Easterly trade winds are found east of the Philippines. In the DRY composite monsoon westerlies extend further eastwards. *It is shown that the deep layer of vorticity from surface to mid troposphere over the low latitudes of western north Pacific during the DRY year is favourable for formation of tropical cyclones there which explains why in DRY monsoons the west Pacific cyclones form in the lower latitudes compared to WET monsoons.* The mean vertical profile of the zonal component (u), by averaging over the longitudes 62.5°E to 67.5°E from latitudes 30°S to 50°N, from 1961 to 1990 for July and August shows the vertical structure of LLJ over Arabian Sea. Here we can see only one axis of LLJ at around 15°N. The vertical cross section obtained averaging over 77.5°E to 82.5°E shows a two core structure of LLJ, one around 8°N and another around 17°N over peninsular India.

The intraseasonal variability of LLJ and its association with convective heating of the atmosphere are described. The important results are,

- The core of the cross equatorial LLJ crosses the equator in a geographically fixed narrow longitudinal belt close to the east African coast as a southerly current and it crosses India as a westerly current at latitudes varying from the equator to 25°N. In active monsoon conditions the core of the LLJ passes through peninsular India between latitudes 10°N and 20°N. In break monsoon conditions the LLJ from the central Arabian sea moves southeastwards and passes eastward close to Sri Lanka in the latitude belt equator to 10°N. There often is seen at this time a weaker LLJ axis through north India around latitude of 25°N.
- The axis or core of LLJ moves north along with the Maximum Cloud Zone of *Sikka and Gadgil* (1980) in their 30-50 day oscillations.

- LLJ does not show splitting into two branches over the Arabian Sea as suggested by *Findlater* (1971). His suggestion which is widely accepted since then is based on the analysis of monthly mean winds. Such an analysis is likely to show the LLJ of active and break monsoons as occurring at the same time, suggesting a split of the LLJ over the Arabian Sea. Two branches of LLJ through India are however seen during break monsoon spells, but the northern branch is at around latitude 25°N and not at about 17°N as found by Findlater.
- Convective heating of the atmosphere over the Bay of Bengal has a high and significant linear Correlation Coefficient with the zonal component of the wind at 850 hPa over peninsular India (70°E–80°E) and the Bay of Bengal (80°E–100°E) all between latitudes 10°N and 20°N. The correlation is maximum for a lag of 2–3 days, convection leading. It is speculated that active convection occurring over the Bay of Bengal between latitudes 10°N and 20°N accelerates the whole inter–hemispheric LLJ and takes the monsoon to an active spell.
- At the time of Break monsoon when there is no active convection in the Bay of Bengal (latitude belt 10°N-20°N), LLJ turns anti-cyclonically over the Arabian Sea conserving its potential vorticity and its axis passes eastwards close to the equator and south of India. It is speculated that the cyclonic vorticity in the frictional boundary layer on either side of the LLJ axis generates vertical upward motion and produces east-west bands of convection on either sides of the equator. From this point of time begins the northward movement of a new Maximum Cloud Zone in the 30–50 day oscillation of the monsoon.

Intense rainfall (24 hr) events observed along the west coast of India during the south Asian monsoon season have been studied. Cases of rainfall of 15 cm

per day or more at 5 coastal stations viz., Kozhikode (11.2°N, 75.7°E), Honavar (14.2°N, 74.4°E), Goa (15.3°N, 73.8°E), Ratnagiri (16.9°N, 73.3°E), and Mumbai (19°N, 72.9°E) for the period 1975–1990 have been studied. *It is found that these heavy rainfall events occur invariably in the region of large cyclonic wind shear at 850 hPa of the LLJ.* Literature has speculated on the existence of an offshore trough and a mesoscale vortex embedded in it in the atmospheric boundary layer in association with these intense rainfall events, although evidence from data has been weak. This aspect was examined with a Mesoscale model (MM5) with input data from NCEP/NCAR Reanalysis on the coarse grid 2.5°×2.5°latitude–longitude. *With the inclusion of realistic Western Ghat orography, a mesoscale vortex appears after 24 hours of model run on the cyclonic shear side of the LLJ. The intensity of this vortex becomes less when orography is removed.*

The results of a study on the association of LLJ with the genesis of monsoon depressions are presented. It is well known that monsoon depressions form in the active phase of the monsoon, when LLJ is strong and its axis passes through central Bay of Bengal. A synoptic model of the temporal evolution of a composite monsoon depression has been produced. There is a systematic temporal evolution of the field of deep convection and the strength and position of the LLJ axis leading to the genesis of monsoon depression. *Monsoon depressions have their genesis after (i) LLJ grows in strength over the central Bay of Bengal and (ii) convection has become strong and extensive over Bay of Bengal on the cyclonic shear side of the LLJ.* It is suggested that MDs form in the strong cyclonic shear zone of the LLJ (large area of strong cyclonic vorticity at and around 850 hPa) which is an area of intense vertical upward motion in the moist atmosphere prevailing during monsoon. As convection increases, LLJ strengthens cyclonic shear vorticity increases and the depression forms through a CISK–like mechanism. This differ from the conventional CISK (applied to synoptic scale systems) because LLJ is a planetary scale phenomenona.

One of the significant outcomes of the present doctoral thesis is that LLJ plays an important role in the intraseasonal variability of Asian Summer monsoon activity. Convection and rainfall are dependent mainly on the cyclonic vorticity in the boundary layer associated with LLJ. In turn, LLJ is maintained by the convective heating of the atmosphere over the Bay of Bengal. LLJ has a large amplitude intraseasonal oscillation. Active and break monsoons are extreme phases of this oscillation. Monsoon depression genesis in the Bay of Bengal and the episodes of very heavy rainfall along the west coast of India are closely related to the cyclonic shear of LLJ in the boundary layer and the associated deep convection. Case studies by a mesoscale numerical model (MM5) have shown the possibility that the heavy rainfall episodes along the west coast of India are associated with generation of mesoscale cyclonic vortices in the boundary layer as speculated in the literature. Thus LLJ should have a prominent place in numerical modeling studies of monsoon. Models should be able to simulate the location and strength of the LLJ correctly in each phase of the monsoon. LLJ associated features like the equatorial cloud band, monsoon depression, etc also should be simulated well in order that models simulate realistic monsoons and their intraseasonal variability.

7.1 Scope for Future Studies

Further work is needed to understand the role of LLJ in the intraseasonal variability of monsoon. We suggest three areas

- A modelling study with an atmospheric GCM using initial input data of an active monsoon day. In the model integration, the convective heating in the Bay of Bengal is slowly and artificially reduced to zero over a period of a week. Does the LLJ shift to the location as in a Break Monsoon?

- A modelling study with an atmospheric GCM using input data of days with strong LLJ axis through Bay of Bengal along latitude 15°N. Integrate the model with different SSTs and different north–south temperature gradients (representing vertical wind shear and the tropical easterly Jet). This study is to understand the role of LLJ in the genesis of monsoon depressions.

- Using an atmospheric GCM fed with initial condition, the data of a break monsoon day with no convection in the Bay of Bengal. The Bay of Bengal SST is increased slowly over a period of 15 days. Does convection increase in the Bay of Bengal as in an active monsoon spell. We may also study the lag between convection and LLJ.

REFERENCES

Ananthakrishnan, R. and Soman, M. K., The onset of southwest monsoon over Kerala 1901-1980, *J. Climatol*, **8**, 283–296, 1988.

Anderson, D. L. T., The low-level jet as western boundary current, *Mon. Weather Rev.*, **104**, 907–921, 1976.

Annamalai, H. and Slingo, J. M., Active/break cycles: Diagnosis of the intraseasonal variability of the Asian summer monsoon, *Clim. Dyn.*, **18**, 85–102, 2001.

Annamalai, H., Slingo, J. M., Sperber, K. R., and Hodges, K., The mean evolution and variability of the Asian summer monsoon: comparison of ECMWF and NCEP/NCAR reanalyses, *Mon. Weather Rev.*, **127**, 1157–1186, 1999.

Anthes, R. A. and Warner, T. T., Development of hydrostatic model suitable for air pollution and other mesometeorological studies, *Mon. Weather Rev.*, **106**, 1045–1078, 1978.

Arakawa, A., The variation of general circulation in the barotropic atmosphere, *J. Met. Soc. Japan.*, **39**, 49–58, 1961.

Arakawa, A. and Moorthi, S., Baroclinic (and barotropic) instability with cumulus heating, in *Proc. WMO program on Research in Tropical Meteorology*, WMO, V-43-V-62, Geneva, Switzerland, 1982.

Arpe, K. L., Dumenil, L., and Giorgetta, M. A., Variability of the Indian monsoon in the ECHAM3 model: Sensitivity to sea surface temperature, soil moisture, and the stratospheric quasi-biennial oscillation, *J. Climate*, **11**, 1837–1858, 1998.

Asnani, G. C., *Tropical Meteorology*, Volume I, G. C. Asnani, Pune, India, 1993.

Bannon, P. R., On the dynamics of the East African Jet. Part 1: Simulation of the mean conditions for July, *J. Atmos. Sci.*, **36**, 2139–2152, 1979.

Bannon, P. R., On the dynamics of the East African Jet. Part III: Arabian Sea branch, *J. Atmos. Sci.*, **39**, 2267–2278, 1982.

Betts, A. K. and Miller, M. J., The Betts–Miller Scheme, in *The representation of cumulus convection in numerical models*, edited by K. A. Emmanuel and D. J.

Raymond, pp. 107–121, American Meteorological Society, 1993.

Bhalme, H. N., Mooley, D. A., and Jadhav, S. K., Fluctuations in drought / flood area over India and relationship with southern oscillation, *Mon. Weather Rev.*, **111**, 86–94, 1983.

Bunker, A. F., Interaction of the summer monsoon air with the Arabian sea, *J. Geophys. Res.*, **102**, 19,495–19,505, 1965.

Chang, C. P. and Li, T., A theory of the tropical biennial oscillation, *J. Atmos. Sci.*, **57**, 2209–2224, 1999.

Charney, J. G. and Shukla, J., Predictability of monsoons, in *Monsoons Dynamics*, edited by J. Lighthill and R. P. Pearce, pp. 99–110, Cambridge University Press, 1981.

Chen, G. T. J. and Chang, C. P., The structure and vorticity budget of an early summer monsoon trough ("Mei-Yu") over southeastern China and Japan, *Mon. Weather Rev.*, **108**, 942–953, 1980.

Chin, P. C., *Tropical cyclone climatology for the China Seas and Western Pacific from 1884 to 1970*, Royal Observatory, Hong Kong, Basic Data, Vol.1, 1972.

Chung, C. and Nigam, S., Asian summer monsoon-ENSO feedback on the Cane-Zebiak model ENSO, *J. Climate*, **12**, 2787–2807, 1999.

De, U. S., Lele, R. R., and Natu, J. C., *Breaks in south west monsoon*, India Meteorological Department, Pune, Pre-Published Scientific Report No. 1998/3, 1998.

Derber, J. C., Parrish, D. F., and Lord, S. J., The new global operational analysis system at the National Meteorological Center, *Wea. Forecasting*, **6**, 538–547, 1991.

Douglas, M. W., Structure and dynamics of two monsoon depressions. Part I: Observed structure, *Mon. Weather Rev.*, **120**, 1524–1547, 1992a.

Douglas, M. W., Structure and dynamics of two monsoon depressions. Part II: Vorticity and Heat Budget, *Mon. Weather Rev.*, **120**, 1548–1564, 1992b.

Dudhia, J., A nonhydrostatic version of the Penn State/NCAR mesoscale model: Validation tests and simulation of an atlantic cyclone and cold front, *Mon. Weather Rev.*, **121**, 1493–1513, 1993.

Findlater, J., A major low-level air current near the Indian Ocean during the northern summer, *Q. J. R. Meteorol. Soc.*, **95**, 362–380, 1969a.

Findlater, J., A major low level current near the Indian Ocean during northern summer, *Q. J. R. Meteorol. Soc.*, *95*, 362–380, 1969b.

Findlater, J., Mean monthly airflow at low levels over the western Indian Ocean, in *Geophysical Memoirs*, HMSO, London, 1971.

Findlater, J., Low level airflow over Kenya and rainfall over India, in *Monsoons Dynamics*, edited by J. Lighthill and R. P. Pearce, pp. 309–319, Cambridge University Press, 1981.

Gadgil, S., Climate change and agriculture–an Indian perspective, in *Climate Variability and Agriculture*, edited by Y. R. Abool, S. Gadgil, and G. B. Pant, pp. 1–18, Narosa, New Delhi, India, 1996.

Gadgil, S. and Asha, G., Intraseasonal variation of the summer monsoon. I: Observational aspects, *J. Met. Soc. Japan.*, **70**, 517–527, 1992.

George, L. and Mishra, S. K., An observational study on the energetics of the onset monsoon vortex 1979, *Q. J. R. Meteorol. Soc.*, **119**, 755–778, 1993.

George, P. A., Effects of off shore vortices on rainfall along west coast of India, *Ind. J. Met. Geophys.*, **7**, 225–240, 1956.

Goswami, B. N., Dynamical predictability of seasonal monsoon rainfall: Problems and prospects, *Proc. Ind. Natl. Sci. Acad.*, **60**, 101–120, 1994.

Goswami, B. N. and Ajayamohan, R. S., Intraseasonal oscillations and interannual variability of the Indian summer monsoon, *J. Climate*, **14**, 1180–1198, 2001.

Goswami, B. N. and Jayavelu, V., On possible impact of the summer monsoon on the ENSO, *Geophys. Res. Lett.*, **28**, 571–574, 2001.

Goswami, B. N. and Shukla, J., Quasi-periodic oscillations in a symmetric general circulation model, *J. Atmos. Sci.*, **41**, 20–37, 1984.

Goswami, B. N., Sengupta, D., and Sureshkumar, G., Intraseasonal oscillations and interannual variability of surface winds over the Indian monsoon region, *Proc. Ind. Acad. Sci. Earth Planet. Sci.*, **107**, 45–64, 1998.

Goswami, B. N., Krishnamurthy, V., and Annamalai, H., A broad scale circulation index for the interannual variability of the Indian summer monsoon, *Q. J. R. Meteorol. Soc.*, **125**, 611–633, 1999.

Gray, W. M., *Tropical cyclone global climatology*, WMO, Geneva, WMO Technical Document, WMO/TD No.72, Vol.1, 1985.

Grossman, R. L. and Durran, D. R., Interaction of low–level flow with the western Ghat Mountains and offshore convection in the summer monsoon, *Mon. Weather Rev.*, **112**, 652–672, 1984.

Gruber, A. and Krueger, A. F., The status of the NOAA outgoing longwave radiation data set, *Bull. Am. Meteorol. Soc.*, **65**, 958–926, 1984.

Halpern, D. and Woiceshyn, P. M., Onset of the Somali Jet in the Arabian Sea during June 1997, *Geophys. Res. Lett.*, **104**, 18 041–18 046, 1999.

Halpern, D. and Woiceshyn, P. M., Somali Jet in the Arabian Sea, El Niño and

India Rainfall, *Mon. Weather Rev.*, **14**, 434–441, 2001.

Halpern, D., Freeilich, M. H., and Weller, R. A., Arabian sea surface winds and ocean transports determined from ERS-1 scatrometer, *Geophys. Res. Lett.*, **103**, 7799–7805, 1998.

Hart, J. E., On the theory of East African low level jetstream, *Pure Appl. Geophys.*, **115**, 1263–1282, 1977.

Hartman, D. and Michelsen, M., Intraseasonal periodicities in the Indian rainfall, *J. Atmos. Sci.*, **46**, 2838–2862, 1989.

Harzallah, A. and Sadourny, R., Internal versus SST forced atmosphere variability simulated by an atmospheric general circulation model, *J. Climate*, **8**, 474–495, 1995.

Hastenrath, S. and Lamb, P. J., On the heat budget of hydrosphere and atmosphere in the Indian ocean, *J. Phys. Oceanogr.*, **10**, 694–708, 1980.

Holton, J. R., *An introduction to dynamic meteorology*, Academic Press, 1992.

Hoskins, B. J. and Rodwell, M. J., A model of the Asian summer monsoon, *J. Atmos. Sci.*, **52**, 1329–1340, 1995.

IMD, Tracks of storms and depressions in the Bay of Bengal and the Arabian Sea 1971-1990, Tech. rep., India Meteorological Department, Pune, India, 1996.

Janjic, Z. I., The step–mountain eta coordinate model: Further development of the convection, viscous sublayer, and turbulent closure schemes, *Mon. Weather Rev.*, **122**, 927–945, 1994.

Joseph, P. V., Climatic change in monsoon and cyclones, Proceedings of the IITM symposium on Tropical Monsoons, Indian Institute of Tropical Meteorology, Pune, 1976.

Joseph, P. V., Subtropical westerlies in relation to large scale failure of Indian summer monsoon, *Ind. J. Met. Hydrol. Geophys.*, **29**, 412–418, 1978.

Joseph, P. V. and Raman, P. L., Existance of low level westerly jet -stream over peninsular India during July, *Ind. J. Met. Geophys.*, **17**, 407–410, 1966.

Joseph, P. V., Eisched, J. K., and Pyle, R. J., Interannual variability of the onset of Indian summer monsoon and its association with atmospheric features, El Niño, *J. Climate*, **7**, 81–105, 1994.

Julian, P. and Madden, R., Comments on a paper of T. Yasunari, a quasi-stationary appearance of 30 to 40 day period in the cloudiness fluctuations during the summer monsoon over India, *J. Met. Soc. Japan.*, **59**, 435–437, 1981.

Kalnay, E., Kanamitsu, M., Kistler, R., Collins, W., Deaven, D., Gandin, L.,

Iredell, M., Saha, S., White, G., Woollen, J., Zhu, Y., Leetmaa, A., Reynolds, R., Chelliah, M., Ebisuzaki, W., Higgins, W., Janowiak, J., Mo, K. C., Ropelewski, C., Wang, J., Jenne, R., and Joseph, D., The NCEP/NCAR 40-year reanalysis project, *Bull. Am. Meteorol. Soc.*, **77**, 437–471, 1996.

Kesavamurty, R. N., Satyan, V., Dash, S. K., and Sinha, H. S., Shift of quasi-stationary features during active and break monsoons, *Proc. Ind. Acad. Sci. Earth Planet. Sci.*, **89**, 209–214, 1980.

Kim, K. M. and Lau, K. M., Dynamics of monsoon-induced biennial variability in ENSO, *Geophys. Res. Lett.*, **28**, 315–318, 2000.

Koteswaram, P. and George, C. A., On the formation of monsoon depression in the Bay of Bengal, *Ind. J. Met. Geophys.*, **9**, 9–22, 1958.

Krishnamurti, T. N., Summer monsoon experiment–A Review, *Mon. Weather Rev.*, *113*, 1590–1629, 1985.

Krishnamurti, T. N. and Bhalme, N. H., Oscillations of a monsoon system. Part I: Observational aspects, *J. Atmos. Sci.*, **33**, 1937–1954, 1976.

Krishnamurti, T. N. and Ramanathan, Y., Sensitivity to monsoon onset to differential heating, *J. Atmos. Sci.*, **39**, 1290–1306, 1982.

Krishnamurti, T. N. and Subrahmanyam, D., The 30-50 day mode at 850 hpa during the MONEX, *J. Atmos. Sci.*, **39**, 2088–2095, 1982.

Krishnamurti, T. N. and Surgi, N., Observational aspects of monsoons, in *Monsoons Meteorology*, edited by C. P. Chang and T. N. Krishnamurti, pp. 501–544, Oxford University Press, New York, 1987.

Krishnamurti, T. N. and Wong, V., A simulation of cross equatorial flow over Arabian Sea, *J. Atmos. Sci.*, **36**, 1895–1907, 1979.

Krishnamurti, T. N., Molinari, J., and Pan, H. L., Numerical simulation of the somali jet, *J. Atmos. Sci.*, **33**, 2350–2362, 1976.

Krishnamurti, T. N., Ardanuy, P., Ramanathan, Y., and Pasch, R., On the onset vortex of summer monsoons, *Mon. Weather Rev.*, **105**, 344–363, 1981.

Krishnamurti, T. N., Wong, V., Pan, H. L., Pasch, R., Molinari, J., and Ardanuy, P., A three dimensional planetary boundary layer model for Somali jet, *J. Atmos. Sci.*, **40**, 894–908, 1983.

Krishnan, R., Zhang, C., and Sugi, M., Dynamics of breaks in the Indian summer monsoon, *J. Atmos. Sci.*, **57**, 1354–1372, 2000.

Kumar, K. K., Rajagopalan, B., and Cane, M., On the weakening relationship between the Indian monsoon and ENSO, *Science.*, **284**, 2156–2159, 1999.

Lander, M. A., An explosive analysis of the relationship between tropical storm in the Western North Pacific and ENSO, *Mon. Weather Rev.*, *122*, 636–651,

1994.

Lau, K. M. and Chan, P. H., Aspects of the 40-50 day oscillation during the northern summer as infrared from outgoing longwave radiation, *Mon. Weather Rev.*, **114**, 1354–1367, 1986.

Lau, K. M. and Peng, L., Origin of low frequency (intraseasonal) oscillations in the tropical atmosphere. Part III: Monsoon dynamics, *J. Atmos. Sci.*, **47**, 1443–1462, 1990.

Lau, K. M. and Sheu, P., Annual cycle, QBO and southern oscillation in global precipitation, *J. Geophys. Res.*, **93**, 10 975–10 913, 1988.

Lau, K. M. and Wu, H. T., An assessment of the impacts of the 1997-98 El Niño on the Asian Australian monsoon, *Geophys. Res. Lett.*, **26**, 1747–1750, 1999.

Lau, K. M. and Wu, H. T., Intrinsic modes of coupled rainfall / SST variability for the Asian summer monsoon: A re-assessment of monsoon-ENSO relationship, *J. Climate*, **14**, 2880–2895, 2001.

Lau, K. M., King, K. M., and Yang, S., Dynamical and boundary forcing characteristics of regional components of the Asian summer monsoon, *J. Climate*, **13**, 2461–2482, 2000.

Lawrence, D. M. and Webster, P. J., Interannual variations of the intraseasonal oscillation in the South Asian summer monsoon region, *J. Climate*, **14**, 2910–2922, 2001.

Lawrence, D. M. and Webster, P. J., The boreal summer monsoon intraseasonal oscillation: Relationship between northward and eastward movement on convection, *J. Atmos. Sci.*, **59**, 1593–1606, 2002.

Lindzen, R. S., Farrell, B., and Rosenthal, A. J., Absolute barotropic instablity and monsoon depressions, *J. Atmos. Sci.*, **40**, 1178–1184, 1983.

Madden, R. A. and Julian, P. R., Description of global scale circulation cells in the tropics with a 40-50 day period, *J. Atmos. Sci.*, **29**, 1109–1123, 1972.

Madden, R. A. and Julian, P. R., Observations of the 40-50 day tropical oscillation: A review, *Mon. Weather Rev.*, **112**, 813–832, 1994.

Magna, V. and Webster, P. J., Atmospheric circulation during active and break periods of the Asian monsoon, in *Preprints of the eighth conference on the Global Ocean-Atmosphere and Land System (GOALS)*, Amer. Meteor. Soc., Atlanta, GA, 1996.

Mak, M., Synoptic–scale disturbances in the summer monsoon, in *Monsoons Meteorology*, edited by C. P. Chang and T. N. Krishnamurti, pp. 435–460, Oxford University Press, New York, 1987.

McGregor, G. R. and Nieuwolt, S., *Tropical Climatology*, John Willy & Sons Ltd, West Sussex, England, 1998.

Meehl, G. A., The annaul cycle and interannual variability in the tropical Indian and Pacific ocean regions, *Mon. Weather Rev.*, **115**, 27–50, 1987.

Meehl, G. A., The south Asian monsoon and the tropospheric biennial oscillation, *J. Climate*, **10**, 1921–1943, 1997.

Mooley, D. A. and Parthasarathy, B., Variability of the Indian summer monsoon and tropical circulation features, *Mon. Weather Rev.*, **111**, 967–978, 1983.

Mooley, D. A. and Parthasarathy, B., Fluctuations in all-India summer monsoon rainfall during 1871-1978, *Clim. Change.*, **6**, 287–301, 1984.

Mooley, D. A. and Shukla, J., Variability and forecasting of the summer monsoon rainfall over India, in *Monsoons Meteorology*, edited by C. P. Chang and T. N. Krishnamurti, pp. 26–59, Oxford University Press, New York, 1987.

Mukherjee, A. K., Dimension of an "offshore vortex" in East Arabian Sea as deduced from observations during MONEX 1979, FGGE Operations Report, Vol.9, Part A- Results on Summer Monex Field Phase Research, World Meteorological Organisation, 1980.

Mukherjee, A. K., Rao, A. K., and Shah, K. C., Vortices embedded in the trough of low pressure off Maharashtra- Goa coasts during the month of July, *Ind. J. Met. Hydrol. Geophys.*, **29**, 61–65, 1978.

Murakami, M., Analysis of deep convective activity over the western Pacific and southeast Asia. Part II: seasonal and intraseasonal variations during northern summer, *J. Met. Soc. Japan.*, **62**, 88–108, 1984.

Ogura, Y. and Yoshizaki, M., Numerical study of orographic convective precipitation over the Eastern Arabian sea and Ghat Mountains during the summer monsoon, *J. Atmos. Sci.*, **15**, 2097–2022, 1988.

Parrish, D. F. and Derber, J., The National Meteorological Center's spectral statistical interpolation analysis system, *Mon. Weather Rev.*, **120**, 1747–1763, 1992.

Parthasarathy, B., Munot, A. A., and Kothawale, D. R., All-India monthly and seasonal rainfall series, *Theor. Appl. Climatol.*, **49**, 219–224, 1994.

Pearce, R. P. and Mohanty, U. C., Onsets of the Asian summer monsoon 1979-1982, *J. Atmos. Sci.*, **41**, 1620–1639, 1984.

Pisharoty, P. R., Evaporation from the Arabian sea and Indian southwest monsoon, in *Proc. of Symposium on Meteorological Results of the International Indian Ocean Expedition*, p. 437, Meteorological Department-INCOR-WMO-UNESCO, Bombay, India, 1965.

Pisharoty, P. R. and Asnani, G. C., Rainfall around monsoon depressions over India, *Ind. J. Met. Geophys.*, **8**, 15–20, 1957.

PSU/NCAR MM5 User's guide, *PSU/NCAR Mesoscale Modeling System Tutorial Class Notes and User's Guide: MM5 Modeling System Version 3*, Mesoscale and Meteorology Division, National Center for Atmospheric Research, 2002.

Rajan, C. K., Ignatious, K., and Joseph, P. V., Inter annual variablity of low level jet stream in relation to Indian Summer Monsoon rainfall, in *Meteorology Beyond 2000*, Proceedings of National Symposium,TROPMET-99, pp. 129–133, Indian Meteorological Society, Chennai, 1999.

Ramage, C., *Monsoon Meteorology*, vol. 15 of *International Geophysics Series*, Academic Press, San Diego, Calif, 1971.

Ramamurthy, K., *Monsoon of India: Some aspects of 'break' in the Indian South west monsoon during July and August*, India Meteorological Department, New Delhi, Forecasting Manual, Part IV.18.3, 1969.

Ramanadham, R., Rao, P. V., and Patnaik, J. K., Break in the Indian summer monsoon, *Pure Appl. Geophys.*, **104**, 635–647, 1973.

Rao, Y. P., *Southwest Monsoon*, India Meteorological Department, New Delhi, Meteorological Monograph, 1976.

Rasmusson, E. M. and Carpenter, T. H., The relation between eastern equatorial Pacific sea surface temperature and rainfall over India and Sri Lanka, *Mon. Weather Rev.*, **111**, 517–528, 1983.

Rasmusson, E. M., Wang, X., and Ropelewski, C. F., The biennial component of ENSO variability, *J. Mar. Sys.*, **1**, 71–96, 1990.

Reiter, E. R., Jet stream meteorology, pp. 265–271, University of Chicago Press, 1961.

Rodwell, M. J. and Hoskins, B. J., A model of the Asian summer monsoon Part II: Cross-equatorial flow and PV behavior, *J. Atmos. Sci.*, **52**, 1341–1356, 1995.

Saha, K. and Chang, C. P., The baroclinic processes of monsoon depressions, *Mon. Weather Rev.*, **111**, 1506–1514, 1983.

Saha, K., Sanders, F., and Shukla, J., Westward propagating predecessers of monsoon depressions, *Mon. Weather Rev.*, **109**, 303–343, 1981.

Sarker, R. P., A dynamical model of orographic rainfall, *Mon. Weather Rev.*, **94**, 555–572, 1966.

Sarker, R. P., Some modifications in a dynamical model of orographic rainfall, *Mon. Weather Rev.*, **95**, 673–684, 1967.

Schulman, L. L., On the summer hemisphere Hadley cell, *Q. J. R. Meteorol. Soc.*, **99**, 197–201, 1973.

Shen, S. and Lau, K. M., Biennial oscillation associated with the east Asian monsoon and tropical sea surface temperature, *J. Met. Soc. Japan.*, **73**, 105–124, 1995.

Shukla, J. and Paolina, D. A., The southern oscillation and long range forecasting of the summer monsoon rainfall over India, *Mon. Weather Rev.*, **111**, 1830–1837, 1983.

Sikka, D. R., Some aspects of the life history, structure and movement on monsoon depressions, *Pure Appl. Geophys.*, **115**, 1501–1529, 1977.

Sikka, D. R., Some aspects of the large-scale fluctuations of summer monsoon rainfall over India in relation to fluctuations in the planetary and regional scale circulation parameters, *Proc. Ind. Acad. Sci. Earth Planet. Sci.*, **89**, 179–195, 1980.

Sikka, D. R. and Gadgil, S., On the maximum cloud zone and the ITCZ over Indian longitudes during the southwest monsoon, *Mon. Weather Rev.*, **108**, 1840–1853, 1980.

Singh, N., Large scale interannual variation of the summer monsoon over Indian emperical prediction, *Proc. Ind. Acad. Sci. Earth Planet. Sci.*, **104 1**, 1–36, 1995.

Singh, N., Mulye, S. S., and Pant, G. B., Some features of the arid area variations over India, *Pure Appl. Geophys.*, **138**, 135–150, 1992.

Smith, R. B., *The influence of mountains on the atmosphere*, vol. 21 of *Advances in Geophysics*, Academic Press, 1979.

Smith, R. B. and Lin, Y. L., Orographic rain on the Western Ghats, in *Proc. First Sino–American Workshop on Mountain Meteorology*, edited by E. R. Reiter, Z. Baozhen, and Q. Yongfu, pp. 71–98, Science Press, Beijing and Amer. Met. Soc., 1983.

Soman, M. K. and Krishnakumar, K., Space-time evolution of meteorological features associated with the onset of Indian summer monsoon, *Mon. Weather Rev.*, **121**, 1177–1194, 1993.

Soman, M. K. and Slingo, J. M., Sensitivity of the Asian monsoon to aspects of sea-surface-temperature anomalies in the tropical Pacific ocean, *Q. J. R. Meteorol. Soc.*, **123**, 309–336, 1997.

Sperber, K. R., Slingo, J. M., and Annamalai, H., Predictability and the relationship between subseasonal and interannual variability during the Asian summer monsoon, *Q. J. R. Meteorol. Soc.*, **126**, 2545–2574, 2000.

Srinivasan, J., Gadgil, S., and Webster, P. J., Meridional propagation of large-scale monsoon convective zones, *Meteorol. and Atmos. Phys.*, **52**, 15–35, 1993.

Tao, S. and Chen, L., A review of recent research on the East Asian summer monsoon in China, in *Monsoon Meteorology*, edited by C. P. Chang and T. N. Krishnamurti, pp. 60–92, Oxford University Press, New York, 1987.

Tian, S. F. and Yasunari, T., Time and space structure of interannual variations in summer rainfall over China, *J. Met. Soc. Japan.*, **70**, 585–596, 1992.

Wainer, I. and Webster, P. J., Monsoon/ El Niño-Southern Oscillation relationships in a simple coupled ocean–atmosphere model, *J. Geophys. Res.*, **101**, 25 599–25 614, 1996.

Wang, B. and Rui, H., Synoptic climatology of transient tropical intraseasonal convection anomalies: 1975-1985, *Meteorol. and Atmos. Phys.*, **44**, 43–61, 1990.

Wang, B. and Xie, X., A model for the boreal summer intraseasonal oscillation, *J. Atmos. Sci.*, **54**, 72–86, 1997.

Warner, C., Core structure of a Bay of Bengal monsoon depression, *Mon. Weather Rev.*, **112**, 137–152, 1984.

Webster, P. J., Mechanisms of low-frequency variability: Surface hydrological effects, *J. Atmos. Sci.*, **40**, 2110–2124, 1983.

Webster, P. J., The variable and interactive monsoon, in *Monsoons*, edited by J. S. Fein and P. L. Stephens, pp. 269–330, Wiley and Sons, New York, 1987.

Webster, P. J., Magana, V. O., Palmer, T. N., Shuka, J., Tomas, R. T., Yanai, M., and Yasunari, T., Monsoons: Processes, predictability and the prospects of prediction, *J. Geophys. Res.*, **103(C7)**, 14 451–14 510, 1998.

Yasunari, T., Structure of the Indian monsoon system with around 40-day period, *J. Met. Soc. Japan.*, **57**, 227–242, 1981.

Yasunari, T., Impact of Indian monsoon on the coupled atmosphere / ocean system in the tropical Pacific, *Meteorol. and Atmos. Phys.*, **44**, 29–41, 1990.

Yasunari, T. and Suppiah, R., Some problems on the interannual variability of Indonesian monsoon rainfall, in *Tropical Rainfall Measurements*, edited by J. S. Theon and N. Fugono, pp. 113–122, Deepak, Hampton, Va., 1988.